



TROPICAL AND MID-LATITUDE CLOUD PROPERTIES DURING PM<sub>2.5</sub>  
LEVELS EXCEEDED THE STANDARD IN DIFFERENT CLIMATE:  
THAILAND AND UK USING SATELLITE DATA

DISSERTATION

By

ORADEE PILAHOME

A Dissertation Submitted in Partial Fulfillment of the Requirements for  
The Doctor of Physics Faculty of Science and Technology  
at Sakon Nakhon Rajabhat University

March 2024

TROPICAL AND MID-LATITUDE CLOUD PROPERTIES DURING PM<sub>2.5</sub>  
LEVELS EXCEEDED THE STANDARD IN DIFFERENT CLIMATE:  
THAILAND AND UK USING SATELLITE DATA

DISSERTATION

BY

ORADEE PILAHOME

A Dissertation Submitted in Partial Fulfillment of the Requirements for  
The Doctor of Physics Faculty of Science and Technology  
at Sakon Nakhon Rajabhat University  
March 2024





**DISSERTATION APPROVAL**  
**SAKON NAKHON RAJABHAT UNIVERSITY**  
**DOCTOR OF PHILOSOPHY**  
**PROGRAM IN PHYSICS**

Dissertation Title: Tropical and Mid-latitude Cloud Properties during PM2.5 Levels Exceeded the Standard in Different Climate: Thailand and UK using satellite data  
Author: Oradee Pilahome

**Dissertation Examination Committee**

  
..... Chairperson .....  Committee  
(Asst. Prof. Dr. Itsara Masiri) (Assoc. Prof. Dr. Wilawan Kumharn) and Advisor

  
..... Committee .....  Committee  
(Asst. Prof. Dr. Sumaman Buntoung) (Prof. Dr. Tosawat Seetawan)


  
..... Committee .....  Committee  
(Assoc. Prof. Dr. Athorn Vora-ud) (Asst. Prof. Dr. Hassakorn Wattanasarn)

Approval by the Curriculum Committee

  
.....  
(Assoc. Prof. Dr. Athorn Vora-ud)

Chair of the Committee for Curriculum  
Administration Approval  
Sakon Nakhon Rajabhat University

Approval by Graduate School

  
.....  
(Asst. Prof. Dr. Surasak Santhaveesuk)

The Director of Graduate School  
Sakon Nakhon Rajabhat University

26 March 2024

## ACKNOWLEDGEMENT

This thesis was accomplished very well. With kindness and great help from Associate Professor Dr. Wilawan Khamhan, Chairman of the Thesis Advisory Committee, kindly advised, made suggestions, and corrected various shortcomings with care throughout. From the beginning until completion, the researcher would like to thank you very much. I would also like to thank all the faculty members who assisted in conducting this research.

Thank you to Assistant Professor Issara Masiri, lecturer in the Department of Physics, Faculty of Science, University, Silpakorn University, for advising and assisting in writing IDL programs to analyze the data in this research. And please sacrifice your time to chair the committee for the outline and thesis defense examinations.

Thank you to the National Research Council of Thailand (NRCT) for granting research and innovation grants. Golden Jubilee Doctoral Project (Contract Number N41A650116)

Thank you, Pollution Control Department and the Climate Change Data Center that provides PM2.5 data for research.

Thank you to NASA for providing satellite data for research.

Finally, the researcher wishes to present the value and benefits of this thesis to his father. Mother of the researcher and all teachers that has been trained and taught until the researcher can maintain himself and achieve success in the present.

Oradee Pilahome

ชื่อเรื่อง	สมบัติของเมฆในเขตร้อนและละติจูดกลางในช่วงที่มีค่า PM2.5 เกินค่ามาตรฐาน ในภูมิภาคที่แตกต่างกัน:ไทย-อังกฤษ โดยใช้ข้อมูลดาวเทียม
ผู้วิจัย	อรดี พิลาโฮม
กรรมการที่ปรึกษา	รองศาสตราจารย์ ดร.วิลาวัรรณ์ คำหาญ
ปริญญา	ปร.ด. (ฟิสิกส์)
สถาบัน	มหาวิทยาลัยราชภัฏสกลนคร
ปีที่พิมพ์	2567

### บทคัดย่อ

การศึกษาสมบัติของเมฆในเขตร้อนและละติจูดกลางในช่วงที่มีค่า PM2.5 เกินค่ามาตรฐานในภูมิภาคที่แตกต่างกันในประเทศไทยและมหาวิทยาลัยแมนเชสเตอร์ โดยใช้ข้อมูลดาวเทียม Terra ตั้งแต่ปี ค.ศ. 2000–2022 และ ดาวเทียม Aqua ตั้งแต่ปี ค.ศ. 2002 –2022 เพื่อประเมินความเป็นไปได้ของเมฆฝนในช่วง PM2.5 สูงเกินค่ามาตรฐาน คุณสมบัติของเมฆที่ศึกษาได้แก่ เมฆปกคลุม (CF) ความลึกเชิงแสงของเมฆ (COD) ปริมาณน้ำในเมฆ (CLW) รัศมีหยดน้ำในเมฆ (CER) ความกดอากาศที่ยอดเมฆ (CTP) และอุณหภูมิที่ยอดเมฆ (CTT) จากการศึกษพบว่า ประเทศไทยมีค่า PM2.5 สูงในช่วงเดือนธันวาคมถึงเดือนเมษายน ส่วนมหาวิทยาลัยแมนเชสเตอร์มีค่า PM2.5 สูงในช่วงเดือนพฤศจิกายนถึงเดือนเมษายน นอกจากนี้ยังพบว่า คุณสมบัติของเมฆในช่วง PM2.5 สูง CF มีค่าน้อยกว่า 0.2 COD มีค่าน้อยกว่า 5.0 CLW มีค่าน้อยกว่า 50 g/m<sup>2</sup> CER มีค่าน้อยกว่า 15  $\mu\text{m}$  CTP มีค่ามากกว่า 800 hPa CTT มีค่ามากกว่า -15 °C การค้นพบนี้ช่วยให้เข้าใจคุณสมบัติของเมฆในช่วงที่มีค่า PM2.5 สูง เพื่อเป็นองค์ความรู้ประกอบการประเมินการเกิดเมฆฝนในช่วงที่มีค่า PM2.5 สูงเกินค่ามาตรฐาน นำไปสู่แนวทางในการแก้ปัญหาหมอกควันได้

คำสำคัญ: PM2.5 ฝุ่นละออง คุณสมบัติของเมฆ ข้อมูลดาวเทียม

<b>TITLE</b>	Tropical and Mid–latitude Cloud Properties during PM <sub>2.5</sub> Levels Exceeded the Standard in Different Climate: Thailand and UK using satellite data
<b>AUTHOR</b>	Oradee Pilahome
<b>ADVISORS</b>	Assist. Prof. Dr.Wilawan Kumhran
<b>DEGREE</b>	Ph.D. (Physics)
<b>INSTITUTION</b>	Sakon Nakhon Rajabhat
<b>YEAR</b>	2024

### ABSTRACT

A study of tropical and mid–latitude cloud properties during PM<sub>2.5</sub> exceeded the standard levels in different climates between Thailand and the University of Manchester by using data from the Terra satellite (2000–2022) and the Aqua satellite (2002–2022) for the possibility of rain clouds occurring. Cloud properties include cloud properties include cloud fraction (CF), cloud optical depth (COD), cloud liquid water path (CLW), cloud effective radius (CER), cloud top pressure (CTP), and cloud top temperature (CTT). It was found that PM<sub>2.5</sub> gave high values from December to April in Thailand. In contrast, high PM<sub>2.5</sub> values were detected from November to April at the University of Manchester station. This study showed that CF was less than 0.2, COD was less than 5.0, CLW was less than 50 g/m<sup>2</sup>, CER was less than 15 μm, CTP was more significant than 800 hPa, and CTT was greater than –15 °C during high PM<sub>2.5</sub> concentration. This finding may help to understand the properties of clouds during high PM<sub>2.5</sub> concentrations as knowledge for evaluating the occurrence of rain clouds during PM<sub>2.5</sub> values exceeding the standard levels. This finding can be a guideline for solving the haze problem in the future.

**Keywords:** PM<sub>2.5</sub>, Aerosol, Cloud properties, Satellite data

## LIST OF CONTENTS

CHAPTER	Page
I	INTRODUCTION ..... 1
	STATEMENT AND SIGNIFICANCE OF THE PROBLEMS..... 1
	RESEARCH OBJECTIVES .....2
	SCOPE OR LIMITATION OF THE STUDY .....3
	EXPECTED BENEFITS .....3
II	THEORY AND LITERATURE REVIEW.....4
	THEORY ..... 4
	Layers of Earth's Atmosphere .....4
	Cloud Formation Processes and Classification of Cloud..... 7
	Cloud condensation nuclei..... 7
	Cloud Classifications and Characteristics.....9
	Cloud formation processes..... 14
	From Cloud to Rain ..... 17
	PM2.5..... 18
	LITERATURE REVIEW..... 19
III	RESEARCH METHODOLOGY .....22
	RESEARCH INSTRUMENT .....22
	Satellite data .....22
	DATA COLLECTION .....24
	1. Study Area.....24
	2. Sensor and PM2.5 data ..... 29
	ANALYSIS.....32

## LIST OF CONTENTS (continued)

CHAPTER	Page
IV	RESULTS ..... 35
	1. VARIATIONS IN AEROSOL PARTICLE AND CLOUD PROPERTIES IN THAILAND ..... 35
	1.1 Aerosol particle ..... 35
	1.2 Cloud properties ..... 41
	2. VARIATIONS IN AEROSOL PARTICLE AND CLOUD PROPERTIES IN THE UNIVERSITY OF MANCHESTER ..... 53
	2.1 Aerosol particle ..... 53
	2.2 Cloud properties ..... 55
	3. DISTRIBUTION OF CLOUD PROPERTIES IN THAILAND AND THE UNIVERSITY OF MANCHESTER ..... 56
	3.1 Thailand ..... 56
	3.2 The University of Manchester ..... 62
	4. CLOUD PROPERTIES IN DIFFERENT CLIMATES (BANGKOK AND THE UNIVERSITY OF MANCHESTER) ..... 64
	5. ASSESS THE POSSIBILITY OF RAIN CLOUDS IN THE DUST PERIOD, PM <sub>2.5</sub> IS HIGHER THAN THE STANDARD ..... 67
V	CONCLUSION ..... 72
	REFERENCES ..... 76
	APPENDICE ..... 79
	APPENDICE A DATA ..... 80
	APPENDICE B CONFERENCE ..... 90



**LIST OF CONTENTS (continued)**

<b>CHAPTER</b>	<b>Page</b>
APPENDICE C PAPER ONLINE.....	93
APPENDICE D SHORT-TERM RESEARCH .....	112
APPENDICE E A BRIEF HISTORY OF RESEARCHER.....	115

## LIST OF TABLES

TABLE	Page
1 Air quality standards for PM <sub>2.5</sub> set by the NATIONAL ENVIRONMENT BOARD, the European Union (EU), and the WHO Air Quality Guidelines (AQG). .....	19
2 Shown the station name in the study area. ....	24
3 Show the basic data of Aerosol Product. ....	29
4 Show the basic data of Cloud Products. ....	30
5 Shows a comparison of cloud properties during the high PM <sub>2.5</sub> and rainy seasons. ....	69

## LIST OF FIGURES

FIGURE	Page
1	Vertical temperature profile after the U.S. Standard Atmosphere and definitions of atmospheric nomenclature. (Liou, 2002) ..... 4
2	Troposphere Diagram.....5
3	Stratosphere Diagram.....6
4	Mesosphere diagram .....6
5	CCN particle count $n$ vs. radius $R$ , for $c = 2,000,000 \mu\text{m}^3/\text{m}^3$ . (Stull, 2016) .....8
6	Cirrus Clouds Photographed by Lisa Gardiner (UCAR, 2023) ..... 10
7	Cirrocumulus clouds Photographed by UCAR ..... 10
8	Cirrostratus clouds Photographed by Anne Pharamond ..... 11
9	Altostratus cloud Photographed by UCAR.....11
10	Altostratus cloud Photographed by Keith G. Diem..... 12
11	Stratus cloud Photographed by Sara Martin ..... 13
12	Stratocumulus clouds Photographed by Carlye Calvin/UCAR..... 13
13	Nimbostratus clouds Photographed by Peggy LeMone..... 14
14	Size comparison for PM particles ..... 19
15	Satellite a. Terra Satellite and b. Aqua Satellite (a. NASA (2023a) and b. iSTAR (2023) .....23
16	MODIS sensor.....23
17	Thailand map is divided into 7 regions. .... 28
18	The United Kingdom map is the University of Manchester ..... 28
19	A website for downloading PM2.5 data from the Pollution Control Department..... 31
20	A website for downloading PM2.5 data from the Climate Change Data Center of Chiangmai University ..... 31
21	A website for downloading PM2.5 data from the CEDA.....32

## LIST OF FIGURES (continued)

FIGURE	Page
22	Time series of the monthly mean AOD derived from Terra satellite data in Thailand..... 36
23	Time series of the monthly mean AOD derived from Aqua satellite data in Thailand.....37
24	Time series of the monthly mean AE derived from Terra satellite data in Thailand..... 38
25	Time series of the monthly mean AE derived from Aqua satellite data in Thailand..... 39
26	Time series of the monthly mean PM2.5 in Thailand.....40
27	Time series of the monthly mean CF derived from Terra satellite data in Thailand..... 41
28	Time series of the monthly mean CF derived from Aqua satellite data in Thailand.....42
29	Time series of the monthly mean CER derived from Terra satellite data in Thailand.....43
30	Time series of the monthly mean CER derived from Aqua satellite data in Thailand..... 44
31	Time series of the monthly mean COT derived from Terra satellite data in Thailand.....45
32	Time series of the monthly mean COT derived from Aqua satellite data in Thailand.....46
33	Time series of the monthly mean CWP derived from Terra satellite data in Thailand..... 47
34	Time series of the monthly mean CWP derived from Aqua satellite data in Thailand.....48

## LIST OF FIGURES (continued)

FIGURE	Page
35	Time series of the monthly mean CTP derived from Terra satellite data in Thailand.....49
36	Time series of the monthly mean CTP derived from Aqua satellite data in Thailand..... 50
37	Time series of the monthly mean CTT derived from Terra satellite data in Thailand..... 51
38	Time series of the monthly mean CTT derived from Aqua satellite data in Thailand.....52
39	Time series of monthly mean AOD derived from Terra and Aqua satellite data at The University of Manchester..... 53
40	Time series of monthly mean AE derived from Terra and Aqua satellite data at The University of Manchester.....54
41	Time series of monthly mean PM <sub>2.5</sub> derived from ground-based in The University of Manchester from 2019 to 2022.....54
42	Time series of monthly mean CF, COT, CTP, CTT, CER, and CWP derived from Terra and Aqua satellite data at The University of Manchester. .... 56
43	Distribution of cloud properties in Bangkok using Terra satellite data. .... 58
44	Distribution of cloud properties in Bangkok using Aqua satellite data. .... 59
45	Distribution of cloud properties in the University of Manchester using Terra satellite data..... 63
46	Distribution of cloud properties in the University of Manchester using Aqua satellite data.....64
47	The relationship between cloud properties in Bangkok and the University of Manchester using Terra satellite data..... 66
48	The relationship between cloud properties in Bangkok and the University of Manchester using Aqua satellite data.....67

**LIST OF FIGURES (continued)**

<b>FIGURE</b>		<b>Page</b>
49	Time series of the monthly mean high PM 2.5 levels in the northern region during the month of December to February. ....	68
50	Time series of the monthly mean high PM 2.5 levels in the central and Northeastern region during the months of December to February. ....	68
51	Distribution of cloud properties in Bangkok during high PM2.5 .....	69

## CHAPTER I

### INTRODUCTION

#### STATEMENT AND SIGNIFICANCE OF THE PROBLEMS

Aerosol particles are solid or liquid particles suspended in atmospheric aerosols which can occur spontaneously and arise from various human activities. The direct aerosol effect is their influence on the amount of solar radiation leaving/entering the Earth's atmosphere. The indirect effects of aerosols, known as cloud condensation nuclei (CCN) – act as a seed of cloud. Therefore, atmospheric aerosol influences cloud properties (Kumharn, 2016). The basis of cloud properties is essential for studying anthropogenic impacts and climate change. Cloud properties affect the rain cycle and climate change, negatively impacting human health and the environment (Gauderman et al., 2002). Increased anthropogenic aerosol emissions led to the radiative forcing associated with cloud albedo, which is the critical driver of effective radiative forcing due to aerosol–cloud interactions. An increase in cloud lifetime may come from CNN obtained from anthropogenic pollution, increasing the amount of solar radiation reflected from clouds (Albrecht., 1989). Low clouds with small liquid water paths are observed in high accumulation mode aerosols, related to the cloud droplets having a smaller effective radius, providing the clouds with higher emissivity (Garreatt & Zhao, 2006). Therefore, increased PM<sub>2.5</sub> levels can enhance CCN concentrations and the density of cloud droplets. Subsequently, the droplet size declines, and the cloud albedo increases, leading to a constant liquid water content (IPCC. (2007).

Satellite data are currently being used to study dust and cloud properties using data from Terra and Aqua satellites equipped with Moderate–resolution Imaging Spectroradiometer sensors. The information obtained from satellites helps monitor various situations at the regional level every day Because MODIS satellite images

have a wide range of imaging that can cover the whole of Thailand in a single shot. Including having many imaging bands, it can be analyzed in many ways with detailed information from 250 to 1,000 meters. Terra satellite will orbit from the North Pole to the South Pole. Via Thailand from 9:30 a.m. – 11:30 a.m. (morning) and Aqua satellite. This work used Aerosol Products) Collection 6.1 Level 2 (MOD04\_L2 for Terra and MYD04\_L2 for Aqua) with the spatial resolution of a 10x10 1-km pixel array (at nadir) (Pilahome et al., 2023) and Cloud properties, including Cloud Fraction, Cloud Effective Radius, Cloud Optical Thickness, Cloud Water Path, Cloud Top Pressure, and Cloud Top Temperature, determine physics and radiative cloud properties and illustrate Earth's upper-air atmosphere state. Cloud Product Collection 6.1 Level 2 (MOD06\_L2 for Terra and MYD06\_L2 for Aqua) has a spatial resolution of 1 km or 5 km (at the nadir).

Consequently, this research investigated cloud properties, including cloud fraction, effective cloud radius, cloud optical thickness, cloud water path, cloud top pressure, and cloud top temperature in different climates, using satellite data as time and spatial changes. Furthermore, to assess the possibility of rain clouds during the PM2.5 exceeds the standard in Thailand.

## RESEARCH OBJECTIVES

1. To study the climate and cloud properties in different climates.
2. To examine cloud variations in the tropics.
3. To evaluate the types and structures of clouds in different climates.
4. To investigate cloud properties in different climates.
5. To assess the possibility of rain clouds in the dust period, PM2.5 is higher than the standard.
6. To broadcast and disseminate works at the national/ international level.



## **SCOPE OR LIMITATION OF THE STUDY**

This study investigated the properties of clouds (cloud optical depth, effective cloud radius, cloud fraction, cloud water path, cloud top temperature, and cloud fraction) using Terra and Aqua satellite data in different climates during high PM<sub>2.5</sub> concentrations: Thailand and the UK.

## **EXPECTED BENEFITS**

1. Knowledge cloud properties during high PM<sub>2.5</sub> concentrations.
2. It is a guideline for solving the haze crisis in Thailand.

## CHAPTER II

### THEORY AND LITERATURE REVIEW

#### THEORY

##### Layers of Earth's Atmosphere

Each stratum in the Earth's atmosphere has unique characteristics. These levels, which rise from the Earth's surface, are known as the troposphere (0–12 km), stratosphere (12–50 km), mesosphere (50–85 km), and thermosphere (>85 km). The outermost region of the atmosphere above the thermosphere is called the exosphere, as shown in Figure 1.

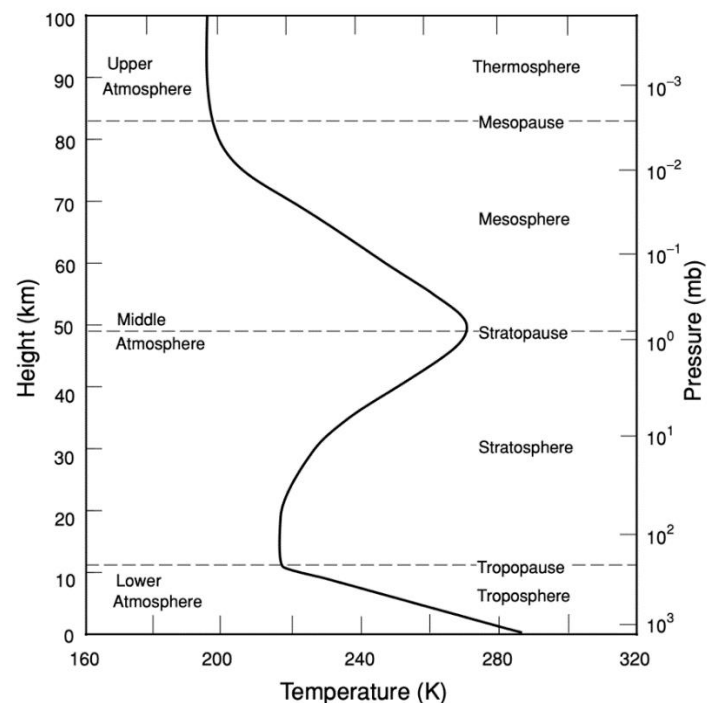


Figure 1 Vertical temperature profile after the U.S. Standard Atmosphere and definitions of atmospheric nomenclature. (Liou, 2002)

The troposphere is the lowest atmospheric stratum, shown in Figure 2. Humans reside in the troposphere, where virtually all weather phenomena occur, and 99% of the atmospheric water vapor is in the troposphere, where clouds form. As one ascends higher into the troposphere, air pressure decreases, and temperatures fall.

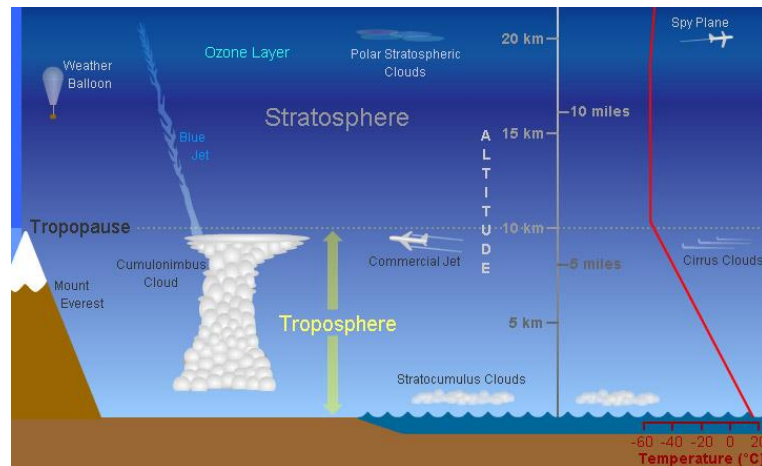


Figure 2 Troposphere Diagram

The stratosphere contains the famed ozone layer, shown in Figure 3. Ozone molecules absorb high-intensity ultraviolet (UV) light from the Sun in this layer, turning UV energy into heat. In contrast to the troposphere, the stratosphere warms up as it ascends! The stratosphere's air lacks the turbulence and updrafts that characterize the troposphere below due to the trend of rising temperatures with altitude. Commercial passenger planes travel in the lower stratosphere because they offer a smoother ride and have less turbulence. The troposphere–stratosphere boundary is where the jet stream passes.

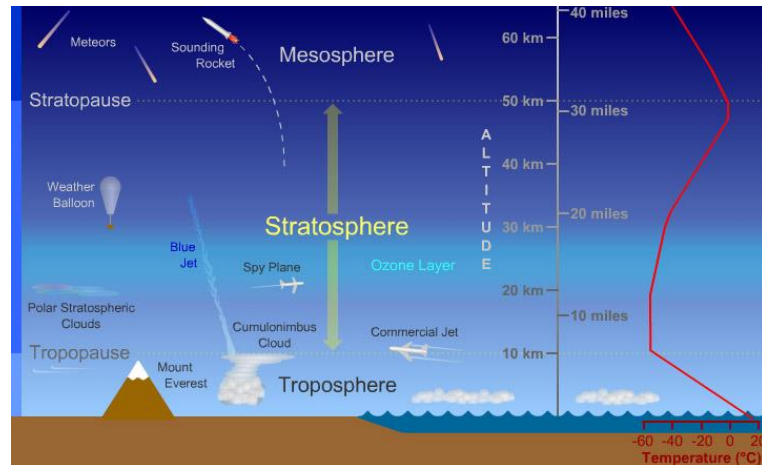


Figure 3 Stratosphere Diagram

The mesosphere is where most meteors burn up, as shown in Fig 4. As you ascend through the mesosphere, temperatures drop again, contrasting with the stratosphere. Near the top of this layer, temperatures as low as  $-90^{\circ}\text{C}$  ( $-130^{\circ}\text{F}$ ) are recorded in the Earth's atmosphere. The air pressure in the mesosphere is far too low to allow for breathing (it starts at well below 1% of sea level and becomes lower as you go higher).

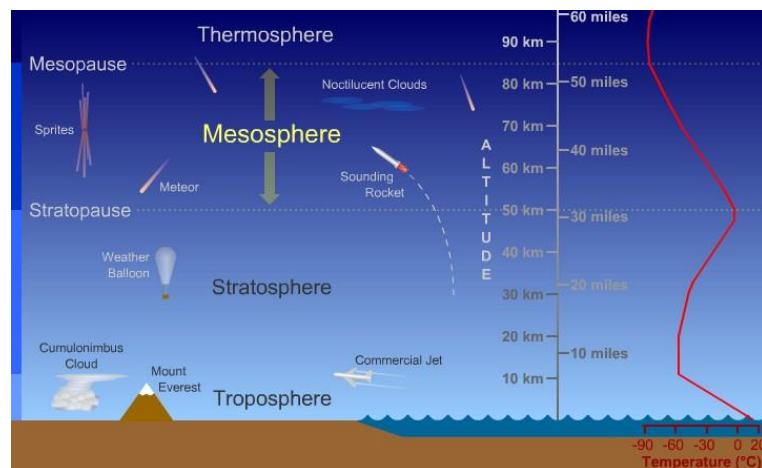


Figure 4 Mesosphere diagram

Although some experts consider the thermosphere the highest stratum of Earth's atmosphere, others consider the exosphere the "final frontier" of the planet's

gaseous envelope. Exospheric "air" is extremely thin, making this layer even more space like than the thermosphere. In actuality, the air in the exosphere is continuous albeit very progressively – "leaking" from the Earth's atmosphere into space. There is no distinct upper limit at which the exosphere gradually dissipates into space.

### **Cloud Formation Processes and Classification of Cloud**

A cloud is a type of hydrometeor comprising tiny particles of ice, liquid water, or a combination of the two (WMO, 2017). These particles are suspended in the air and do not typically contact the ground below them. It can also contain bigger particles of liquid water or ice and non-aqueous liquid or solid particles, such as fumes, smoke, or dust. Nowadays, various human activities have modified the properties of clouds, Affecting the rainwater cycle and climate change.

Can you classify clouds based on their shape and height? Most clouds are divided into groups based on the height of the cloud base above the Earth's surface, while others are based on specific characteristics such as cloud formation.

### **Cloud condensation nuclei**

An aerosol is any tiny solid or liquid particle suspended in the air. The subset of aerosol particles that can nucleate cloud droplets is called cloud condensation nuclei (CCN). To nucleate a droplet, a solid aerosol must either be soluble in water (such as various salt particles) or sufficiently large in diameter (radius > 0.1  $\mu\text{m}$ ) and have a wettable surface (i.e., be hydrophilic).

Boundary-layer air over oceans has smaller concentrations of aerosols than continental air. Over oceans, of the 150 to 1000 total aerosol particles/cm<sup>3</sup> of air, only about 90 to 200 particles/cm<sup>3</sup> are CCN at average relative humidity (RH  $\approx$  101%) inside clouds. Over continents, of the 2,000 to 70,000 total aerosol particles/cm<sup>3</sup> of air, only about 200 to 700 particles/cm<sup>3</sup> are CCN. At higher relative humidities, more significant percentages of aerosols act as CCN. Exceptionally clean air over the Arctic

can have only 30 CCN particles/cm<sup>3</sup>; over industrial cities, the CCN count can approach 10<sup>6</sup> particles/cm<sup>3</sup>.

CCN particles can form when pollutant gases (of molecular size 10 to 10<sup>-3</sup> μm) in the air cluster form ultrafine aerosols (size 10<sup>-3</sup> to 10<sup>-2</sup> μm) or are oxidized in sunlight. Over the oceans, sulfate and sulfuric acid CCN can form this way from gases such as dimethyl sulfide and methane sulfonic acid, produced by phytoplankton (microscopic drifting plant life in the ocean).

Further condensation of more pollutant gases and coagulation (sticking together) cause the aerosols to quickly grow to 0.01 to 1 μm size, called fine aerosols. Beyond this size range they grow more slowly. As a result, aerosols in this size range tend to accumulate — a process called accumulation mode. At larger 1 to 10 μm sizes, coarse mode CCN can form by other processes, such as strong winds that pick up fine dirt from the ground.

Small nuclei are much more abundant than larger ones (thin, wiggly line in Figure 5. Instead of a smooth decrease in the number of particles as their size increases, the aerosol curve often has two or three peaks corresponding to the ultrafine, accumulation, and coarse modes.

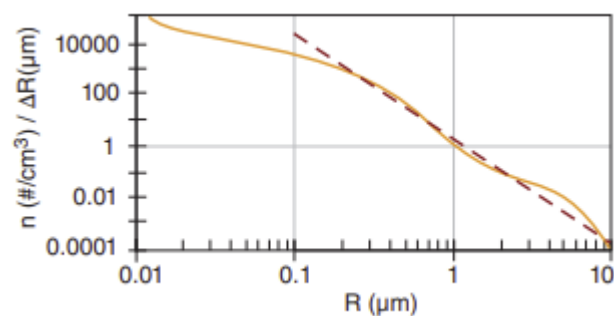


Figure 5 CCN particle count  $n$  vs. radius  $R$ , for  $c = 2,000,000 \mu\text{m}^3/\text{m}^3$ . (Stull, 2016)

Over continental regions, the number density ( $n$  = count of particles per volume of air) of particles with radius between  $R - 0.5 \cdot \Delta R$  and  $R + 0.5 \cdot \Delta R$  can be approximated by:

$$n(R) = c \cdot R^{-4} \cdot \Delta R \quad (1)$$

for particles larger than 0.2  $\mu\text{m}$ , and for small  $\Delta R$ . Constant  $c$  depends on the total concentration of particles. This distribution called the Junge distribution, is the dashed straight line in Figure 5.

### Cloud Classifications and Characteristics

Classify clouds based on their shape and height. Most clouds are divided into groups based on the height of the cloud base above the Earth's surface, while other clouds are based on specific cloud characteristics such as cloud formation.

#### 1. Cloud types based on their appearance and shape

Clouds are formed in 2 features: Cumuliform cloud and Stratiform.

– Cumuliform cloud called "Cumulus" if the clouds float close together. We put the two names together called "Stratocumulus" in the case of a rain cloud add the word "nimbo" or "nimbus" which means "rain" calling the clouds that cause rainstorms. thunder that "Cumulonimbus".

– Stratiform clouds are known as "Stratus". Stratiform clouds with peaceful drizzle are called Nimbostratus clouds.

#### 2. Cloud types according to height

– High cloud

The prefix "cirro" is applied to clouds that exist above approximately 20,000 feet. As a result of the frigid tropospheric temperatures at these altitudes, the clouds are composed primarily of ice crystals and frequently appear thin, streaky, and white. (although a low sun angle, e.g., near sunset, can create an array of colors on the clouds). Cirrus (Figure 6), cirrostratus (Figure 7), and cirrocumulus (Figure 8) are the three primary varieties of high clouds.



Figure 6 Cirrus Clouds Photographed by Lisa Gardiner (UCAR, 2023)

Cirrus clouds are composed of ice crystals and appear in the sky as long, thin, feathery white ribbons. They are commonly known as "mare's tails" due to their resemblance to a horse's tail. Cirrus clouds are frequently observed during sunny weather. However, if they continue to grow and are followed by cirrostratus clouds, a warm front may be approaching.



Figure 7 Cirrocumulus clouds Photographed by UCAR

Cirrocumulus clouds are small, round, high-altitude clouds that appear in continuous chains. Cirrocumulus are typically white but can occasionally appear gray. They are the same width or smaller than your smallest finger when your hand is held at arm's length. Cirrocumulus are prevalent in the winter and signal cloudy, chilly conditions.





Figure 8 Cirrostratus clouds Photographed by Anne Pharamond

– Middle cloud

The prefix "alto-" refers to the appearance of cloud bases in the middle troposphere, which are located between 6,500 and 20,000 feet. These clouds may consist of liquid water droplets, ice crystals, or a combination of the two, including supercooled droplets (i.e., liquid droplets with temperatures below freezing), depending on the altitude, season, and vertical temperature structure of the troposphere. In terms of mid-level clouds, altostratus (Figure 9) and altocumulus (Figure 10) are the two types.



Figure 9 Altocumulus cloud Photographed by UCAR

Altocumulus clouds are mid-level, grayish-white, with one part darker than the other. Typically formed in groups, altocumulus clouds are a kilometer thick. When you hold up your hand at arm's length, the width of an altocumulus cloud is about the same as your thumb. On a hot, muggy morning, there can be a thunderstorm by late afternoon if you notice altocumulus clouds.



Figure 10 Altostratus cloud Photographed by Keith G. Diem

Altostratus clouds are mid-level, gray or blue-gray clouds that usually cover the whole sky. An altostratus cloud can let the Sun or Moon show through, although it will look watery or fuzzy. Altostratus clouds indicate the possibility of a storm with persistent rain or snow. On rare occasions, an altostratus cloud will produce rain. When rain falls to the earth, the cloud transforms into a nimbostratus.

– Low cloud

Low-level clouds are not given a prefix, although their names are derived from "strato-" or "cumulo-", depending on their characteristics. Low clouds are those that are less than 6500 feet in altitude and are typically made up of liquid water droplets or even supercooled droplets, apart from icy winter storms when ice crystals (and snow) make up the majority of the clouds. The two primary varieties of low clouds are stratus (Figure 11), which grows vertically, and stratocumulus (Figure 12), which grows horizontally.



Figure 11 Stratus cloud Photographed by Sara Martin

Stratus clouds are low and have a uniform gray in color and can cover most or all the sky. Sometimes stratus clouds can resemble a groundless fog. There may occasionally be a light mist or drizzle when stratus clouds are present.



Figure 12 Stratocumulus clouds Photographed by Carlye Calvin/UCAR

Stratocumulus clouds are low, lumpy, and gray. They sometimes arrange themselves in rows and other times they are dispersed. Stratocumulus clouds only produce mild rain, which usually falls as drizzle. Point your hand in the direction of the cloud to tell a stratocumulus cloud from an altocumulus cloud. It is a stratocumulus cloud if it is roughly the size of your fist.



Figure 13 Nimbostratus clouds Photographed by Peggy LeMone

Nimbostratus clouds feature ragged bases, are dark gray in color, and are low in the sky (Figure 13). Continuous rain or snow is a characteristic of nimbostratus clouds. Sometimes they fill the entire sky, making it impossible to see the cloud borders.

### **Cloud formation processes**

The process of cloud formation begins with the condensation of suspended water particles and ice crystals. Some amount of invisible water vapor is always present in the air, and this invisible water vapor is the first phase in the process of cloud formation. Condensation of water vapor occurs because of a decrease in temperature, causing the vapor to transform into a liquid. The air in this region is saturated with water vapor, resulting in the formation of clouds.

#### **1. Growth of cloud particles**

Cloud particle growth refers to the process by which tiny water droplets or ice crystals in the atmosphere increase in size through various mechanisms. Cloud particles typically start as very small condensation nuclei, such as dust, pollen, or other aerosols, upon which water vapor condenses or freezes. As these particles grow, they eventually become large enough to fall as precipitation. Several processes contribute to the growth of cloud particles:

Condensation: Water vapor in the air condenses onto the surfaces of aerosol particles, forming tiny water droplets. This process is crucial in the initial formation of clouds.

Collision–Coalescence: Cloud droplets collide with each other, and when they collide, they may coalesce, or join, forming larger droplets. This process is particularly important in warm clouds where droplets are larger, and collisions occur more frequently.

Collection: Larger cloud droplets or ice crystals may collect smaller droplets or ice crystals as they fall through the cloud. This process, known as collection or aggregation, contributes to the growth of precipitation particles.

Ice Nucleation: In clouds that are cold enough, water droplets may freeze to form ice crystals. These ice crystals can grow through the deposition of water vapor directly onto their surfaces.

Riming: In certain conditions, such as in mixed–phase clouds where both supercooled water droplets and ice crystals coexist, ice crystals may grow by colliding with and accreting onto supercooled droplets. This process, known as riming, can rapidly increase the size of ice particles.

Growth by Vapor Deposition: Ice crystals can grow through the deposition of water vapor directly onto their surfaces, especially in supersaturated environments.

The growth of cloud particles is influenced by various factors including temperature, humidity, and the presence of aerosols. Different types of clouds and atmospheric conditions lead to variations in the mechanisms and rates of particle growth, ultimately impacting cloud dynamics and precipitation processes.

## 2. Cloud properties

Cloud properties include Cloud Fraction, Cloud Effective Radius, Cloud Optical Thickness, Cloud Liquid Water Path, Cloud Top Temperature, and Cloud Top Pressure.

2.1. Cloud Fraction (CF) refers to the proportion of each pixel or grid box in a weather or climate model that is covered by clouds. A cloud fraction of one indicates that the pixel is completely covered with clouds, while a fraction of zero indicates that the pixel is cloud-free (NASA, 2023c).

2.2. Cloud Effective Radius (CER) is a weighted mean of the cloud particle size distribution (NASA, 2023b). It is a physically weighted radius of cloud droplets. This is mathematically expressed as:

$$r_e = \frac{\int_0^{\infty} r^3 n(r) dr}{\int_0^{\infty} r^2 n(r) dr} \quad (2)$$

Where  $r_e$  is Cloud effective radius ( $\mu\text{m}$ ).

$r$  is particle radius.

$n(r)$  is particle size distribution (number of particles per  $\text{cm}^2$  with radius in the range  $r$  and  $r + dr$   $\mu\text{m}$ ).

2.3. Cloud Optical Thickness (COT) is a measurement of the light attenuation caused by the scattering and absorption of cloud droplets. Instead of absorbing visible wavelengths of sunlight, clouds scatter and reflect the most visible light.

2.4. Cloud Liquid Water Path (LWP) is measure of the weight of the liquid water droplets in the atmosphere above a unit surface area on the earth, given in units of  $\text{kg}/\text{m}^2$  or  $\text{g}/\text{m}^2$  (NCAR, 2023). This variable is essential for determining the type of cloud present. Identifying cloud varieties is extremely beneficial for weather forecasting. Cumulonimbus clouds are associated with thunderstorms and torrential precipitation. Even though cirrus clouds are not directly proportional to the quantity of precipitation. It can be calculated using the equation(AMS, 2023):

$$\text{LWP} = \int \rho_{\text{air}} r_L dz \quad (3)$$

Where  $\text{LWP}$  is liquid water path

$\rho_{\text{air}}$  is the density of the (wet) air

$r_L$  is the liquid water mixing ratio

The liquid water path also contributes to important cloud properties. As the value of the liquid water path increases, the albedo of the cloud also increases. This increase in albedo occurs most rapidly at the lower end of the liquid water path spectrum, i.e., as the total volume of water decreases, the albedo rises more rapidly. Clouds' radiative absorption is also dependent on the path of liquid water. An increase in the liquid water path causes a rise in absorption. Again, the greatest increase is observed at lower liquid water path levels (Hartmann, 2016).

2.5. Cloud Top Temperature (CTT) refers to the temperature at the uppermost portion of a cloud, typically measured in the troposphere, which is the lowest layer of the Earth's atmosphere where most weather phenomena occur. CTT is an essential parameter used in meteorology and remote sensing to characterize clouds and infer information about their properties and behavior.

2.6. Cloud Top Pressure (CTP) refers to the atmospheric pressure at the uppermost portion of a cloud, usually measured in the troposphere, the lowest layer of the Earth's atmosphere. Like Cloud Top Temperature (CTT), CTP is an essential parameter in meteorology and remote sensing to characterize clouds and infer information about their properties and behavior.

### **From Cloud to Rain**

The transition from clouds to rain involves several steps in the atmospheric process.

Cloud Formation: Clouds are formed when water vapor in the atmosphere condenses into tiny water droplets or ice crystals around tiny particles such as dust, pollen, or smoke. This process typically occurs as air rises, cools, and reaches its dew point, the temperature at which the air becomes saturated with water vapor.

Cloud Growth: Within clouds, water droplets or ice crystals continue to collide and combine through a process called coalescence or aggregation. As these particles collide and merge, they grow larger in size. The larger the particles become, the more likely they are to fall out of the cloud.

Precipitation Formation: When cloud droplets or ice crystals grow too heavy to remain suspended in the air, they begin to fall toward the Earth's surface. The form of precipitation (rain, snow, sleet, or hail) depends on the temperature profile through which the precipitation falls.

Rain Formation: In the case of rain, water droplets within the cloud continue to collide and merge until they reach a size where air resistance can no longer keep them aloft. These larger droplets fall as rain. The intensity of rain can vary based on factors such as the size of the droplets and the speed at which they fall.

Rainfall: Once the water droplets reach the Earth's surface, they become what we commonly refer to as rain. The rate and duration of rainfall depend on various atmospheric conditions, such as the size of the cloud, the intensity of updrafts and downdrafts within the cloud, and the presence of atmospheric disturbances.

Replenishment: The water that falls as rain contributes to the Earth's water cycle. Some of it infiltrates into the ground to replenish groundwater, some is absorbed by vegetation, and some runs off into rivers, lakes, and oceans, eventually evaporating back into the atmosphere to begin the cycle anew.

Overall, the transformation from clouds to rain is a crucial aspect of the Earth's hydrological cycle, playing a significant role in weather patterns and the distribution of water across the planet.

## **PM2.5**

PM stands for particulate matter (also called particle pollution) the term for a mixture of solid particles and liquid droplets found in the air. Some particles, such as dust, dirt, soot, or smoke, are large or dark enough to be seen with the naked eye. Others are so small that they can only be detected using an electron microscope.



Particle pollution includes:

- PM10 inhalable particles, with diameters that are generally 10 micrometers and smaller.
- PM2.5 fine inhalable particles, with diameters that are generally 2.5 micrometers and smaller.

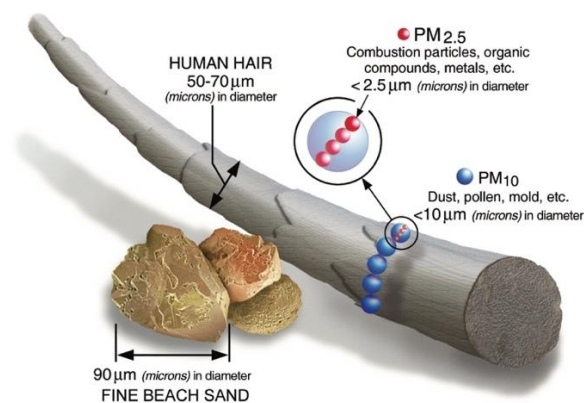


Figure 14 Size comparison for PM particles

Table 1 Air quality standards for PM2.5 set by the NATIONAL ENVIRONMENT BOARD, the European Union (EU), and the WHO Air Quality Guidelines (AQG).

Pollutant	Thailand		WHO (AQG)		EU standard	
	Annual	24 hours	Annual	24 hours	Annual	24 hours
PM2.5	25	50	10	25	25	n/a

## LITERATURE REVIEW

Cloud properties have been retrieved from the Moderate Resolution Imaging Spectroradiometer (MODIS) over 12 years of continuous observations from Terra and over nine years from Aqua. Results include the spatial and temporal distribution of cloud fraction, the cloud top pressure and cloud top temperature, and the cloud optical thickness and effective radius of both liquid water and ice clouds.

Globally, the cloud fraction derived by the MODIS cloud mask is  $\sim 67\%$ , with somewhat more clouds over land during the afternoon and less clouds over ocean in the afternoon, with very little difference in global cloud cover between Terra and Aqua. Overall, the cloud fraction over land is  $\sim 55\%$ , with a distinctive seasonal cycle, whereas the ocean cloudiness is much higher, around  $72\%$ , with much reduced seasonal variation. Aqua and Terra have comparable zonal cloud top pressures, with Aqua having somewhat higher clouds (cloud top pressures lower by  $100\text{ hPa}$ ) over land due to afternoon deep convection. The coldest cloud tops (colder than  $230\text{ K}$ ) generally occur over Antarctica and the high clouds in the tropics. The cloud effective particle radius of liquid water clouds is significantly larger over ocean (mode  $12\text{--}13\ \mu\text{m}$ ) than land (mode  $10\text{--}11\ \mu\text{m}$ ), consistent with the variation in hygroscopic aerosol concentrations that provide cloud condensation nuclei necessary for cloud formation. We also find the effective radius to be  $2\text{--}3\ \mu\text{m}$  larger in the southern hemisphere than in the northern hemisphere, likely reflecting differences in sources of cloud condensation nuclei. (King et al., 2013).

Fan et al. (2020) Study the dependence of rain intensity on cloud properties for marine boundary layer water clouds over the Southern Hemisphere Ocean. Found that rain is sharply intensified when droplets at the cloud top grow larger than  $14\ \mu\text{m}$ , and precipitation decreases with increasing cloud drop number concentration ( $N_d$ ). A simple framework to explain the relationship between precipitation and aerosols is proposed here by showing the dependence of precipitation on  $N_d$  and cloud geometric thickness. We also discussed why using aerosol optical depth (AOD) as CCN proxy in previous studies could lead to great uncertainties and why sorting cloud geometrical thickness is necessary.

Koren et al. (2012) Examine the relationship between aerosol abundance and rain rate key factor in climate and hydrological processes rain data from a satellite-based instrument sensitive to stronger rain rates (Tropical Rainfall Measuring Mission<sup>3</sup>, TRMM), aerosol and cloud property data from the Moderate Resolution Imaging Spectroradiometer onboard the Aqua satellite and meteorological information

from the Global Data Assimilation System. We show that for a range of conditions, increases in aerosol abundance are associated with the local intensification of rain rates detected by the TRMM. The relationship is apparent over both the ocean and land and, in the tropics, subtropics, and mid-latitudes. Further work is needed to determine how aerosols influence weaker rain rates, not picked up in the analysis. We also find that increases in aerosol levels are associated with a rise in cloud-top height. We suggest that the invigoration of clouds and the intensification of rain rates is a preferred response to an increase in aerosol concentration.

## CHAPTER III

### RESEARCH METHODOLOGY

This chapter presents the step detail of the study Aerosol, cloud properties (Cloud Fraction, Cloud Effective Radius, Cloud Optical Thickness, Cloud Water Path, Cloud Top Pressure, and Cloud Top Temperature), and PM<sub>2.5</sub> in Thailand and the University of Manchester were studied. Using satellite data from Terra and Aqua, details of the study process are as follows.

#### RESEARCH INSTRUMENT

The data used in this research was obtained from satellite data. Most of the data obtained from satellites are radar and infrared images. Since satellites can cover a large area at once, they can continuously measure both during the day and at night. Data resolution part: The spatial and radiographic resolutions depend on the device's capabilities and the area's elevation.

##### **Satellite data**

MODIS (Moderate resolution Imaging Spectroradiometer) is a key instrument aboard the Terra (originally known as EOS AM-1) is shown in Figure 15a. and Aqua (originally known as EOS PM-1) is shown in Figure 15b. satellites. Terra's orbit around the Earth is timed so that it passes from north to south across the equator in the morning, while Aqua passes south to north over the equator in the afternoon. Terra MODIS and Aqua MODIS view the entire Earth's surface every 1 to 2 days, acquiring data in 36 spectral bands or groups of wavelengths. These data will improve our understanding of global dynamics and processes occurring on land, in the oceans, and in the lower atmosphere. MODIS (shown in Figure 16) plays a vital role in developing validated, global, interactive Earth system models able to accurately

predict global change enough to assist policymakers in making sound decisions concerning protecting our environment. (NASA (2023d)). In this research, we will use 2 products from MODIS, namely Aerosol Product and Cloud Product.

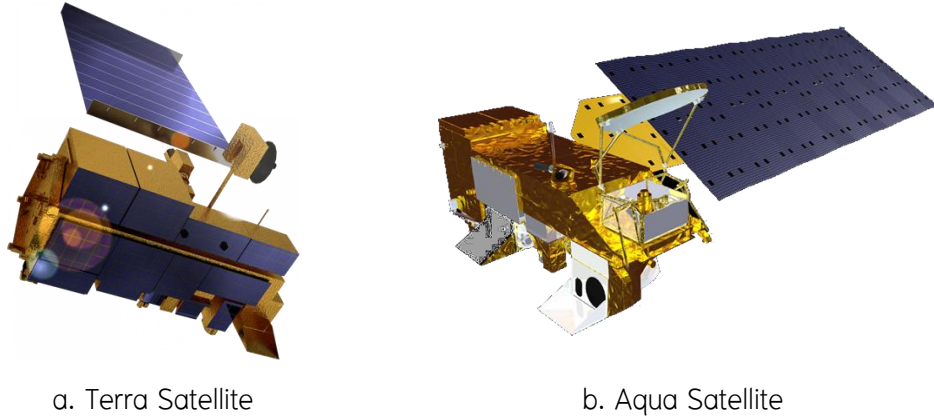


Figure 15 Satellite a. Terra Satellite and b. Aqua Satellite (a. NASA (2023a) and b. iSTAR (2023))

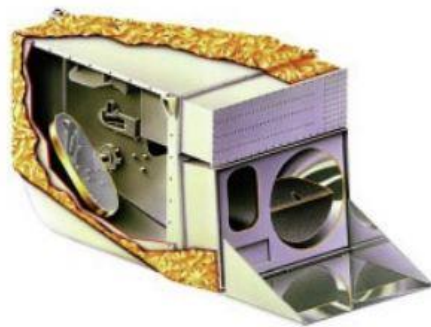


Figure 16 MODIS sensor

### 1. Aerosol Product

The MODIS Aerosol Product monitors the ambient aerosol optical thickness over the oceans globally and over the continents. Furthermore, the aerosol size distribution is derived over the oceans, and the aerosol type is derived over the continents. “Fine” aerosols (anthropogenic/pollution) and “course” aerosols (natural particles, e.g., dust) are also derived. Daily Level 2 data are produced at the spatial resolution of a  $10 \times 10$  1-km (at nadir) pixel array. The aerosol product includes the

“deep–blue” algorithm recently developed to get aerosol optical thickness over bright land areas (NASA (2023e)). There are two MODIS Aerosol data product files: MOD04\_L2, containing data collected from the Terra platform; and MYD04\_L2, containing data collected from the Aqua platform.

## 2. Cloud Product

The MODIS Cloud Product combines infrared and visible techniques to determine both physical and radiative cloud properties. Daily global Level 2 data is provided. Cloud–particle phase (ice vs. water, clouds vs. snow), effective cloud–particle radius, and cloud optical thickness are derived using the MODIS visible and near–infrared channel radiances. An indication of cloud shadows affecting the scene is also provided. Cloud–top temperature, height, effective emissivity, phase (ice vs. water, opaque vs. non–opaque), and cloud fraction are produced by the infrared retrieval methods both day and night at 5x5 1–km–pixel resolution. Finally, the MODIS Cloud Product includes the cirrus reflectance in the visible at the 1–km–pixel resolution, which is useful for removing cirrus scattering effects from the land–surface reflectance product. There are two MODIS Cloud data product files: MOD06\_L2, containing data collected from the Terra platform; and MYD06\_L2, containing data collected from the Aqua platform (NASA (2023f)).

## DATA COLLECTION

### 1. Study Area

Researchers conducted studies in all 77 tropical stations in Thailand, which can be divided into 7 regions, namely the Northern with 15 stations. The Central with 18 stations; the Northeastern with 20 stations; the Eastern with 8 stations; the East Coast of Southern with 10 stations; the West Coast of Southern with 6 stations; and areas in the middle latitudes 1 station in England, namely the University of Manchester, is shown in Figure 17, 18 and Table 2.

Table 2 Shown the station name in the study area.

Region	Stations
Tropical (Thailand)	
North	Chiang Mai
	Chiang Rai
	Lampang
	Lamphun
	Mae Hong Son
	Nan
	Phayao
	Phrae
	Uttaradit
	Kamphaeng Phet
	Tak
	Phitsanulok
	Phetchabun
	Sukhothai
Central	Kanchanaburi
	Chai Nat
	Phra Nakhon Si Ayutthaya
	Nakhon Nayok
	Nakhon Sawan
	Ratchaburi
	Lopburi
	Saraburi
	Sing Buri
	Suphan Buri
Ang Thong	

(continued)

Region	Stations
	Uthai Thani Bangkok Nakhon Pathom Nonthaburi Pathum Thani Samut Prakan Samut Songkhram Samut Sakhon
Northeastern	Kalasin Khon Kaen Chaiyaphum Nakhon Phanom Nakhon Ratchasima Bueng Kan Maha Sarakham Mukdahan Yasothon Roi Et Loei Sakon Nakhon Surin Sisaket Nong Khai Nong Bua Lamphu Udon Thani Ubon Ratchathani Amnat Charoen



(continued)

Region	Stations
Eastern	Burirum
	Chanthaburi
	Chachoengsao
	Chonburi
	Trat
	Prachinburi
	Rayong
	Sa Kaeo
East Coast of Southern	Phetchaburi
	Prachuap Khiri Khan
	Chumphon
	Surat Thani
	Nakhon Si Thammarat
	Phatthalung
	Songkhla
	Pattani
	Yala
	Narathiwat
West Coast of Southern	Ranong
	Phang Nga
	Phuket
	Krabi
	Trang
	Satun
Middle latitudes (United Kingdom)	The University of Manchester

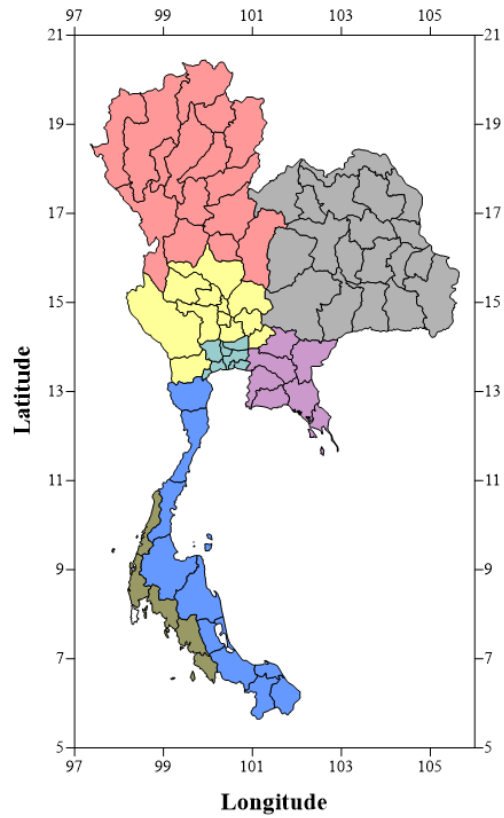


Figure 17 Thailand map is divided into 7 regions.

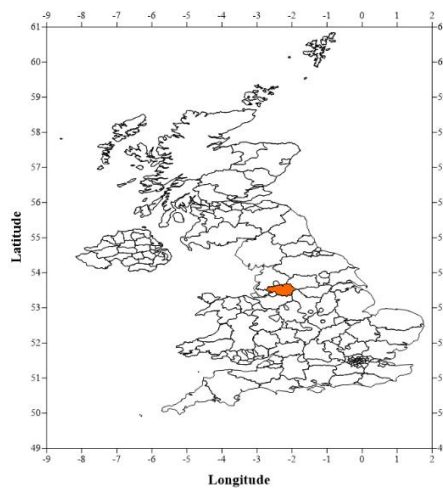


Figure 18 The United Kingdom map is the University of Manchester

## 2. Sensor and PM2.5 data

### 2.1 Aerosol data

The researcher has collected data collected daily Aerosol and Angstrom Exponent data from Aerosol Product I Collection 6.1 level 2 for 78 stations from 2000 to 2022 for Terra (available for download [https://adsweb.modaps.eosdis.nasa.gov/search/order/2/MOD04\\_L2--61](https://adsweb.modaps.eosdis.nasa.gov/search/order/2/MOD04_L2--61)) and from 2002 – 2020 for Aqua satellites (available for downloaded [https://adsweb.modaps.eosdis.nasa.gov/search/order/2/MYD04\\_L2--61](https://adsweb.modaps.eosdis.nasa.gov/search/order/2/MYD04_L2--61)).

Table 3 Show the basic data of Aerosol Product.

satellite	Data	Unit	Algorithm	period
Terra	AOD	unitless	Deep_Blue_Aerosol_Optical_Depth_550_Land	2000 –
	AE	unitless	Deep_Blue_Angstrom_Exporment_Land	2022
Aqua	AOD	unitless	Deep_Blue_Aerosol_Optical_Depth_550_Land	2002 –
	AE	unitless	Deep_Blue_Angstrom_Exporment_Land	2022

### 2.2 Cloud properties data

The researcher has collected data on cloud properties from Cloud Product Collection 6.1 level 2 as daily data for all 78 stations. Data can be downloaded from Terra satellite ([https://adsweb.modaps.eosdis.nasa.gov/search/order/2/MOD06\\_L2--61](https://adsweb.modaps.eosdis.nasa.gov/search/order/2/MOD06_L2--61)) and Aqua satellites ([https://adsweb.modaps.eosdis.nasa.gov/search/order/2/MYD06\\_L2--61](https://adsweb.modaps.eosdis.nasa.gov/search/order/2/MYD06_L2--61)).

Table 4 Show the basic data of Cloud Products.

satellite	Data	Unit	Algorithm	period
Terra	CF	unitless	Cloud_Fraction	2000 – 2022
	CER	$\mu\text{m}$	Cloud_Effective_Radius	
	COT	unitless	Cloud_Optical_Thickness	
	CWP	$\text{g}/\text{m}^2$	Cloud_Water_Path	
	CTP	hPa	Cloud_Top_Pressure	
	CTT	$^{\circ}\text{C}$	Cloud_Top_Temperature	
Aqua	CF	unitless	Cloud_Fraction	2002 – 2022
	CER	$\mu\text{m}$	Cloud_Effective_Radius	
	COT	unitless	Cloud_Optical_Thickness	
	CWP	$\text{g}/\text{m}^2$	Cloud_Water_Path	
	CTP	hPa	Cloud_Top_Pressure	
	CTT	$^{\circ}\text{C}$	Cloud_Top_Temperature	

### 2.3 PM2.5 data in Thailand

Daily PM2.5 data were collected from 45 stations of the Pollution Control Department database and 25 stations from Climate Change Data of Chiang Mai University. Data can be downloaded from <http://air4thai.pcd.go.th/webV3/#/History> for the Pollution Control Department database(Figure 19.) and <https://www.cmuccdc.org> for Climate Change Data of Chiang Mai University(Figure 20.). Standards for PM2.5 dust particles in the atmosphere, in general, the 24-hour average must not exceed  $50 \mu\text{g}/\text{m}^3$ , and the annual average must not exceed  $25 \mu\text{g}/\text{m}^3$  (Environment, 2010).

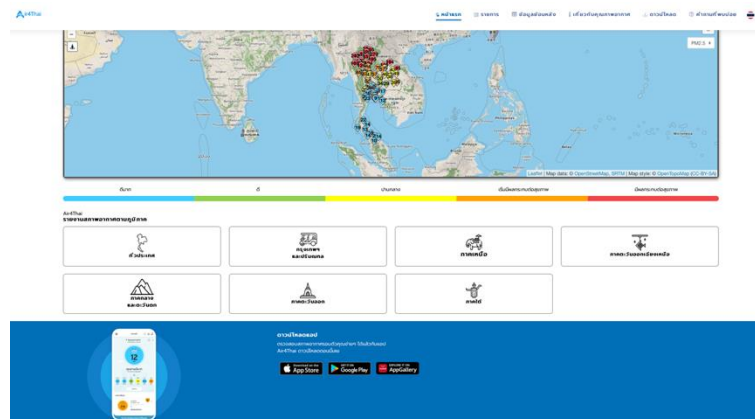


Figure 19 A website for downloading PM2.5 data from the Pollution Control Department.

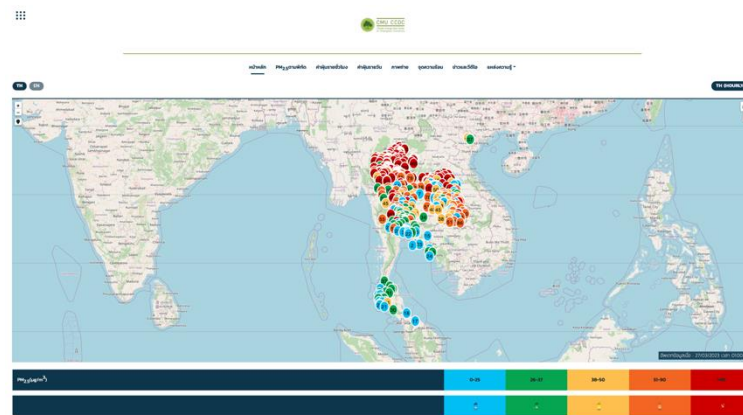


Figure 20 A website for downloading PM2.5 data from the Climate Change Data Center of Chiangmai University

#### 2.4 PM2.5 data in The University of Manchester

Particulate matter data measured at 7m above ground level by a Palas FIDAS 200 Instrument at Manchester Air Quality Site (MAQS) for the Integrated Research Observation System for Clean Air (OSCA) project.

Measurements include the abundance of mass concentration of PM1 ambient aerosol in air, mass concentration of PM2.5 ambient aerosol in air, mass concentration of PM10 ambient aerosol in Air, and the concentration of ambient aerosol particles.

Daily PM<sub>2.5</sub> data were collected The CEDA Archive forms part of NERC's Environmental Data Service (EDS). Data can be downloaded <https://data.ceda.ac.uk/badc/osca/data/manchester>.

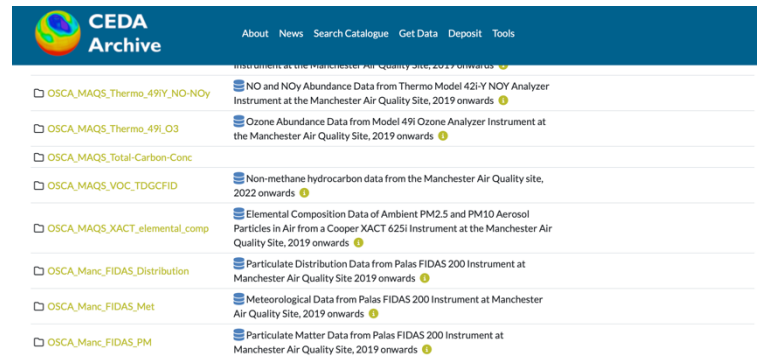


Figure 21 A website for downloading PM<sub>2.5</sub> data from the CEDA.

## ANALYSIS

The researcher used Aerosol, Angstrom Exponent, PM<sub>2.5</sub>, and cloud properties data for analysis change trend, and data frequency distribution. To study the relationship between aerosol and cloud properties by using statistics. Pearson correlation coefficient and to study the correlation of cloud properties during PM<sub>2.5</sub> exceeding the standard value.

1. To study of the trend of changes monthly, yearly Aerosols, Angstrom Exponent, PM<sub>2.5</sub>, and cloud properties (CF, CER, COT, CWP, CTP, and CTT) data were averaged and the standard deviation of each parameter was determined using mean represents the average value in a dataset. It is calculated as:

$$\text{mean} = \frac{\sum x_i}{n} \quad (4)$$

Where  $\sum$  is A symbol that means “sum

$x_i$  is The observation in a dataset

$n$  is The total number of observations in the dataset

The standard deviation represents how spread out the values are in a dataset relative to the mean. It is calculated as:

$$S.D. = \frac{\sqrt{\sum (x_i - \bar{x})^2}}{(n-1)} \quad (5)$$

Where  $\sum$  is A symbol that means “sum”

$X_i$  is The observation in a dataset

$\bar{x}$  is The mean of the sample

$n$  is The sample size

Finally, take the average value of each parameter to create monthly mappings.

## 2. Data frequency distribution

The daily AOD, AE, PM2.5, and cloud properties (CF, CER, COT, CWP, CTP, and CTT) data were frequency-distributed to find the range of the parameter data each of them is divided by year and it's season. using a histogram frequency distribution.

Frequency distribution is the data that is the variable's value we are interested in arranged in order of and divided into equal periods. The amount of data in each score range is called frequency if the difference between the highest and lowest scores is insignificant. There is no need to segment scores into segments; each interval has 1 point. The frequency distribution aims to provide a systematic overview of the distribution of all data. Organizing and presenting preliminary information Data can be given as tables and charts. In this case, we would like to separate into two parts in the presentation: frequency distribution tables and various graphs and charts (Chula (2023))

A histogram is to bring the data that has already been distributed frequently in a distribution table. The frequency is shown as an image, which consists of rectangular bars. The horizontal axis is divided into intervals. The width of each

interval is equal to the width of the layer. The midpoint of each square is the midpoint of each layer. The height of each square bar will be the frequency of each floor.

3. To study the relationship of Aerosol, PM<sub>2.5</sub> and cloud properties.

The distribution of cloud properties was examined in Thailand using Terra and Aqua satellite data. In Thailand and The University of Manchester.

4. Assessment of particulate matter and cloud properties during PM<sub>2.5</sub> exceeds the standard.

PM<sub>2.5</sub> exceeds the standard take data on dust and cloud properties of each parameter to consider the range of data that each parameter has data in. and correlated with PM<sub>2.5</sub> values in the range above the standard.



## CHAPTER IV

### RESULTS

This work aims to study aerosol and cloud properties in Thailand and the University of Manchester. The aerosol parameters were PM<sub>2.5</sub> (particulate matter with a diameter of fewer than 2.5 microns), Angstrom Exposure (AE), and Aerosol Optical Depth (AOD). At the same time, there are six-parameter of cloud properties, including Cloud Fraction (CF), Cloud Effective Radius (CER), Cloud Optical Thickness (COT), Cloud Water Path (CWP), Cloud Top Pressure (CTP), Cloud Top Temperature (CTT), Cloud Fraction (CF), and Cloud Effective Radius (CER).

#### VARIATIONS IN AEROSOL PARTICLE AND CLOUD PROPERTIES IN THAILAND

##### 1. Aerosol particle

###### 1.1 AOD

AOD values over Thailand were obtained from Terra and Aqua satellite data. Daily AOD data from 2002 to 2022 were average monthly, as shown in Figures 22–23. Low AOD values are represented in blue, while high AOD values are defined in brown. Overall, AOD values were highest in the North, Northeast, and Central regions. High AOD values were observed from February to April (summer) and low AOD values from October to January (dry). In contrast, the southern region experiences consistent AOD values except in monsoon season. The monthly AOD obtained from the Terra and Aqua satellite data gave similar results.

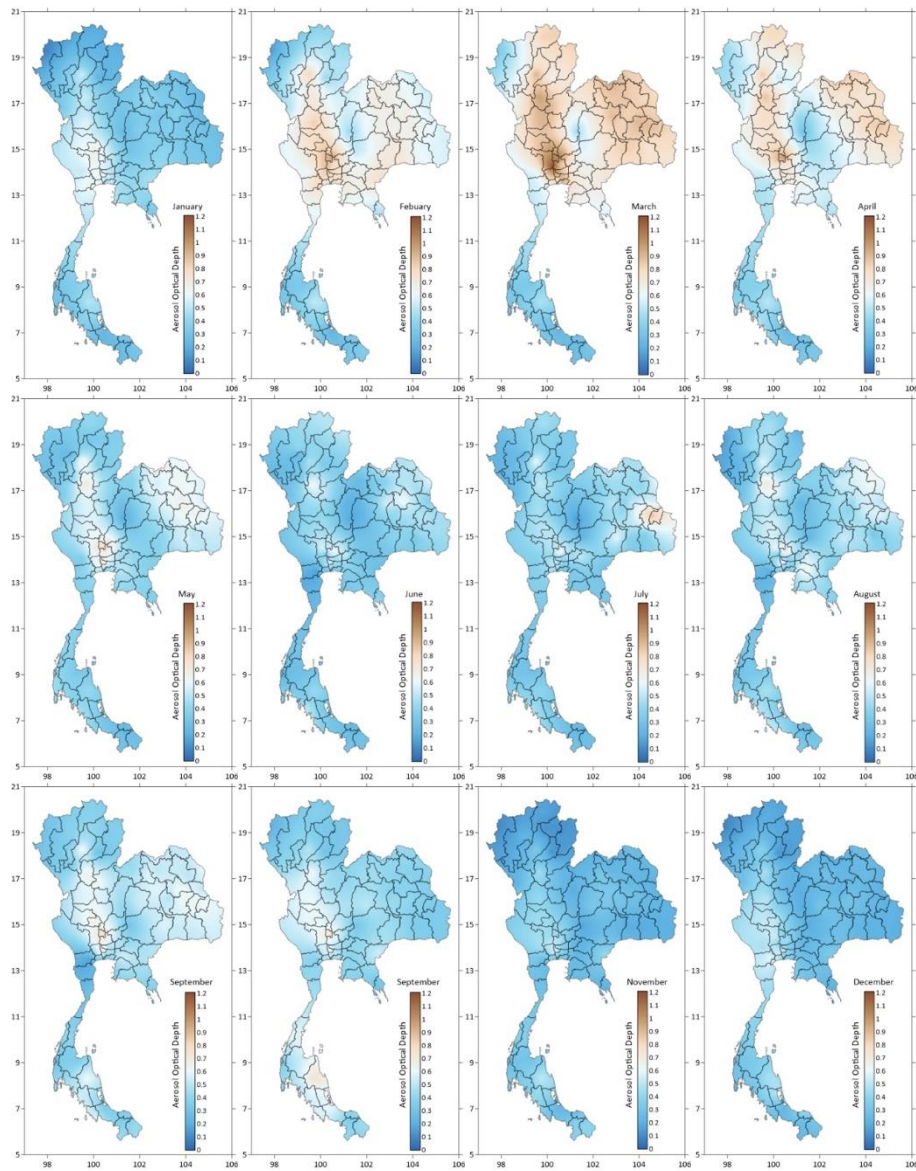


Figure 22 Time series of the monthly mean AOD derived from Terra satellite data in Thailand.

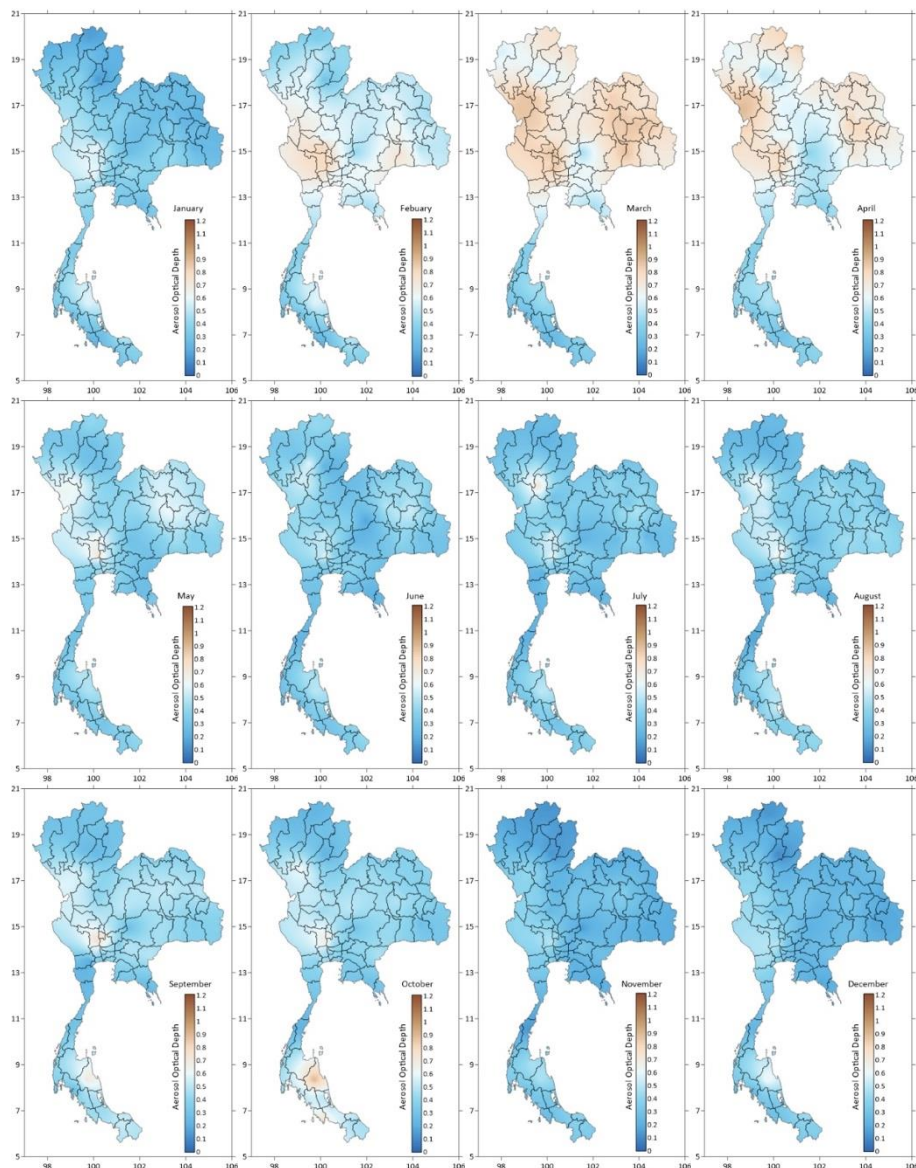


Figure 23 Time series of the monthly mean AOD derived from Aqua satellite data in Thailand.

### 1.2 AE

Monthly variations in AE in were represented in green for lower AE values, whereas brown indicates higher AE values (Figure 24). It was discovered that higher AE values obtained from Terra satellite were detected in rainy season (June to November) over the Northeast, while the lower AE were found in the North (February to June) and the central in December.

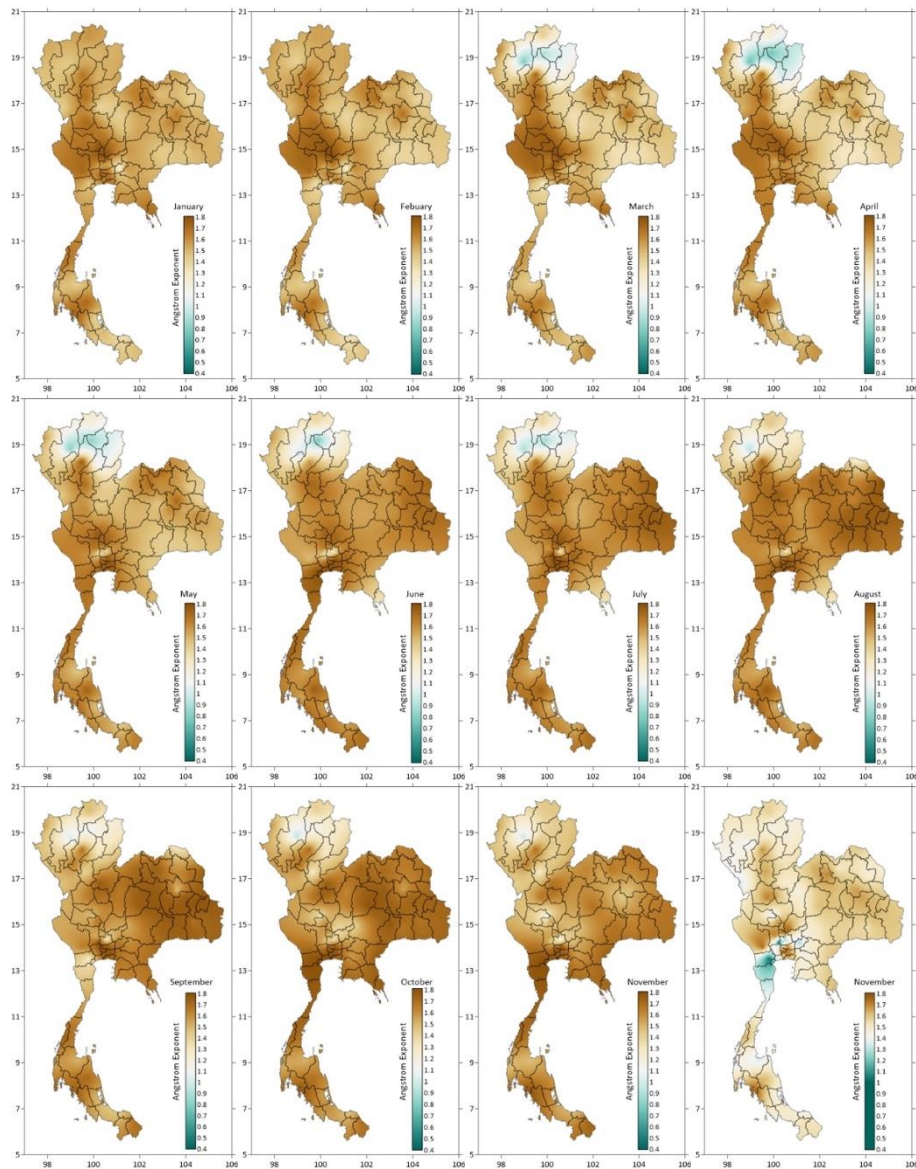


Figure 24 Time series of the monthly mean AE derived from Terra satellite data in Thailand.

Monthly variations in AE were represented in green for lower AE values, whereas brown indicates higher AE values, as shown in Figure 25. It was discovered that higher AE values obtained from the Aqua satellite were detected in the Northeast during the rainy season (June to November), and lower AE data were found in the north during the same period.

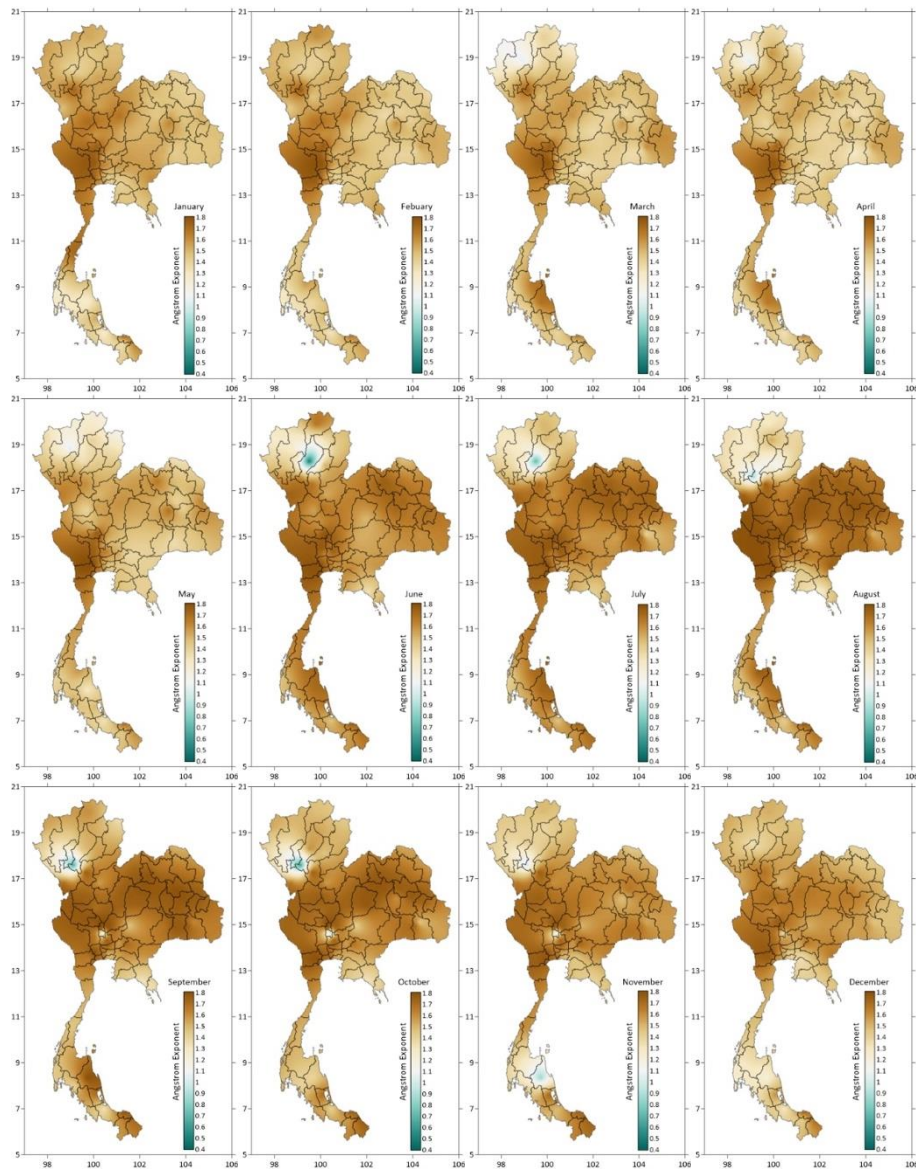


Figure 25 Time series of the monthly mean AE derived from Aqua satellite data in Thailand.

### 1.3 PM2.5

Figure 26 shows the monthly average of PM2.5 in Thailand. It was found that the northern region tends to have high PM2.5 values starting in January to April. Higher PM2.5 in the north was observed in Mae Hong Son, Chiang Mai, and Chiang Mai provinces, which showed high PM2.5 values in March (summer). The central region demonstrated high PM2.5 values from December to April. The

Northeastern and the Northern trends are similar except in the Southern region, with the PM2.5 trend remaining constant throughout the year. PM2.5 concentrations are low in all areas throughout Thailand from May to October (rainy).

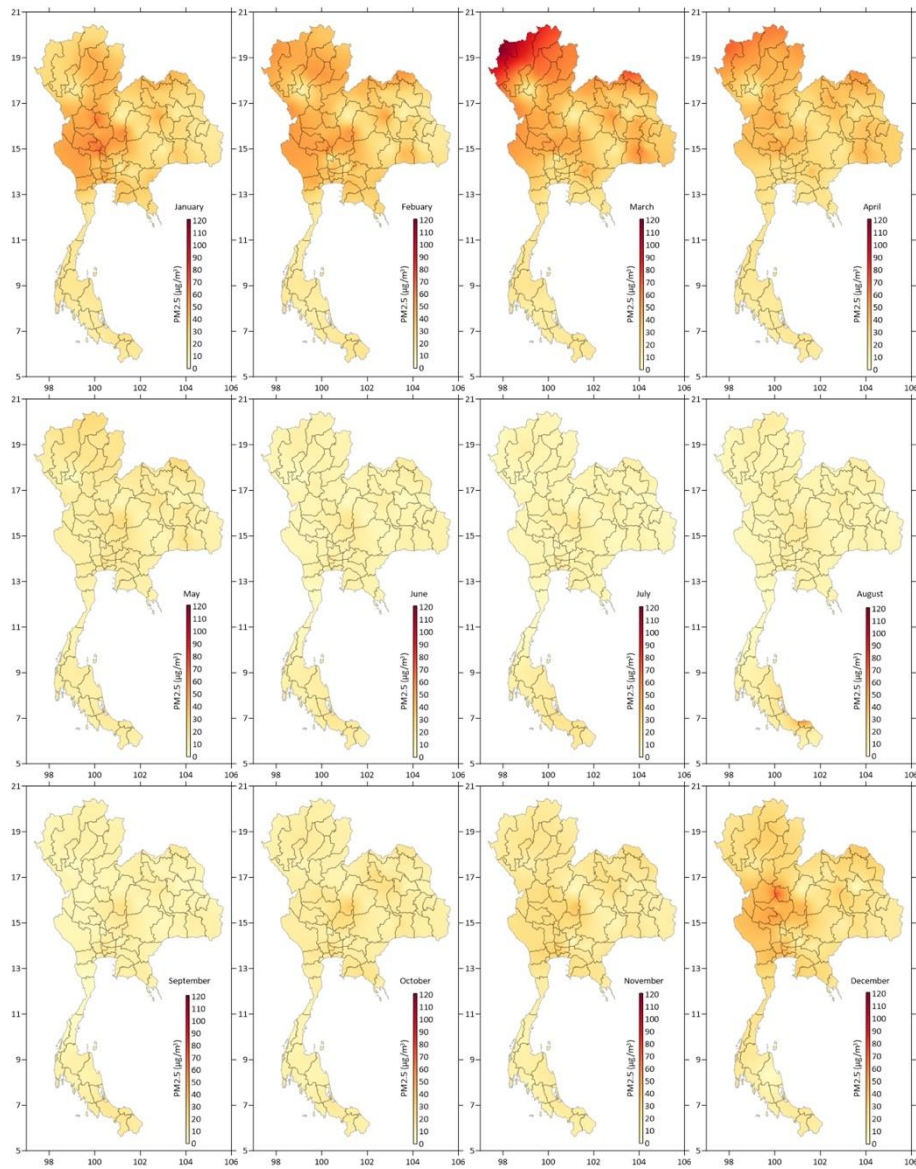


Figure 26 Time series of the monthly mean PM2.5 in Thailand.

## 2. Cloud properties

### 2.1 Cloud Fraction

White light indicates a low cloud fraction, while blue light indicates a high one (Figures 27–28). High CF data were found from May to July (during the rainy season), while low data were detected from December to February (during the winter). There is a similar pattern over Thailand, except in the Southern region. The monthly CF obtained from the Terra and Aqua satellite data gave similar results.

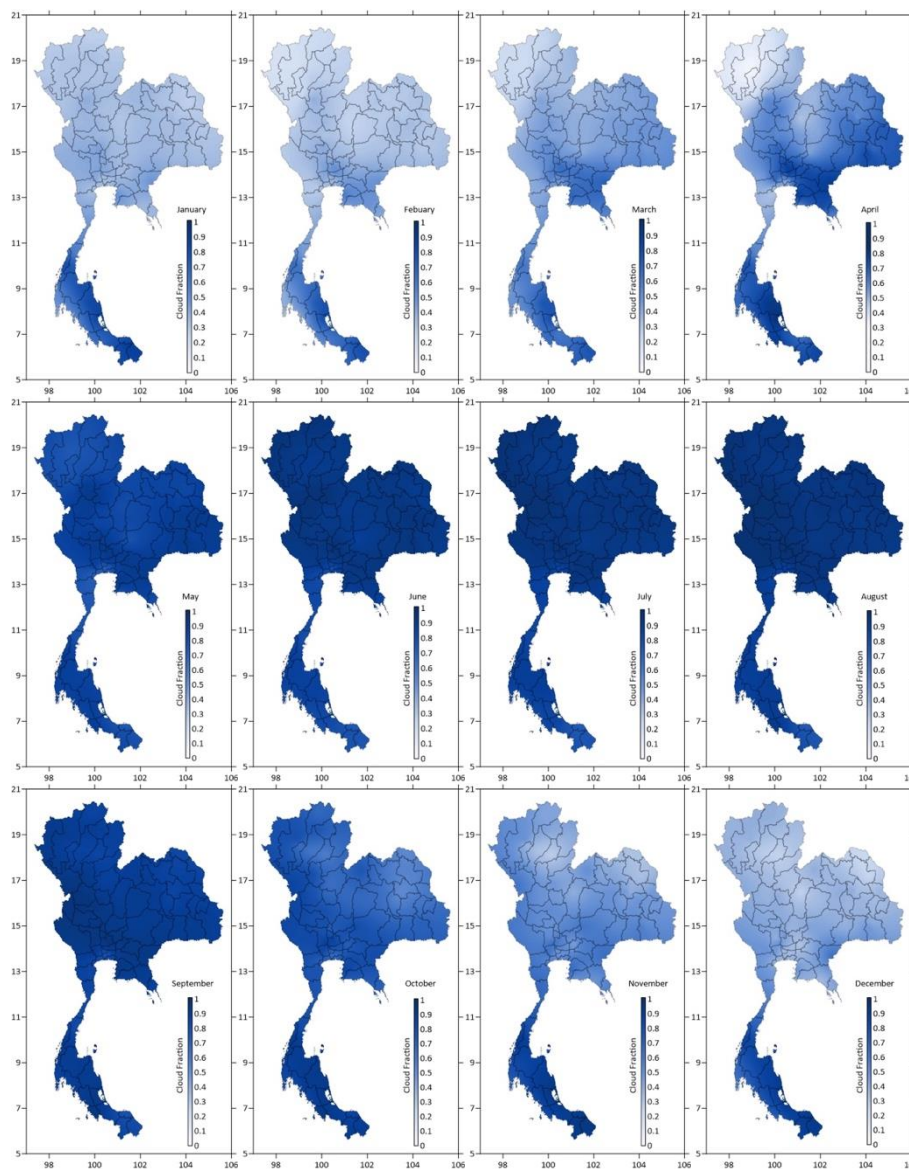


Figure 27 Time series of the monthly mean CF derived from Terra satellite data in Thailand.

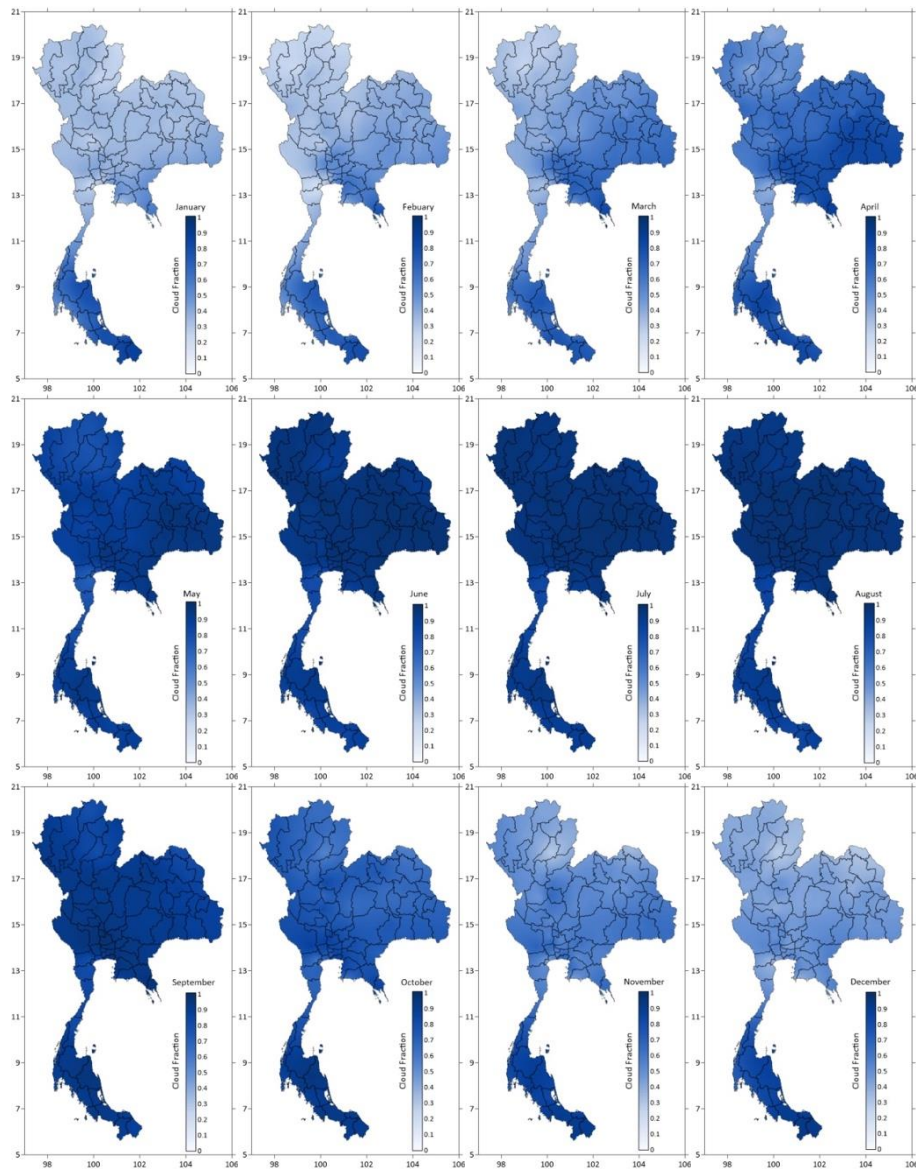


Figure 28 Time series of the monthly mean CF derived from Aqua satellite data in Thailand.

## 2.2 Cloud Effective Radius

As shown in Figures 29–30, high CER values are represented by the orange color, while white represents low CER values. CER levels were high from May to August, coinciding with the rainfall season, and low from December to February, coinciding with the rainfall season. There is a similar pattern over Thailand, except in



the Southern region. The monthly CF obtained from the Terra and Aqua satellite data gave identical results.

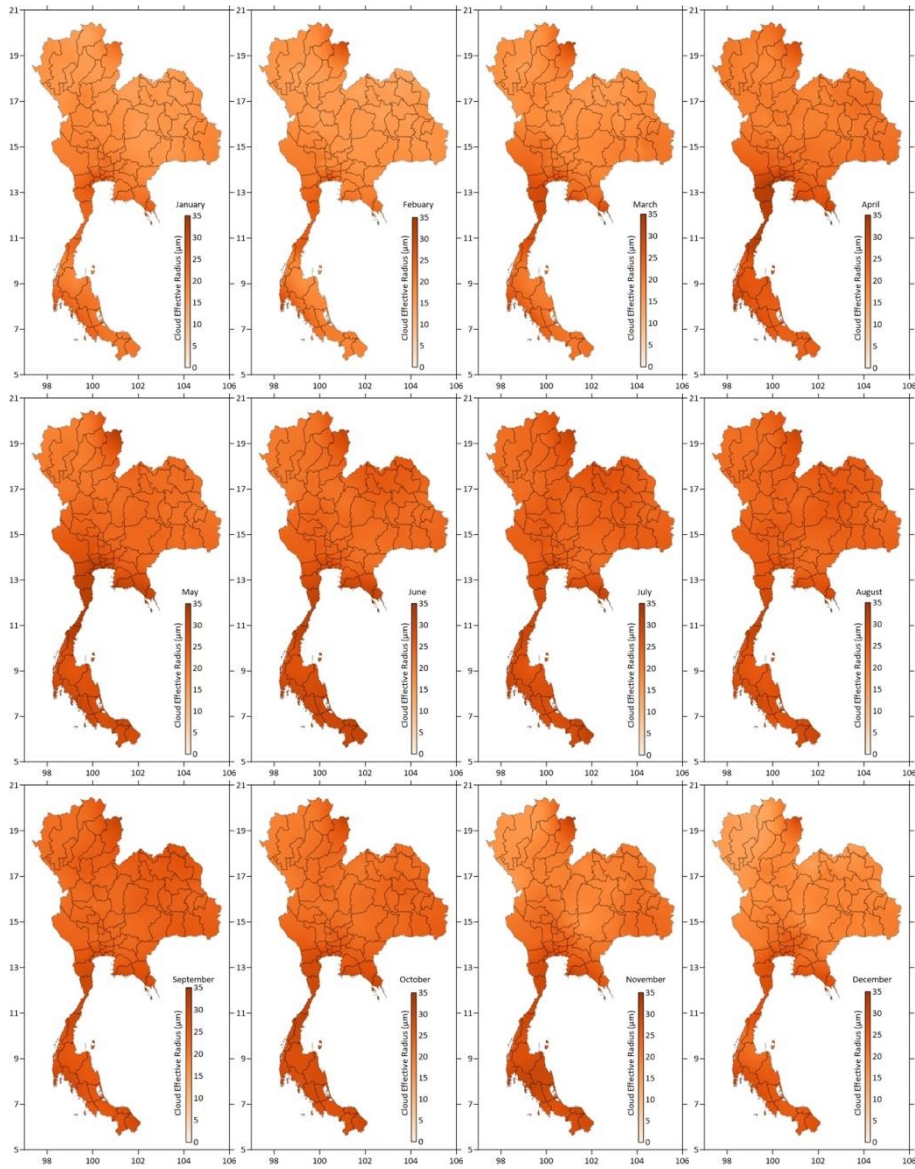


Figure 29 Time series of the monthly mean CER derived from Terra satellite data in Thailand.

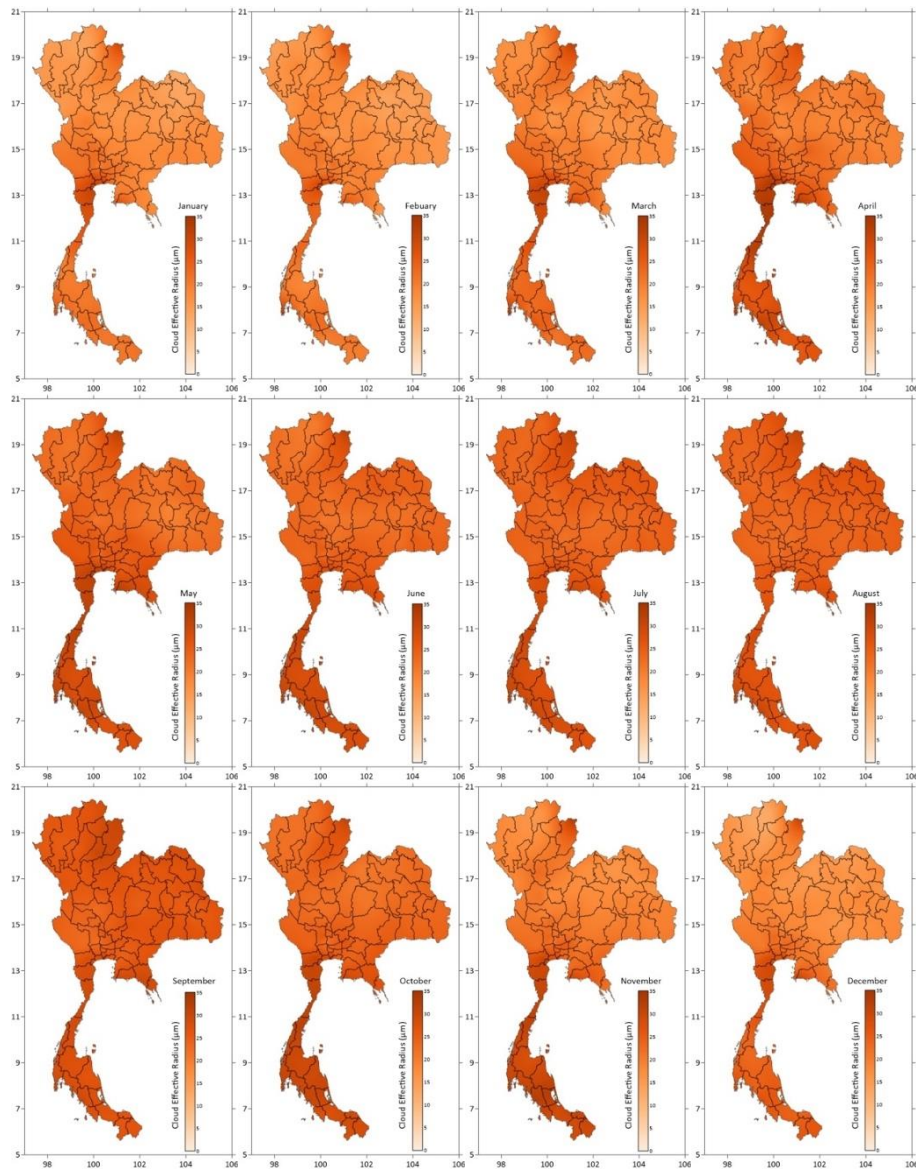


Figure 30 Time series of the monthly mean CER derived from Aqua satellite data in Thailand.

### 2.3 Cloud Optical Thickness

Brown shows high COD values, and white shows low COD value, as shown in Figures 31–32. COD is found to be high during the rainy season, from May to October. and low during the winter from November to April. In the southern region, COD high values are evident during the rainy season from October to January. There

is a similar pattern over Thailand, except the Southern region. The monthly COD obtained from the Terra and Aqua satellite data gave identical results.

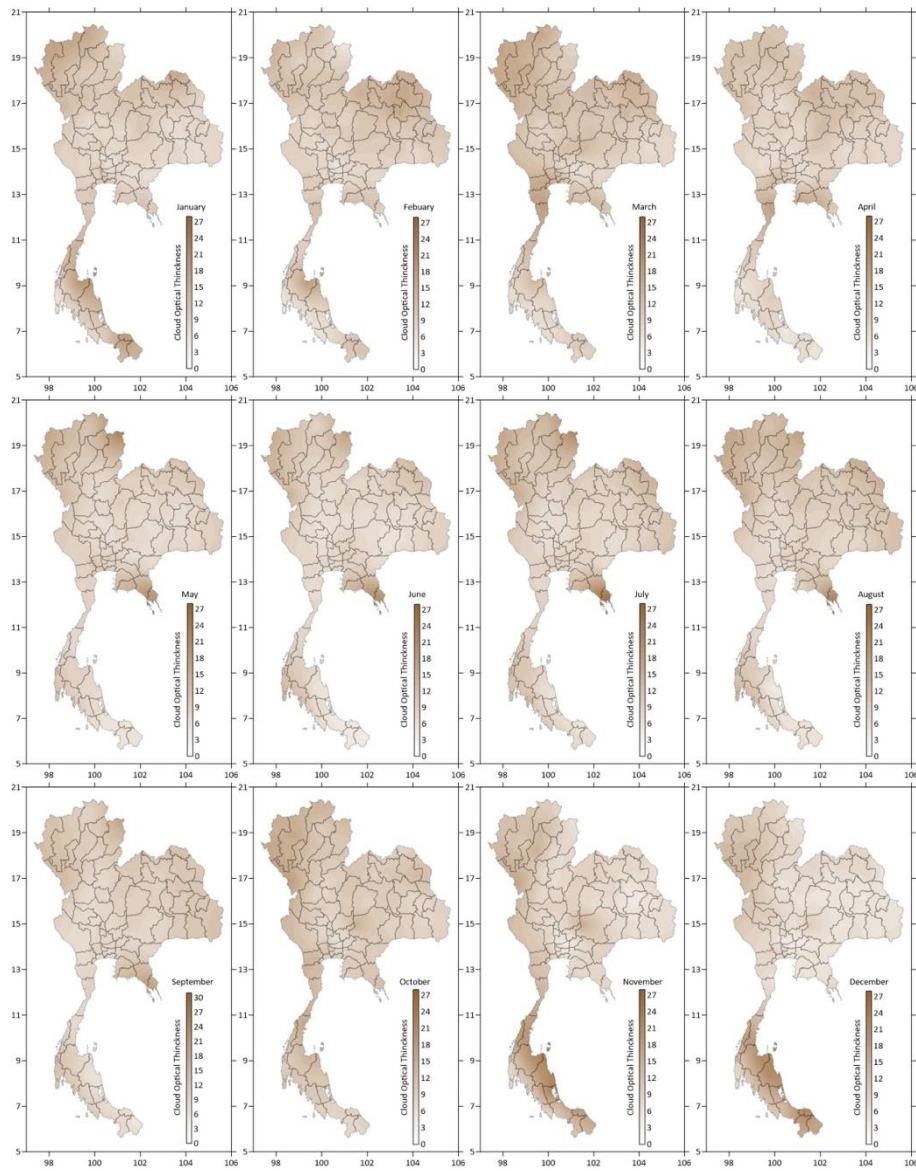


Figure 31 Time series of the monthly mean COT derived from Terra satellite data in Thailand.

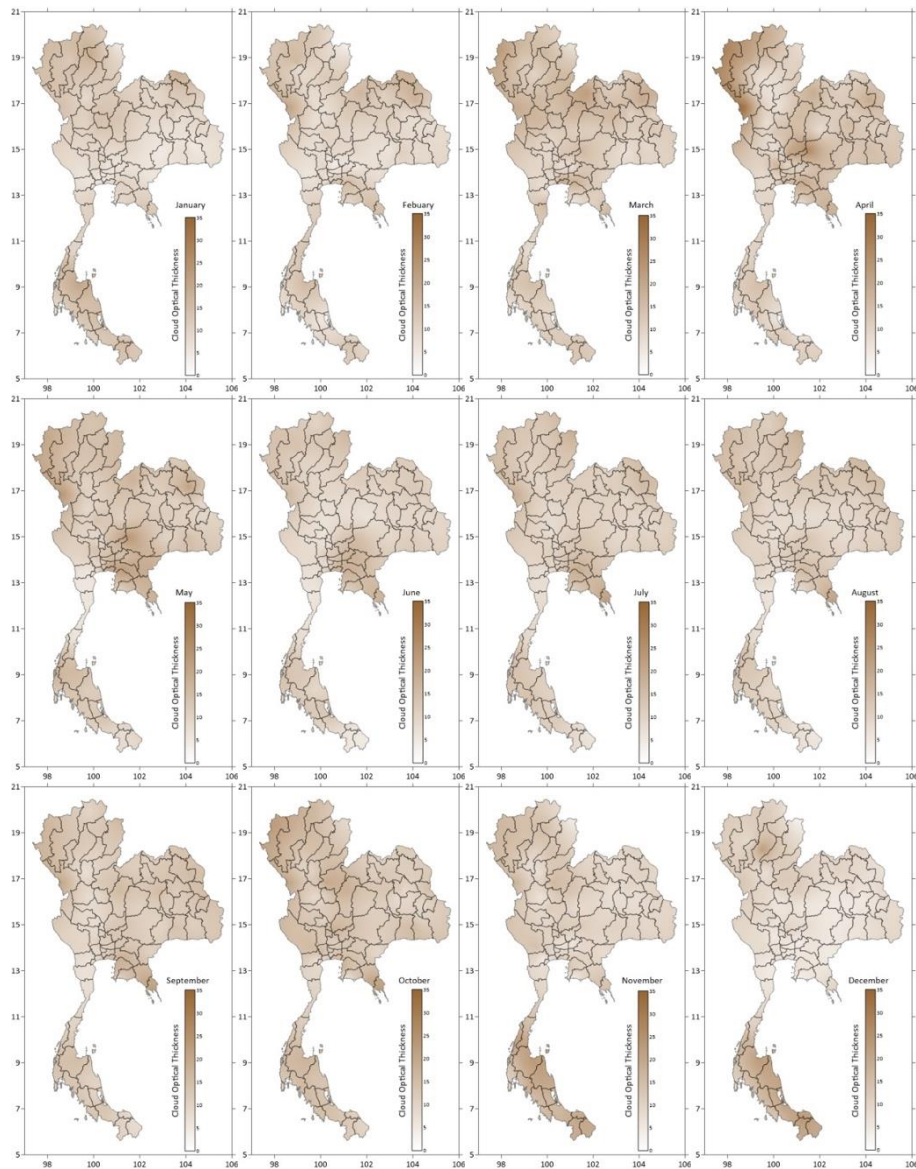


Figure 32 Time series of the monthly mean COT derived from Aqua satellite data in Thailand.

#### 2.4 Cloud Water Path

Blue gives high CWP values, and blue gives low CWP values, as in Figures 33–34. CWP values are high from summer to rainy times (March to October). It has low values during the winter, from November to February. It is evident in the Southern region that the values are high during the rainy season from October to

December. There is a similar pattern in Thailand, except in the Southern region. The monthly COD obtained from the Terra and Aqua satellite data gave identical results.

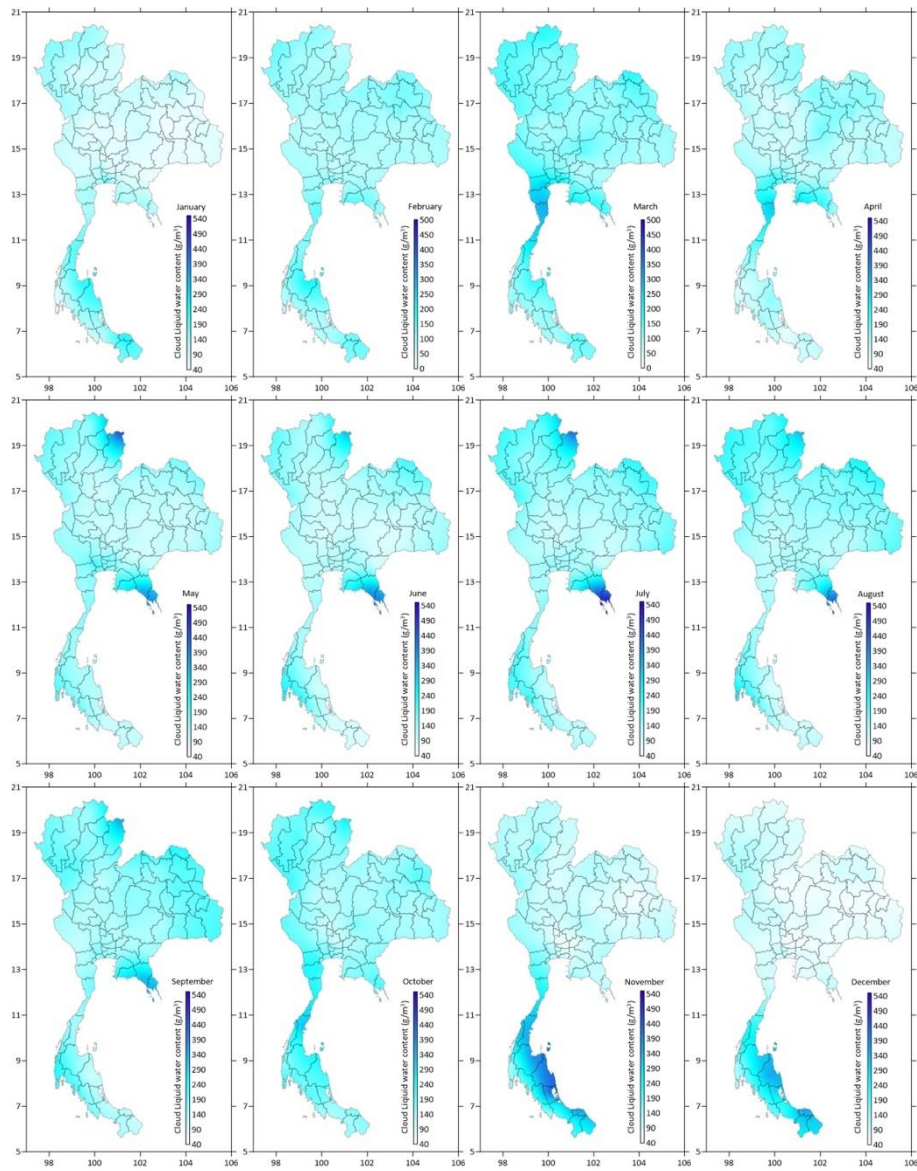


Figure 33 Time series of the monthly mean CWP derived from Terra satellite data in Thailand.

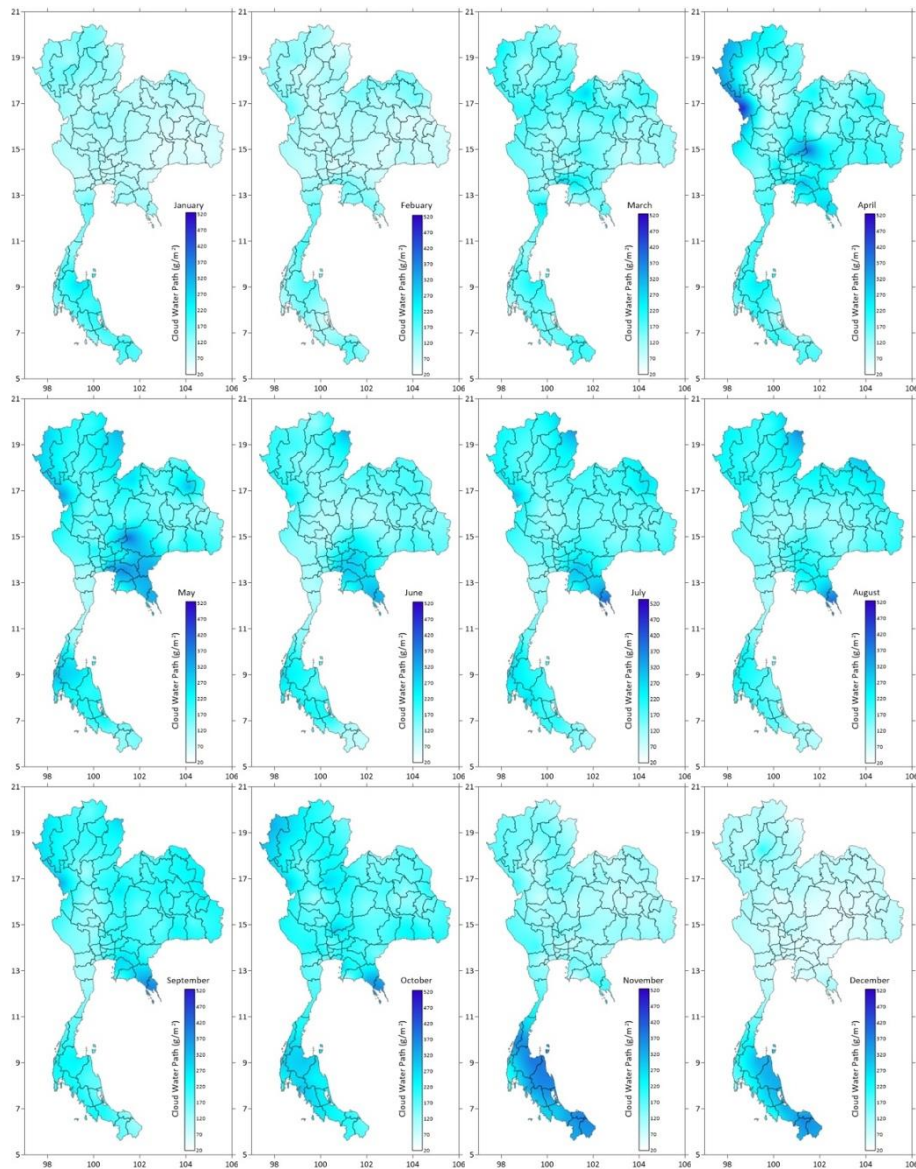


Figure 34 Time series of the monthly mean CWP derived from Aqua satellite data in Thailand.

### 2.5 Cloud Top Pressure

Purple shows high CTP values, and white shows low CTP values.

Figures 35–36 show that CTP values are high from November to February during the winter and low from June to July during the rainy season in all regions of Thailand. The pattern is similar in Thailand, except in the southern region. The monthly COT obtained from the Terra and Aqua satellite data gave identical results.

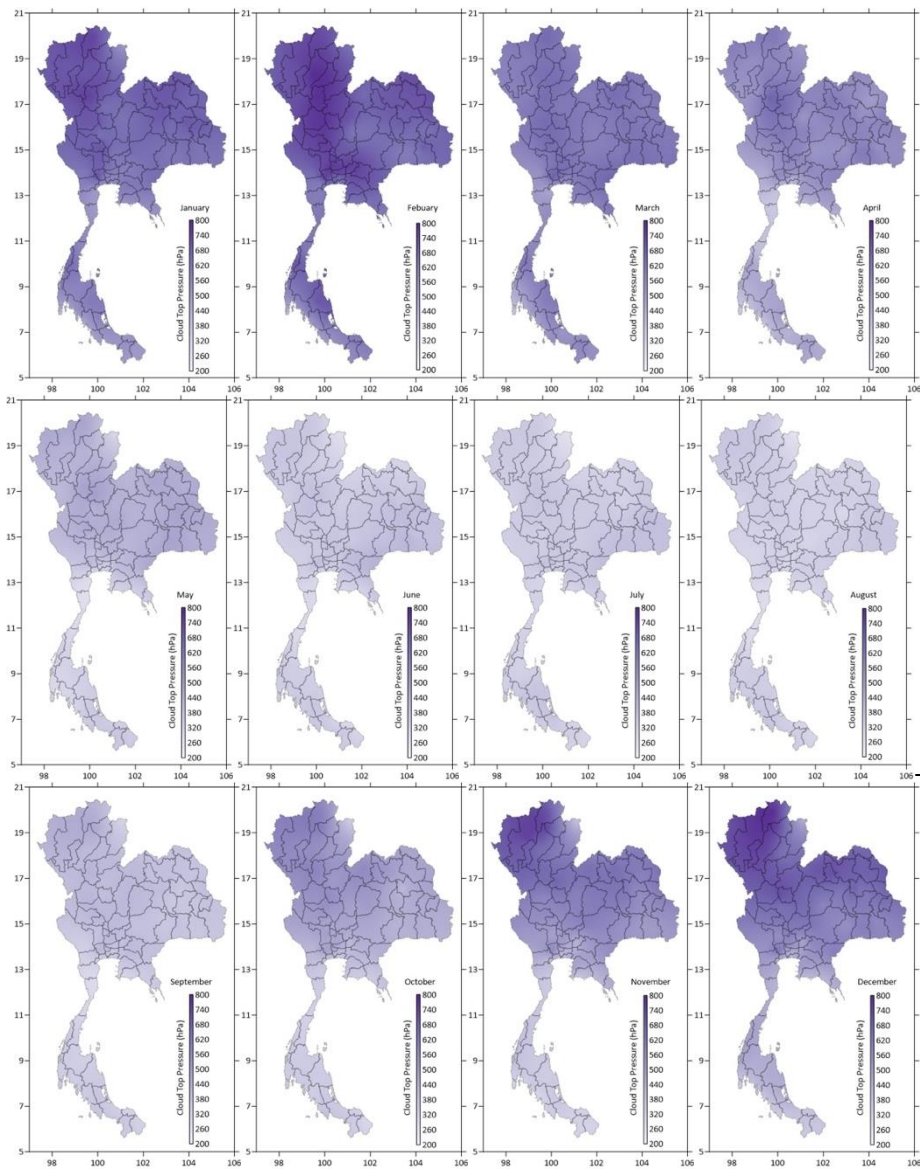


Figure 35 Time series of the monthly mean CTP derived from Terra satellite data in Thailand.

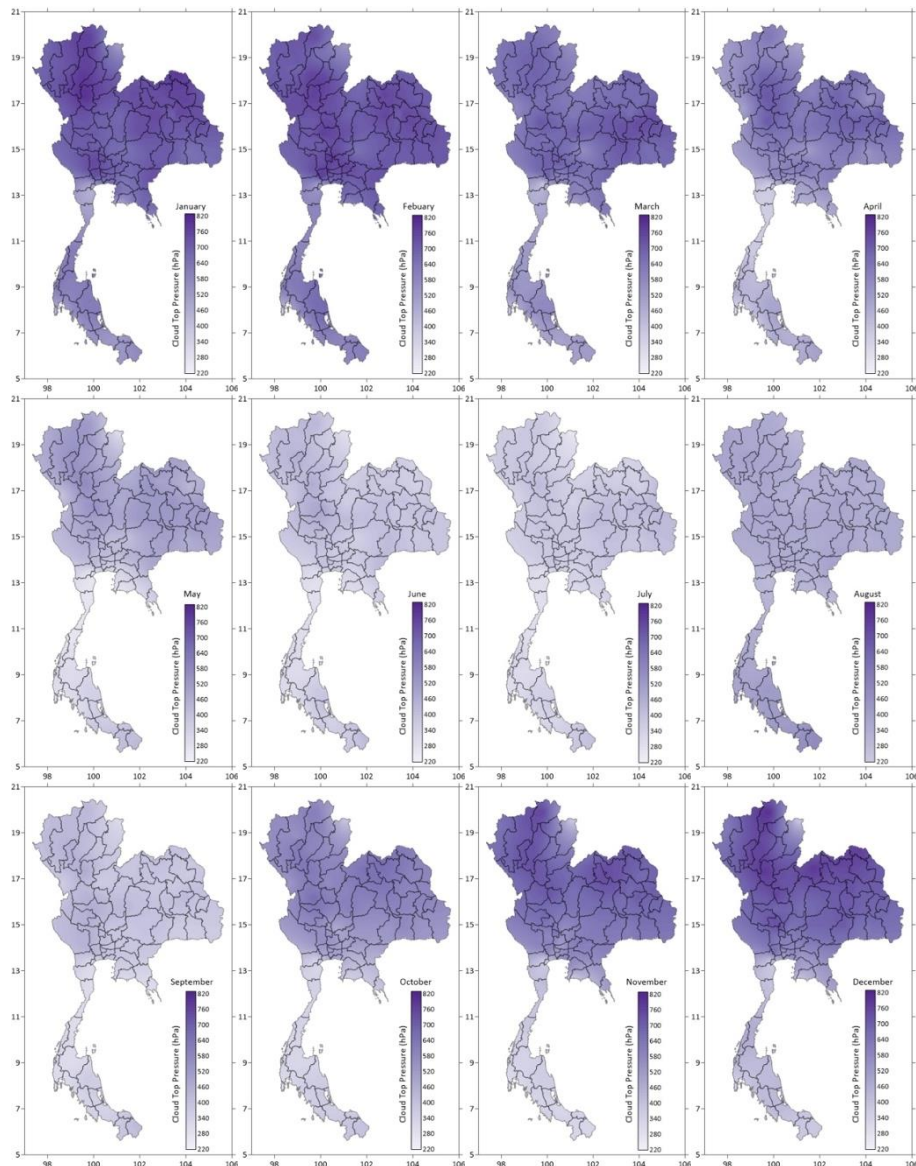


Figure 36 Time series of the monthly mean CTP derived from Aqua satellite data in Thailand.

## 2.6 Cloud Top Temperature

The white color indicates a high CTT value, and the red color indicates a low CTT value, as shown in Figures 37–38. The CTT value is found to be high during the winter season from November to February. It has low values during the rainy season, from May to October. In the south, it is high from May to December (during the rainy season) and low during the summer. The pattern is similar in



Thailand, except in the Southern region. The monthly COD obtained from the Terra and Aqua satellite data gave identical results.

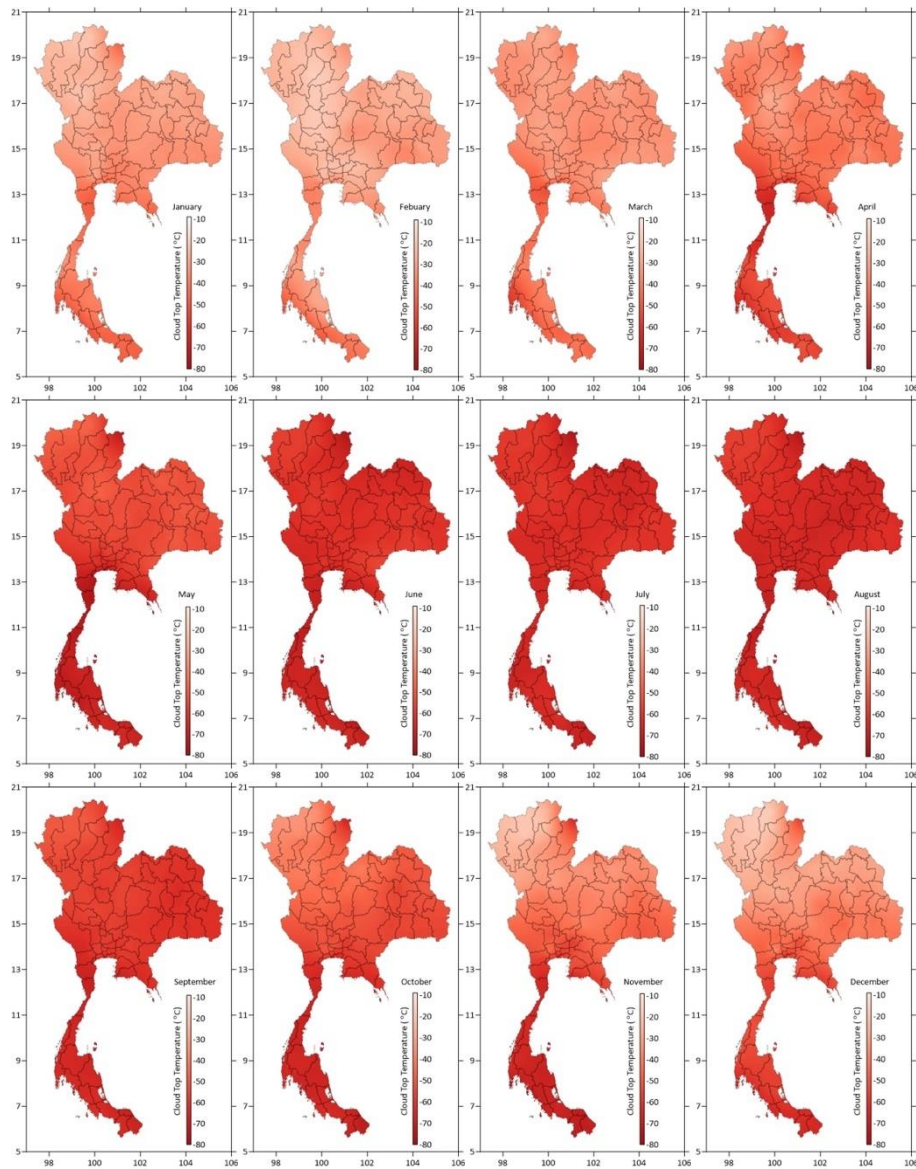


Figure 37 Time series of the monthly mean CTT derived from Terra satellite data in Thailand.

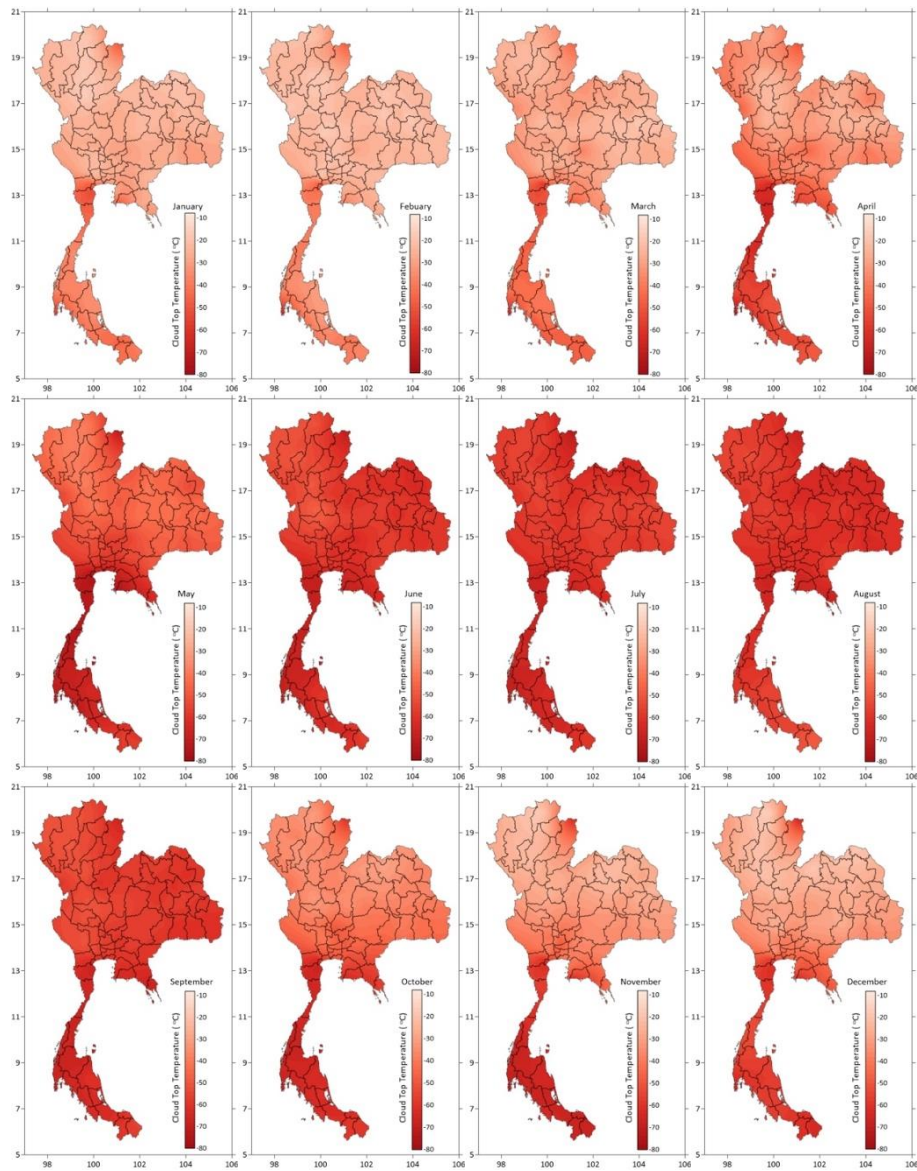


Figure 38 Time series of the monthly mean CTT derived from Aqua satellite data in Thailand.

## VARIATIONS IN AEROSOL PARTICLE AND CLOUD PROPERTIES IN THE UNIVERSITY OF MANCHESTER

### 1. Aerosol particle

The variation in Aerosol and Angstrom Exponent was examined at The University of Manchester using Terra and Aqua satellite data. In the UK, seasons are defined as follows:

Spring (March to May)

Summer (June to August)

Autumn (September to November)

Winter (December to February)

#### 1.1 AOD

Based on the Terra and Aqua satellite data, the monthly AOD (Figure 39) values were determined to be most significant in June (summer) at 0.21 compared with January (winter). Based on the Aqua satellite data, June (summer) has the maximum average value of 0.30, while December (winter) has the lowest average value of 0.07.

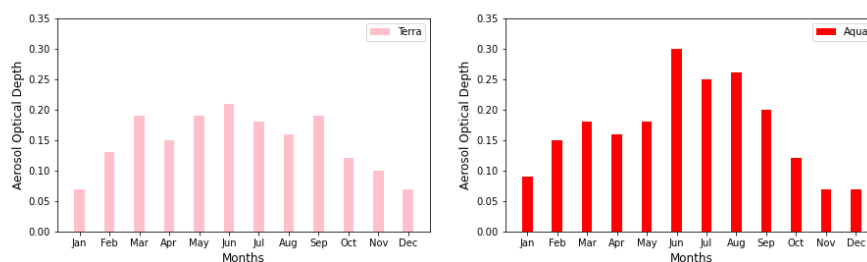


Figure 39 Time series of monthly mean AOD derived from Terra and Aqua satellite data at The University of Manchester.

#### 1.2 AE

Figure 40 illustrates the results of the analysis of the monthly average in AE. The highest average AE value for the Terra satellite was 1.59 in June

(Summer), and the lowest was 1.47 in December (Winter). For the Aqua satellite, the AE value peaks in July (Summer) and averages 1.60, with a low of 1.46 in March (Spring).

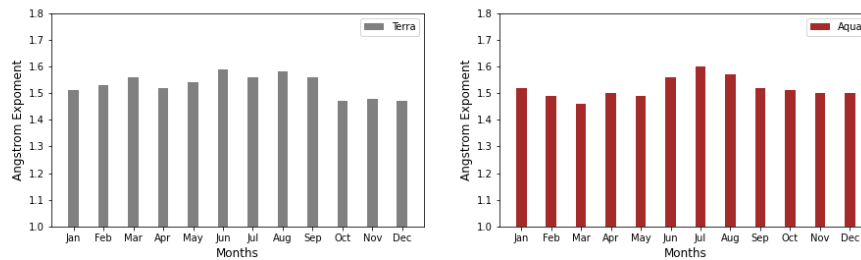


Figure 40 Time series of monthly mean AE derived from Terra and Aqua satellite data at The University of Manchester.

### 1.3 PM2.5

The variations in PM2.5 at the University of Manchester from 2019 to 2022 are shown in Figure 41. High PM2.5 concentrations were detected from November to April. The highest PM2.5 was found in March ( $12.59 \mu\text{g}/\text{m}^3$ ). Low PM2.5 concentrations were detected from May to October, and lowest PM2.5 was found in July ( $5.52 \mu\text{g}/\text{m}^3$ )

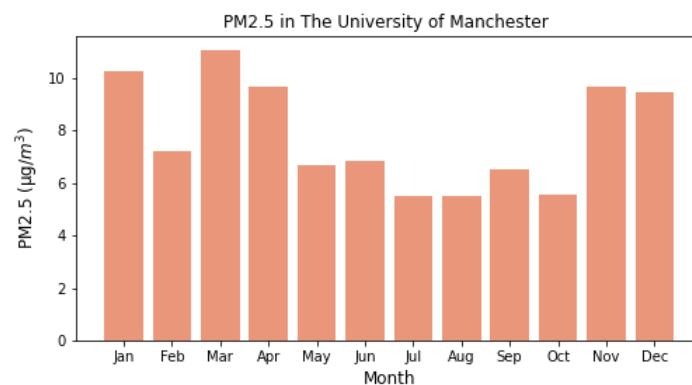


Figure 41 Time series of monthly mean PM2.5 derived from ground-based in The University of Manchester from 2019 to 2022.

## 2. Cloud properties

The seasonal variation of cloud properties (CER, CF, COD, CTP, CTT, and CLW) is examined using Aqua satellite data from 2002 to 2022 and Terra satellite data from 2000 to 2022 at The University of Manchester, as shown in Figure 42. It was found as follows:

- High CF was observed from October to February (autumn to winter), while low CF was detected from June to September (summer to autumn). The highest CF is found in January (0.8) on both satellites, while the lowest CF is detected in June (0.5 for the Terra satellite) and July (0.5 for the Aqua satellite).

- High COT was observed from November to February (autumn to winter), while low COT was detected from March to October (spring to autumn). The highest COT is found in December (25.51 for Terra and 20.76 for Aqua), while the lowest COT is detected in March (9.46 for Terra) and October (9.17 for Aqua).

- High CTP was observed from June to August (summer), while low CTP was detected from September to January (autumn to winter). The highest CTP is found in August (702 hPa for Terra and 733 for Aqua), while the lowest CTP is detected in October (572 hPa for Terra and 525 hPa for Aqua).

- High CTT was observed from June to August (summer), while low CTT was detected from November to February (autumn to winter). The highest CTT is found in August ( $-30.13$  °C for Terra, and  $-27.68$  °C for Aqua), while the lowest CTT is detected in October ( $-46.14$  for Terra) and March ( $-52.34$  °C for Aqua).

- High CER was observed from September to November (autumn), while low CER was detected from December to July (winter to summer). The highest CER is found in October (26.45  $\mu\text{m}$  for Terra and 27.15  $\mu\text{m}$  for Aqua), while the lowest CER is detected in July (17.93  $\mu\text{m}$  for Terra) and August (16.44  $\mu\text{m}$  for Aqua)

- High CWP was observed from November to February (autumn to winter), while low CWP was detected from May to August (spring to summer). The highest CWP is found in November (326.70  $\text{g/m}^2$  for Terra and 245.47  $\text{g/m}^2$  for Aqua),

while the lowest CWP is detected in August ( $119.43 \text{ g/m}^2$  for Terra) and July ( $90.63 \text{ g/m}^2$  for Aqua)

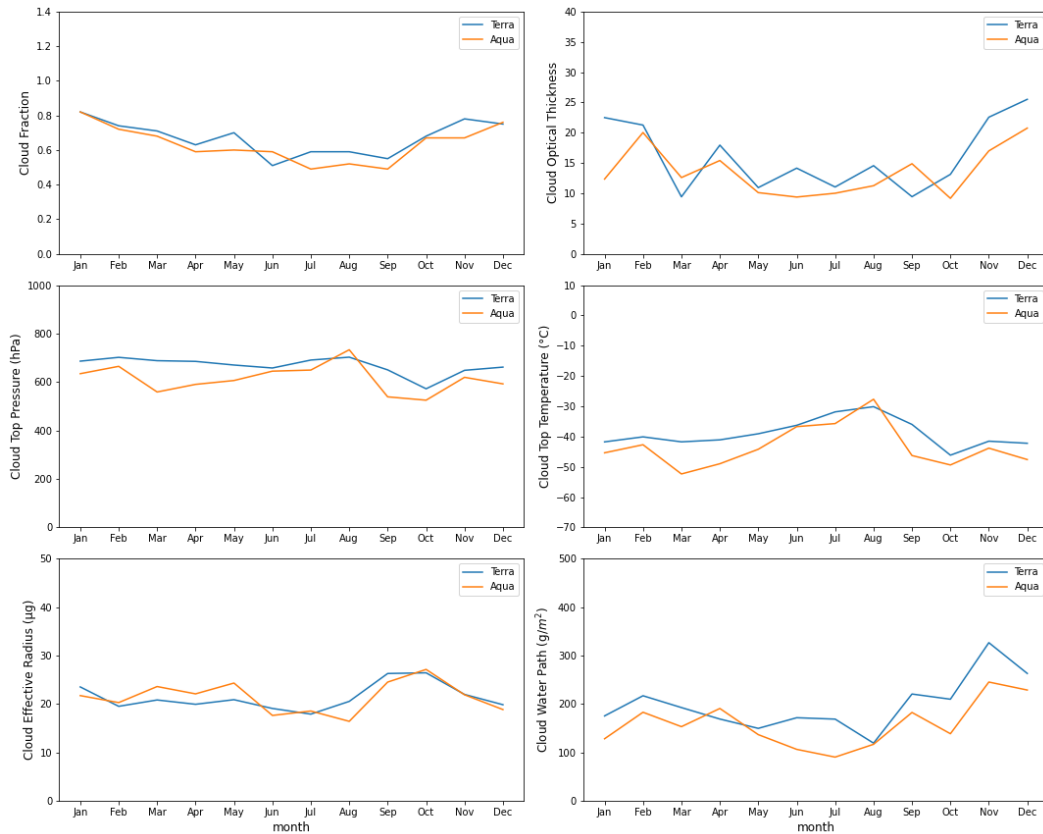


Figure 42 Time series of monthly mean CF, COT, CTP, CTT, CER, and CWP derived from Terra and Aqua satellite data at The University of Manchester.

## DISTRIBUTION OF CLOUD PROPERTIES IN THAILAND AND THE UNIVERSITY OF MANCHESTER

### 1. Thailand

The distribution of cloud properties was examined in Thailand using Terra and Aqua satellite data. In Thailand, seasons are defined as follows:

Summer (March to May)

Rain (June to October)

Winter (November to February)

The southern region is divided into two seasons: the rainy season (May to December) and the summer season (January to April).

The distribution of cloud properties, including Cloud Fraction (CF), Cloud Effective Radius (CER), Cloud Water Path (CLW), Cloud Optical Thickness (COD), Cloud Top Temperature (CTT), and Cloud Top Pressure (CTP) in Thailand from Terra and Aqua satellite data with seasonal distributions of cloud properties are shown in Figures 43–44.

Figures 43–44 show an example of the distribution of cloud properties in Bangkok's winter, summer, and rainy seasons. It was found that the CF distributions are high in the winter ( $\leq 0.2$ ) at 56%, summer ( $> 0.8$ ) at 48%, and rainy season ( $> 0.8$ ) at 75%. CTP values have a large seasonal distribution of 100.1 hPa to 200 hPa at 39%, 50%, and 48%, respectively. CTT data are large distributions in winter ( $-15\text{ }^{\circ}\text{C}$  to  $-1\text{ }^{\circ}\text{C}$ ) at 31%, summer ( $-90\text{ }^{\circ}\text{C}$  to  $-76\text{ }^{\circ}\text{C}$ ) at 26%, and the rainy season ( $90\text{ }^{\circ}\text{C}$  to  $-76\text{ }^{\circ}\text{C}$ ) at 30%. CLW distributions are in the winter, summer, and rainy seasons in the range ( $\leq 50\text{ g/m}^2$ ) at 61%, 47%, and 45%, respectively. CER data are to be more widely distributed in the winter ( $10.1\text{ }\mu\text{m}$  to  $15.0\text{ }\mu\text{m}$ ) at 18%, summer values are ( $30.1\text{ }\mu\text{m}$  to  $40\text{ }\mu\text{m}$ ) at 47%, and rainy seasons ( $15.1\text{ }\mu\text{m}$  to  $20.0\text{ }\mu\text{m}$ ) at 16%. COD distributions are significant in all three seasons in the range  $\leq 5.0$  at 65%, 59%, and 54%, respectively. The Terra and Aqua satellite data distribution gives similar results except for CF; an extensive distribution is found in winter ( $> 0.8$ ) at 27%. CTT is found in a large distribution in winter ( $> -1\text{ }^{\circ}\text{C}$ ) at 26%, while CTT is in the range of  $> -1\text{ }^{\circ}\text{C}$  at 26% in summer for the Aqua satellite data.

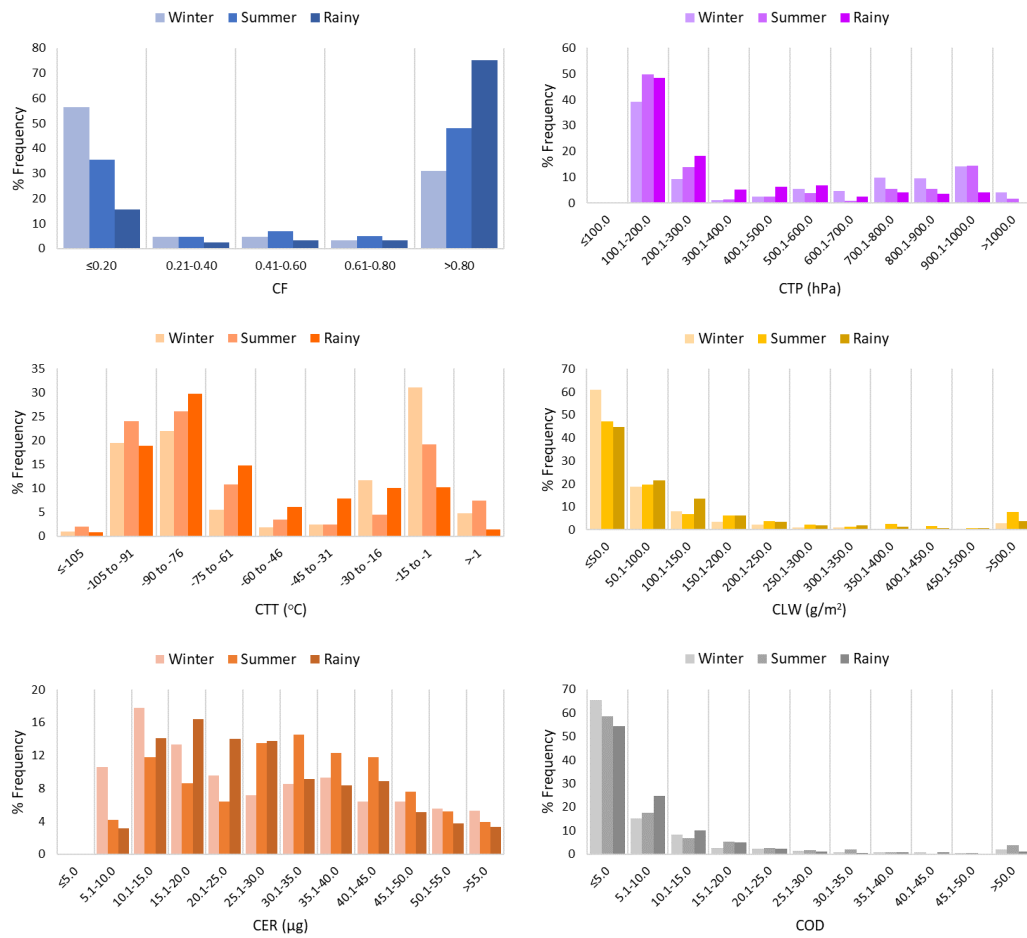


Figure 43 Distribution of cloud properties in Bangkok using Terra satellite data.



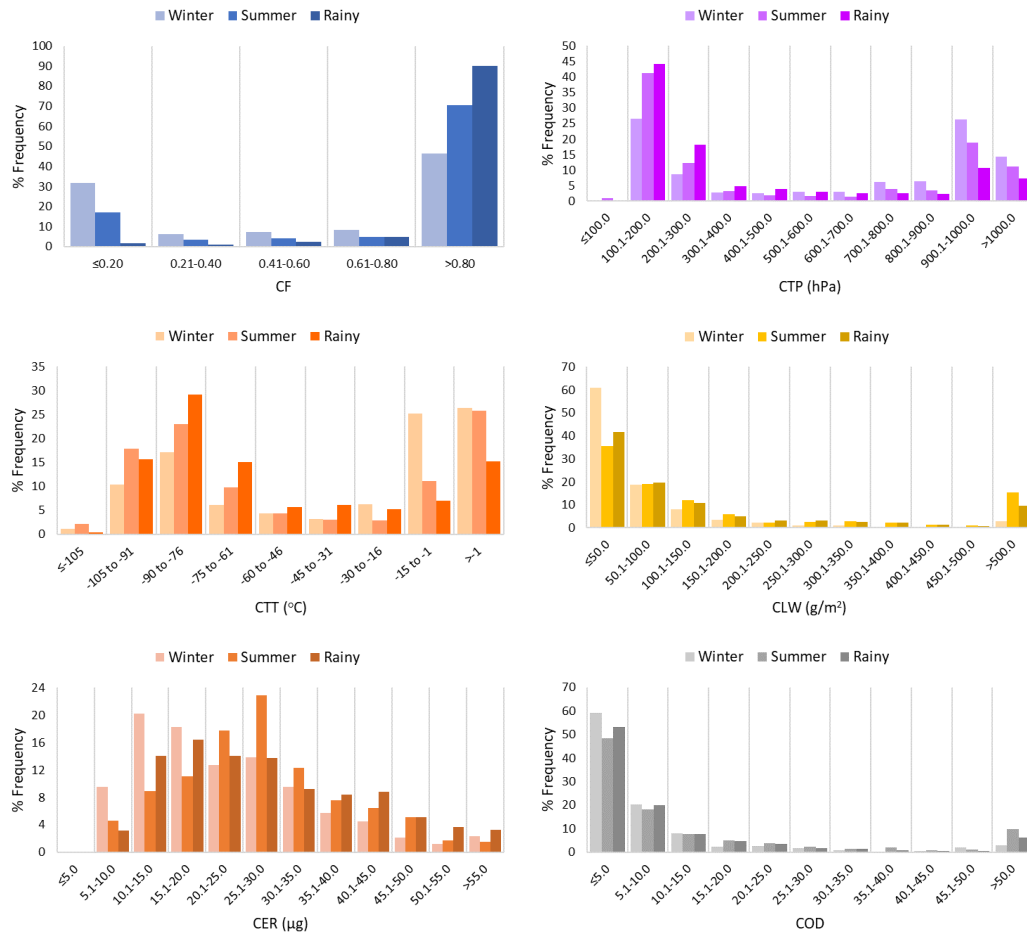


Figure 44 Distribution of cloud properties in Bangkok using Aqua satellite data.

A summary of the distribution of cloud properties in Thailand is divided into seven regions: the northern region, Eastern region, Central region, and Southern region (West and East coasts).

The distribution of cloud properties in the northern region shows that CF values are found chiefly in winter ( $\leq 0.2$ ) at 52%, summer ( $> 0.8$ ) at 40%, and the rainy season ( $> 0.8$ ) at 82%. CTP finds the majority distribution in the season. Winter and summer range from 900.1 hPa to 1000 hPa at 38% and 25%, and the rainy season ranges from 100.1 hPa to 200 hPa at 35%. CTT shows distributions mostly in winter ( $-15$  C to  $-1$ °C) at 57% and 31%, summer ( $> -1$ °C) at 27% and the rainy season ( $-90$ °C to  $-76$ °C) at 24%. CLW displays a large distribution in the winter, summer, and rainy seasons ( $\leq 50$  g/m<sup>2</sup>) at 51%, 39%, and 25%, respectively. CER

finds a large distribution in winter and summer (10.1  $\mu\text{m}$  to 15.0  $\mu\text{m}$ ) at 36% and 32% and in the rainy season (15.1  $\mu\text{m}$  to 20.0  $\mu\text{m}$ ) at 23%. COD obtains a large distribution in the range  $\leq 5.0$  at 42%, 41%, and 30%, respectively, in all three seasons. The distributions received from the Terra and Aqua satellite data give similar results.

The distribution of cloud properties in the Northeast shows that CF values are primarily found in winter ( $\leq 0.2$ ) at 38%, summer ( $>0.8$ ) at 72%, and the rainy season ( $>0.8$ ) at 85%. CTP finds the majority distribution in the season. Winter and summer range from 900.1 hPa to 1000 hPa at 42% and 34%, and the rainy season, 100.1 hPa to 200 hPa at 47%. CTT finds the distribution mostly in winter ( $-15\text{ }^{\circ}\text{C}$  to  $-1\text{ }^{\circ}\text{C}$ ) at 33%. Summer ( $> -1\text{ }^{\circ}\text{C}$ ) and the rainy season ( $-90\text{ }^{\circ}\text{C}$  to  $-76\text{ }^{\circ}\text{C}$ ) at 31% and 31%. CLW finds a large distribution in winter, summer, and the rainy season ( $\leq 50\text{ g/m}^2$ ) at 56%, 47%, and 35%, respectively. CER found a large distribution in the winter, in the range of 5.1  $\mu\text{m}$  to 10  $\mu\text{m}$  at 28%. The summer ranges from 10.1  $\mu\text{m}$  to 15.0  $\mu\text{m}$  at 22%, and the winter and rainy season (25.1  $\mu\text{m}$  to 30.0  $\mu\text{m}$ ) at 18%. COD shows a significant distribution in all three seasons in the range  $\leq 5.0$  at 56%, 48%, and 45%, respectively. The distributions obtained from the Terra and Aqua satellite data show similar results.

The distribution of cloud properties in the central region reveals that the CF distribution is found in winter ( $\leq 0.2$ ) at 56%, summer ( $>0.8$ ) at 48%, and the rainy season ( $>0.8$ ) at 75%. CTP finds an extensive distribution throughout the season in the 100.1 hPa–200 hPa range at 39%, 50%, and 48%, respectively. CTT has a vast distribution in the winter ( $-15\text{ }^{\circ}\text{C}$  to  $-1\text{ }^{\circ}\text{C}$ ) at 39% and then summer ( $-90\text{ }^{\circ}\text{C}$  to  $-76\text{ }^{\circ}\text{C}$ ) at 26%, and rainy season ( $-90\text{ }^{\circ}\text{C}$  to  $-76\text{ }^{\circ}\text{C}$ ) at 30%. CLW shows large distributions in the winter, summer, and rainy seasons in the range ( $\leq 50\text{ g/m}^2$ ) at 61%, 47%, and 45%, respectively. CER demonstrates large distributions in winter (10.1  $\mu\text{m}$  to 15.0  $\mu\text{m}$ ) at 18%, summer (30.1  $\mu\text{m}$  to 40  $\mu\text{m}$ ) at 15%, and the rainy season (15.1  $\mu\text{m}$  to 20.0  $\mu\text{m}$ ) at 16%. COD reveals a large distribution in all three seasons in the range  $\leq 5.0$  at 65%, 59%, and 54%, respectively. The distributions obtained from the Terra and Aqua satellite data have similar results.

In the distribution of cloud properties in the eastern region, CF values are found mostly in all three seasons ( $>0.8$ ) at 38%, 67%, and 86%, respectively. CTP obtains the distribution mostly in winter, in the range of 900.1 hPa to 1000 hPa at 28%; in summer and the rainy season (100.1 hPa to 200 hPa) at 35% and 42%, respectively. CTT appears to have a large distribution in winter ( $-15\text{ }^{\circ}\text{C}$  to  $-1\text{ }^{\circ}\text{C}$ ) at 46%, summer ( $>-1\text{ }^{\circ}\text{C}$ ), and rainy season ( $-90\text{ }^{\circ}\text{C}$  to  $-76\text{ }^{\circ}\text{C}$ ) at 30%. CLW finds a large distribution in the range ( $\leq 50\text{ g/m}^2$ ) at 48%, 28%, and 22%, respectively. CER distributions are found mainly in winter in the range of 10.1  $\mu\text{m}$  to 15  $\mu\text{m}$  at 48%, and then summer (10.1  $\mu\text{m}$  to 15.0  $\mu\text{m}$ ) at 23%, and the rainy season (25.1  $\mu\text{m}$  to 30.0  $\mu\text{m}$ ) at 22%. COD discovers a large distribution in all three seasons in the range  $\leq 5.0$  at 49%, 36%, and 19%. The distributions obtained from the Terra and Aqua satellite data give similar results.

The distribution of cloud properties in the southern and eastern regions shows that CF values are found mainly in the summer and rainy seasons ( $>0.8$ ) at 62% and 83%. CTP is found primarily in the summer and rainy season distributions at 100.1 hPa–200 hPa at 31% and 47%. CTT found a large distribution in the summer ( $-15\text{ }^{\circ}\text{C}$  to  $-1\text{ }^{\circ}\text{C}$ ) at 39% and the rainy season ( $-90\text{ }^{\circ}\text{C}$  to  $-76\text{ }^{\circ}\text{C}$ ) at 34%. CLW finds a large distribution in the summer and rainy seasons ( $\leq 50\text{ g/m}^2$ ) at 40% and 29%. CER displays a large distribution in the summer in the range of 10.1  $\mu\text{m}$  to 15  $\mu\text{m}$  at 21% and in the rainy season in the range of 25.1  $\mu\text{m}$  to 30.0  $\mu\text{m}$  at 21%. COD demonstrates a large distribution in the range  $\leq 5.0$  at 49% and 43% in all two seasons. The distributions obtained from the Terra and Aqua satellite data give similar results.

The distribution of cloud properties in the southern western region shows that CF values are found mainly in the summer and rainy seasons ( $>0.8$ ) at 45%. CTP gives most of the distribution in the summer and rainy seasons at 100.1 hPa – 200 hPa at 44% and 52%. CTT shows a significant distribution in the summer ( $-15\text{ }^{\circ}\text{C}$  to  $-1\text{ }^{\circ}\text{C}$ ) at 27% and the rainy season ( $-90\text{ }^{\circ}\text{C}$  to  $-76\text{ }^{\circ}\text{C}$ ) at 38%. CLW found a large distribution in the summer and rainy seasons ( $\leq 50\text{ g/m}^2$ ) at 49% and 31%. CER finds

a large distribution in the summer in the range of 10.1  $\mu\text{m}$  to 15  $\mu\text{m}$  at 21% and in the rainy season in the range of 30.1  $\mu\text{m}$  to 35.0  $\mu\text{m}$  at 21%. COD retrieves a large distribution in both seasons in the range  $\leq 5.0$  at 57% and 47%. The distributions obtained from the Terra and Aqua satellite data show similar results.

## 2. The University of Manchester

The distribution of cloud properties in Spring, Summer, Autumn, and Winter at The University of the distribution of cloud properties in Spring, Summer, Autumn, and Winter at The University of Manchester is shown in Figures 45–46. The CF distributions are  $>0.8$  all seasons at 61%, 50%, 61%, and 73%, respectively. The CTP values have a large distribution every season, ranging from 900.1 to 1000 at 27%, 29%, 23%, and 26%, respectively. CTT had a distribution value of  $-30$  °C to  $-16$  °C every season at 44%, 39%, 34%, and 40%, respectively. CLW had a value  $\leq 50$  g/m<sup>2</sup> every season at 34%, 44%, 37%, and 34%, respectively. CER values have a significant distribution value in spring, which range from 10.1  $\mu\text{m}$  to 15.0  $\mu\text{m}$  at 23%. Summer ranges from 5.1  $\mu\text{m}$  to 10.0  $\mu\text{m}$  at 26%. Autumn is in the range of 10.1  $\mu\text{m}$  to 15.0  $\mu\text{m}$  at 20%, and winter is in the range of 5.1  $\mu\text{m}$  to 10.0  $\mu\text{m}$  at 25%. COD values have a large distribution every season, with a value of  $\leq 5.0$  at 33%, 40%, 44%, and 39%, respectively. The distributions obtained from the Terra and Aqua satellite data give similar results. The distributions of cloud properties in each season have a similar distribution pattern.

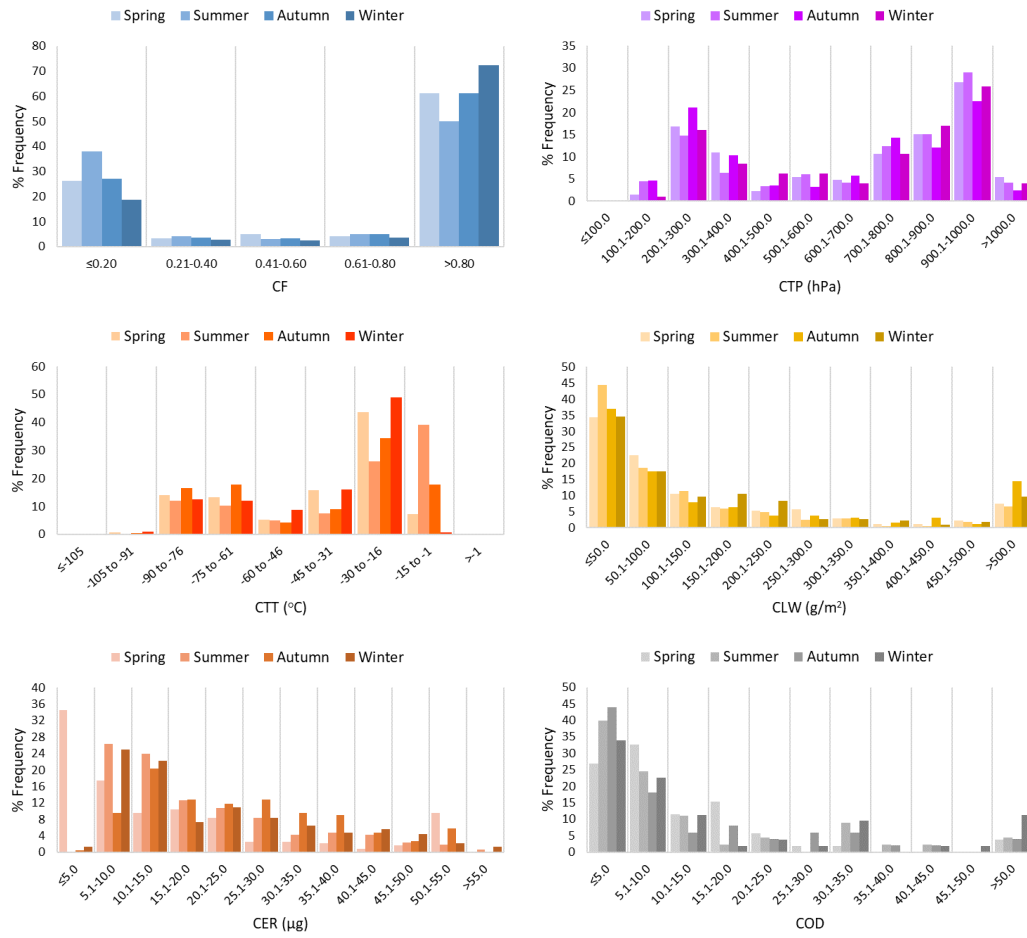


Figure 45 Distribution of cloud properties in the University of Manchester using Terra satellite data.

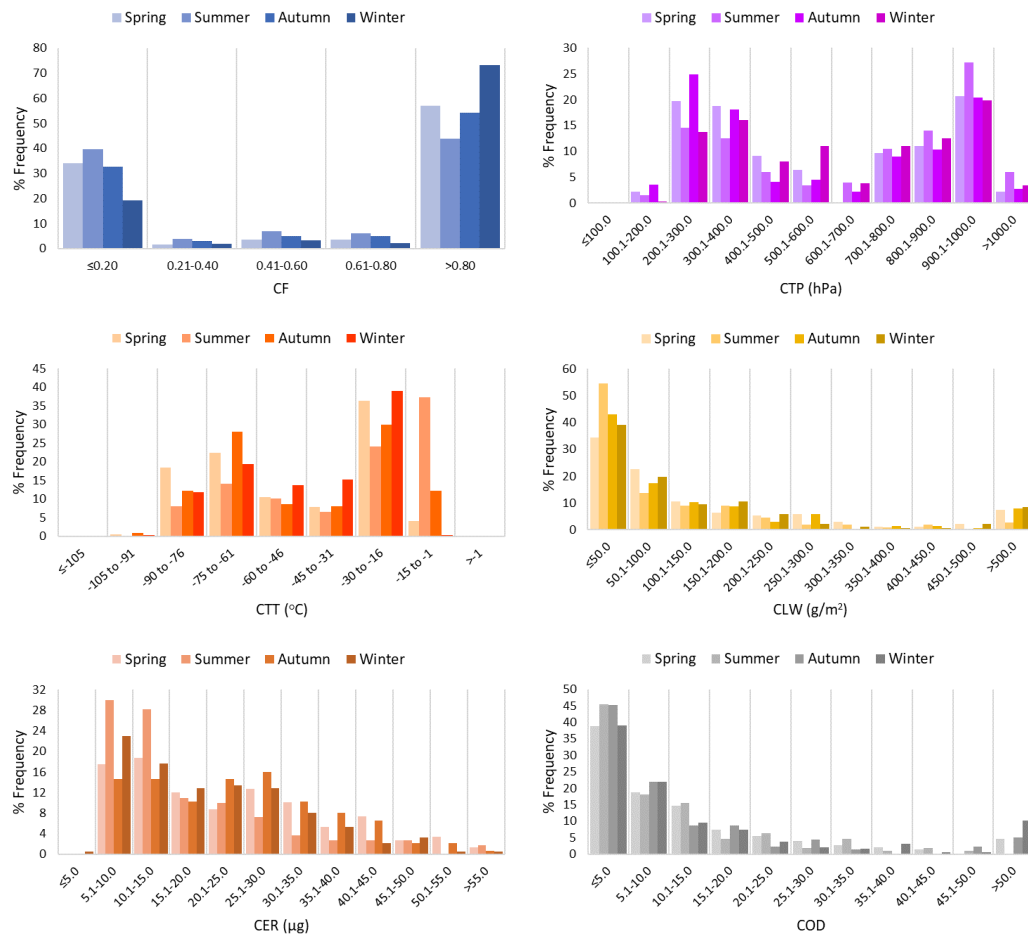


Figure 46 Distribution of cloud properties in the University of Manchester using Aqua satellite data.

### CLOUD PROPERTIES IN DIFFERENT CLIMATES (BANGKOK AND THE UNIVERSITY OF MANCHESTER)

Comparing the properties of clouds in the Thai meteorology department and The University of Manchester stations shown in Figures 47–48, the monthly changes in cloud properties are as follows

CF values in Bangkok station are high in the rainy season (June to September) and low in the winter (November–February), while The University of Manchester station is high in the Autumn to winter (October to February) and low in the summer to autumn (June to September).

COD values in Bangkok station are high from January to March (winter) and low during the rainy season. While The University of Manchester station is high from March to October (spring to autumn), while low COD was detected from March to October (spring to autumn).

CTP in Bangkok is high during winter. From December to February and low during the rainy season, The University of Manchester was high in June to August (summer), while low CTP was detected from September to January (autumn to winter).

CTT in Bangkok is high during winter, from December to February, and low during the rainy season. The University of Manchester's CTT was high from June to August (summer), while low CTT was detected from November to February (autumn to winter).

CER in Bangkok is high during the summer. From March to May and low during the rainy season From June to September. The University of Manchester was high from September to November (autumn), while low CER was detected from December to July (winter to summer).

CLW in Bangkok is high during rainy times (March to October). It is low during the winter, from November to February. The University of Manchester has high values from November to February (autumn to winter), while low CLW was detected from May to August (spring to summer).

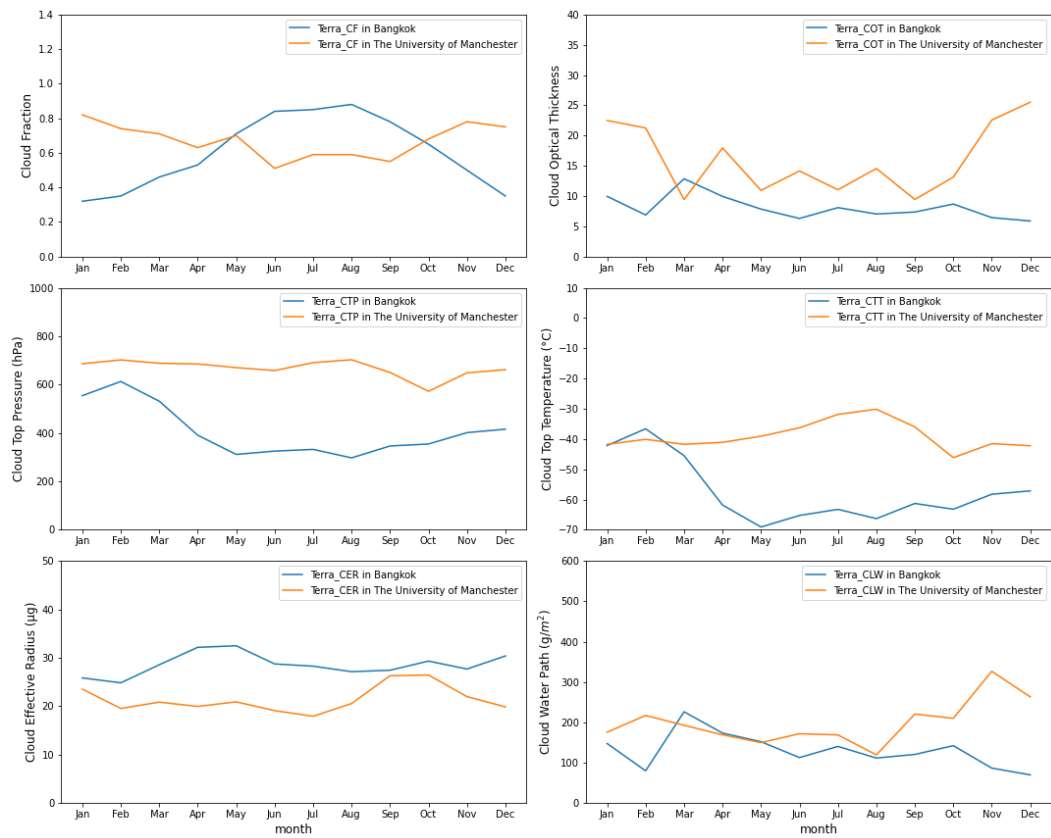


Figure 47 The relationship between cloud properties in Bangkok and the University of Manchester using Terra satellite data.



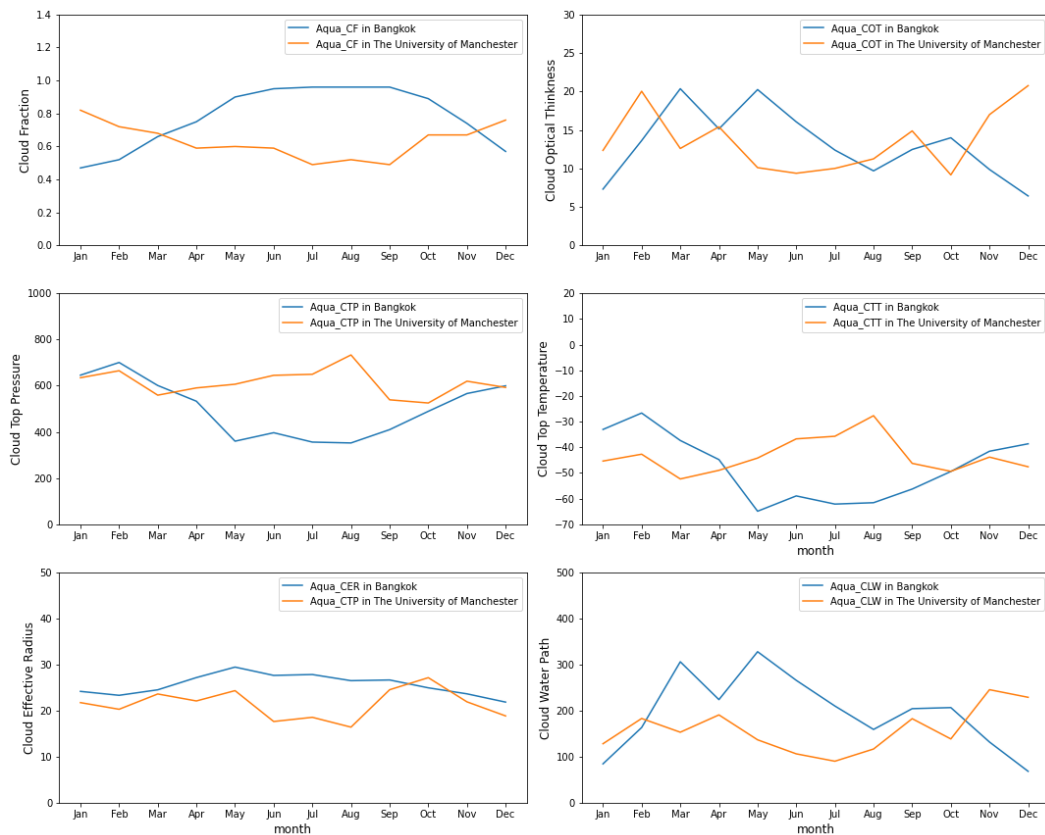


Figure 48 The relationship between cloud properties in Bangkok and the University of Manchester using Aqua satellite data.

## ASSESS THE POSSIBILITY OF RAIN CLOUDS IN THE DUST PERIOD, PM2.5 IS HIGHER THAN THE STANDARD

The variation in high PM2.5 concentration values in Thailand. It was found that:

The central region had high PM2.5 concentration values from December to February (Figure 49).

The northern and northeast had high PM2.5 concentration values from February to April (Figure 50).

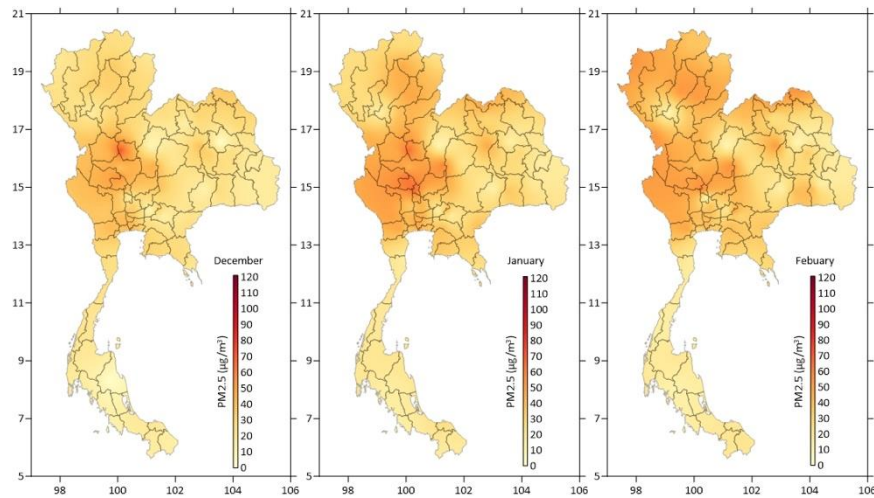


Figure 49 Time series of the monthly mean high PM 2.5 levels in the northern region during the month of December to February.

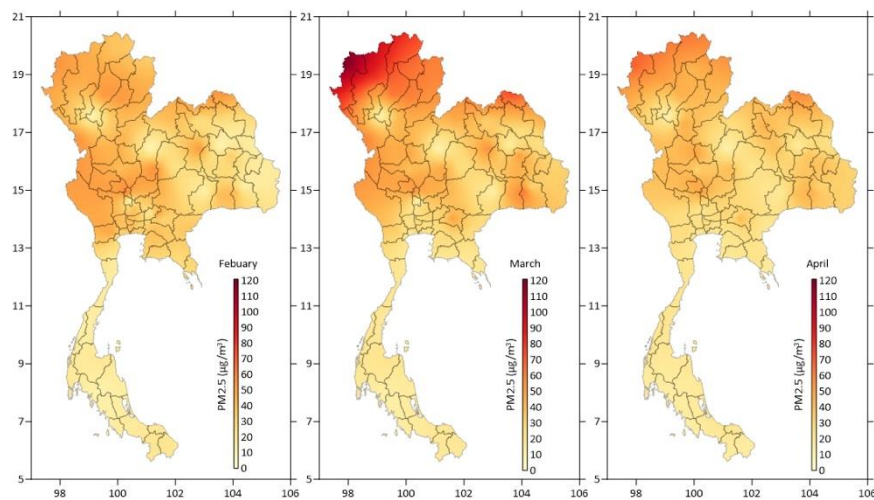


Figure 50 Time series of the monthly mean high PM 2.5 levels in the central and Northeastern region during the months of December to February.

Distribution of cloud properties during periods of high PM<sub>2.5</sub> concentration values in Thailand (Table 5). The results of the study are as follows:

1. Cloud Fraction (CF) is less than 0.2, accounting for 67% of the distribution, while CF is greater than 0.8, accounting for 20%.
2. Cloud Top Pressure (CTP) values greater than 800 hPa account for 31% of the distribution, followed by values less than 200 hPa, which account for 10%.

3. Cloud Top Temperatures (CTT) greater than  $-15\text{ }^{\circ}\text{C}$  account for 60% of the distribution, followed by CTTs less than  $-76\text{ }^{\circ}\text{C}$ , accounting for 8%.

4. Cloud Effective Radius (CER), which is less than  $15\text{ }\mu\text{m}$ , accounts for 32% of the distribution.

5. Cloud Optical Thickness (COD) less than 5.0 accounted for 63% of the distribution. However, COD did not vary seasonally.

6. Cloud Water Path (CLW) less than  $50\text{ g/m}^2$ , accounting for 61% of the distribution, with no seasonal differences.

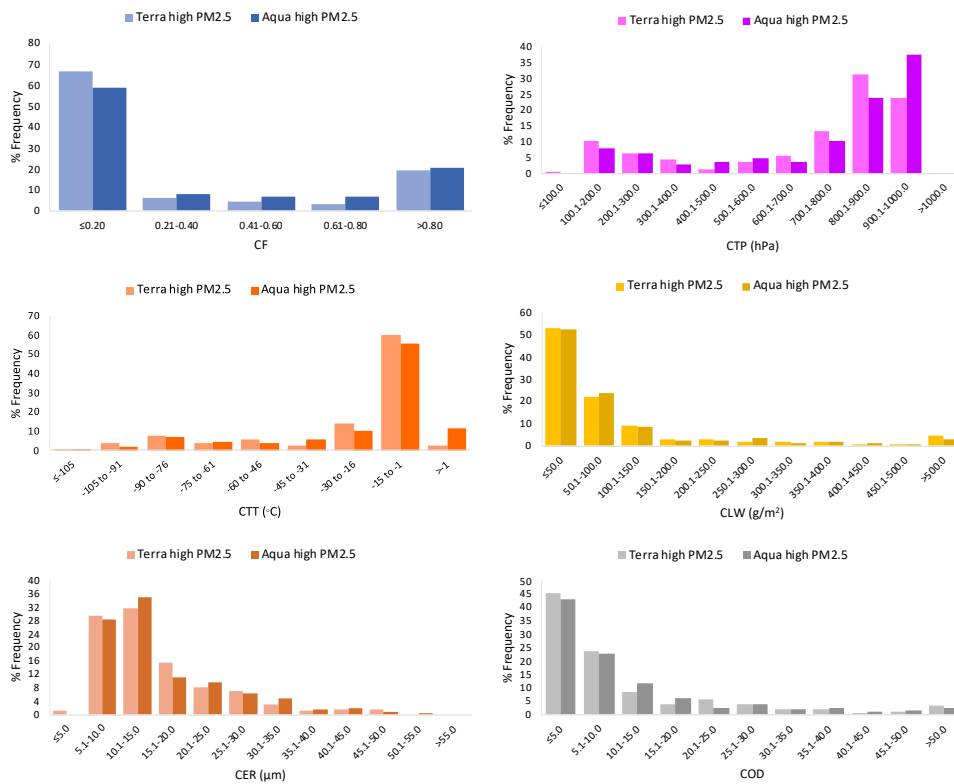


Figure 51 Distribution of cloud properties in Bangkok during high PM2.5

Table 5 Shows a comparison of cloud properties during the high PM2.5 and rainy seasons.

Cloud properties	High PM2.5	Rainy
------------------	------------	-------

CF	$\leq 0.2$	$> 0.8$
CTP	$> 800$ hPa	$< 200$ hPa
CTT	$> -15$ °C	$< -76$ °C
CLW	$< 50$ g/m <sup>2</sup>	$< 50$ g/m <sup>2</sup>
CER	$< 15$ $\mu$ m	$< 20$ $\mu$ m
COD	$< 5$	$< 5$

Considering Table 5, the distribution of cloud properties during the rainy season and dry season, the Rain cloud properties are defined. From the conditions of rain cloud properties, on days with PM<sub>2.5</sub> values exceeding the standard, were found Rain cloud properties, divided by region as follows:

Central Region is Bangkok, Nakhon Pathom, Kanchanaburi, Nakhon Sawan, Samut Prakan, Samut Sakhon, and Saraburi

Northeast Region is Khon Kaen, Nakhon Ratchasima, Bueng Kan, Buriram, and Roi Et

Northern Region is Chiang Mai, Lampang, Lamphun, Nan, Phayao, Phrae, Phichit, and Tak

Southern Region: Songkhla, and Pattani

Eastern Region: Chon Buri, Chachoengsao, and Prachin Buri

Each province in each region is counted together, and the results of the study are as follows:

Northern Region: The days with PM<sub>2.5</sub> levels exceeding the standard were 2,349 days, and days with PM<sub>2.5</sub> levels exceeding the standard and observed rain cloud properties were 11 days.

Central Region: The days with PM<sub>2.5</sub> levels exceeding the standard were 1,996 days, and days with PM<sub>2.5</sub> levels exceeding the standard and observed rain cloud properties were 17 days.

Northeastern Region: The days with PM2.5 levels exceeding the standard were 1,259 days, and days with PM2.5 levels exceeding the standard and observed rain cloud properties were 30 days.

Eastern Region: The days with PM2.5 levels exceeding the standard were 196 days, and days with PM2.5 levels exceeding the standard and observed rain cloud properties were 7 days.

Southern Region: The days with PM2.5 levels exceeding the standard were 51 days, and days with PM2.5 levels exceeding the standard and observed rain cloud properties were 3 days.

This section evaluated the possibility of rain cloud occurrence during high PM2.5 concentrations. It was found that rain cloud properties on days with high PM2.5 concentrations were observed in all regions. The funding was slight but valuable enough to use those clouds to operate Royal Rainmaking.

## CHAPTER V

### CONCLUSION

A study of monthly variations in aerosol particles and cloud properties in Thailand and The University of Manchester using Terra (2002–2022) and Aqua (2000–2022) satellite data. In a whole region, high AOD values were observed from February to April (summer), and low AOD values were observed from October to January (dry season). In contrast, the Southern region experiences consistent AOD values except in monsoon season. The monthly AOD obtained from the Terra and Aqua satellite data gave similar results.

The northern region tends to have high PM<sub>2.5</sub> values from January to April. The central region demonstrated high PM<sub>2.5</sub> values from December to April. The Northeastern and northern trends are similar except in the southern region, with the PM<sub>2.5</sub> trend remaining constant throughout the year. PM<sub>2.5</sub> concentrations are low in all areas throughout Thailand from May to October (rainy).

High CF data were found from May to July (during the rainy season), while low data were detected from December to February (during the winter). There is a similar pattern over Thailand, except in the Southern region.

CER levels were high from May to August, coinciding with the rainfall season, and low from December to February, coinciding with the rainfall season. There is a similar pattern over Thailand, except in the Southern region.

COD data showed high levels during the rainy season from May to October and low levels during the winter from November to April. In the southern region, COD high values are evident during the rainy season from October to January.

CWP values were high from summer to rainy times (March to October). They were low during the winter from November to February. It is evident in the

Southern region that the values were high during the rainy season from October to December.

CTP values are high from November to February during the winter and low from June to July during the rainy season in all regions of Thailand. The pattern is similar in all regions except the southern region.

CTT values were found to be high from November to February during the winter season. They are low during the rainy season, from May to October. In the south, they are high from May to December (during the rainy season) and low during the summer.

PM<sub>2.5</sub> concentrations in the Thai meteorological department and The University of Manchester found that Thailand has high PM<sub>2.5</sub> concentration values from the beginning of winter to the start of summer (December to April). In the Southern region, PM<sub>2.5</sub> remains the same. There are also concentrations variations at the University of Manchester, with high PM<sub>2.5</sub> concentration values from November to April. Low PM<sub>2.5</sub> concentrations were detected from May to October (late Spring to late Autumn)

Finding cloud properties during high PM<sub>2.5</sub> concentrations is vital because aerosol in the atmosphere influences the properties of clouds. Clouds are an essential variable in the occurrence of rain. To solve the problem of PM<sub>2.5</sub>, we study the properties of clouds, including Cloud Fraction (CF), Cloud Effective Radius (CER), Cloud Water Path (CLW), Cloud Optical Thickness (COD), Cloud Top Temperature (CTT), and Cloud Top Pressure (CTP) during high PM<sub>2.5</sub> concentrations. It was found as below:

1. Cloud Fraction (CF) less than 0.2.
2. Cloud Top Pressure (CTP) values greater than 800 hPa.
3. Cloud Top Temperatures (CTT) greater than  $-15$  °C.
4. Cloud Optical Thickness (COD) less than 5.0
5. Cloud Effective Radius (CER) less than  $15$  g/m<sup>2</sup>.
6. Cloud Water Path (CLW) less than 50  $\mu$ m.

While cloud properties during the rainy season are as follows:

1. Cloud Fraction (CF) is more significant than 0.8.
2. Cloud Top Pressure (CTP) values less than 200 hPa.
3. Cloud Top Temperatures (CTT) less than  $-76$  °C.
4. Cloud Optical Thickness (COD) less than 5.0
5. Cloud Effective Radius (CER) less than 20  $\mu\text{m}$ .
6. Cloud Water Path (CLW) less than 50  $\text{g/m}^2$ .



## REFERENCES

## REFERENCES

- Albrecht., B. A. (1989). Aerosols, Cloud Microphysics, and Fractional Cloudiness. *Science*, 245, 1227–1230.  
<https://doi.org/https://doi.org/10.1126/science.245.4923.1227>
- AMS. (2023). liquid water path. Retrieved 18 April from  
[https://glossary.ametsoc.org/wiki/Liquid\\_water\\_path](https://glossary.ametsoc.org/wiki/Liquid_water_path)
- Chula. (2023, 28 March 2023). Chapter II Descriptive statistics.  
<http://pioneer.netserv.chula.ac.th/~jaimorn/b2st.htm>
- Environment, N. (2010). Set standards for particulate matter less than 2.5 microns in the atmosphere in general. <http://slbkb.psu.ac.th/jspui/bitstream/2558/2556/1/ฉบับที่%2036%20%28พ.ศ.%202553%29%20เรื่อง%20กำหนดมาตรฐานฝุ่นละอองขนาดไม่เกิน%202.5%20ไมครอน%20ในบรรยากาศโดยทั่วไป.pdf>
- Fan, C., Wang, M., Rosenfeld, D., Zhu, Y., Liu, J., & Chen, B. (2020). Strong Precipitation Suppression by Aerosols in Marine Low Clouds. *Geophysical Research Letters*, 47. <https://doi.org/10.1029/2019GL086207>
- Garreatt, T. J., & Zhao, C. (2006). Increased Arctic cloud longwave emissivity associated with pollution from mid-latitudes. *Nature*, 440.  
<https://doi.org/10.1038/nature04636>
- Gauderman, W. J., Gilliland, G. F., Vora, H., Avol, E., Stram, D., McConnell, R., Thomas, D., Lurmann, F., Margolis, H. G., Rappaport, E. B., Berhane, K., & Peters, J. M. (2002). Association between air pollution and lung function growth in southern California children: results from a second cohort. *Am J Respir Crit Care Med*, 166, 76–84. <https://doi.org/10.1164/rccm.2111021>
- Hartmann, D. L. (2016). *Global physical climatology*. In: Elsevier, Amsterdam, Netherlands.
- IPCC. (2007). *Climate Change Geneva*.

- iSTAR. (2023). MODIS imagery. Retrieved from [https://istar-gis-features-testing.data.bas.ac.uk/remote\\_sensing/modis/](https://istar-gis-features-testing.data.bas.ac.uk/remote_sensing/modis/)
- King, M. D., Member, S., IEEE, Platnick, S., Menzel, W. P., A, S., Ackerman, & Ackerman, S. A. (2013). Spatial and Temporal Distribution of Clouds Observed by MODIS Onboard the Terra and Aqua Satellites. *IEEE*, 50, 3826–3852.
- Koren, I., Altaratz, O., Remer, L. A., Feingold, G., Martins, J. V., & Heiblum, R. H. (2012). Aerosol-induced intensification of rain from the tropics to the mid-latitudes. *Nature Geoscience*, 5, 118–122.
- Kumharn, W. (2016). *Atmospheric Aerosol* (1 ed.). Chulalongkorn University.
- Liou, K. N. (2002). *An Introduction to Atmospheric Radiation* (Vol. 84).
- NASA. (2023a). In (pp. Image of the Terra spacecraft with transparent background.).
- NASA. (2023b). Cloud Effective Radius. Retrieved 18 April from [https://web.archive.org/web/20090724155507/http://disc.sci.gsfc.nasa.gov/PIP/shtml/cloud\\_effective\\_radius.shtml](https://web.archive.org/web/20090724155507/http://disc.sci.gsfc.nasa.gov/PIP/shtml/cloud_effective_radius.shtml)
- NASA. (2023c). Cloud Fraction. Retrieved 18 April from [https://earthobservatory.nasa.gov/global-maps/MODAL2\\_M\\_CLD\\_FR](https://earthobservatory.nasa.gov/global-maps/MODAL2_M_CLD_FR)
- NASA. (2023d). MODERATE RESOLUTION IMAGING SPECTRORADIOMETER. Retrieved from <https://modis.gsfc.nasa.gov/>
- NASA. (2023e). MODIS Aerosol Product. Retrieved from <https://modis.gsfc.nasa.gov/data/dataproduct/mod04.php>
- NASA. (2023f). MODIS Cloud Product. Retrieved from <https://modis.gsfc.nasa.gov/data/dataproduct/mod06.php>
- NCAR. (2023). Liquid Water Path: Overview. Retrieved 18 April from [https://climatedataguide.ucar.edu/climate-data/liquid-water-path-overview?fbclid=IwAR1A9fhV9\\_k29vFhvhFTkYyqiQpoG3hhF1AENyrAdhL2qbWqHmmi2VYW-lo](https://climatedataguide.ucar.edu/climate-data/liquid-water-path-overview?fbclid=IwAR1A9fhV9_k29vFhvhFTkYyqiQpoG3hhF1AENyrAdhL2qbWqHmmi2VYW-lo)
- Pilahome, O., Nissawan, W., Jankondee, Y., Masiri, I., & Kumharn, W. (2023). Variations in aerosols and aerosols–cloud interactions in Bangkok using MODIS

satellite data during high PM<sub>2.5</sub> concentrations. *Advances in Space Research*, 71, 3166–3174. <https://doi.org/https://doi.org/10.1016/j.asr.2022.12.018>

Stull, R. (2016). *Practical Meteorology: An Algebra-based Survey of Atmospheric Science*. Sundog Publishing LLC.

UCAR. (2023). Cirrus Clouds. Retrieved 12 April from <https://scied.ucar.edu/image/cirrus-clouds>

WMO. (2017). Definition of a cloud. Retrieved 10 April from <https://cloudatlas.wmo.int/en/clouds.html>

## APPENDICE

APPENDICE A

DATA

## APPENDICE A

## DATA

APPENDICE Table A1 Cloud Fraction average monthly data on Aqua satellite.

Stations	Jan	Feb	Mar	Apr	May	Jun	Jul	Aug	Sep	Oct	Nov	Dec
Bangkok	0.44	0.53	0.65	0.73	0.88	0.95	0.96	0.96	0.96	0.86	0.69	0.56
Samut Prakan	0.32	0.41	0.57	0.66	0.82	0.87	0.90	0.91	0.87	0.74	0.57	0.48
Nonthaburi	0.43	0.54	0.65	0.79	0.93	0.97	0.99	0.99	0.99	0.87	0.69	0.56
Samut Sakhon	0.32	0.35	0.50	0.67	0.88	0.90	0.93	0.94	0.92	0.77	0.56	0.50
Pathum Thani	0.38	0.51	0.65	0.79	0.95	0.97	0.96	0.97	0.97	0.83	0.56	0.43
Phra Nakhon Si Ayutthaya	0.36	0.51	0.65	0.78	0.94	0.98	0.97	0.99	0.98	0.82	0.54	0.47
Saraburi	0.34	0.36	0.44	0.65	0.89	0.96	0.97	0.96	0.91	0.64	0.52	0.43
Ratchaburi	0.25	0.20	0.34	0.42	0.73	0.80	0.85	0.88	0.80	0.62	0.51	0.39
Rayong	0.33	0.40	0.48	0.58	0.84	0.83	0.86	0.85	0.85	0.63	0.44	0.39
Chon Buri	0.54	0.63	0.71	0.82	0.94	0.97	0.97	0.98	0.97	0.88	0.71	0.57
Chiang Mai	0.31	0.25	0.25	0.52	0.78	0.95	0.96	0.94	0.87	0.67	0.44	0.41
Lampang	0.38	0.36	0.36	0.54	0.79	0.93	0.94	0.94	0.85	0.68	0.42	0.41
Nakhon Sawan	0.33	0.40	0.46	0.65	0.89	0.97	0.96	0.98	0.97	0.82	0.60	0.38
Phuket	0.42	0.39	0.48	0.66	0.81	0.80	0.85	0.78	0.84	0.79	0.75	0.71
Surat Thani	0.79	0.72	0.67	0.77	0.92	0.91	0.91	0.92	0.93	0.93	0.88	0.87
Songkhla	0.81	0.74	0.75	0.80	0.88	0.89	0.89	0.86	0.92	0.93	0.90	0.91
Khon Kean	0.36	0.42	0.56	0.71	0.93	0.99	0.98	0.97	0.90	0.64	0.49	0.43
Nakhon Ratchasima	0.35	0.42	0.56	0.73	0.86	0.95	0.98	0.98	0.92	0.73	0.58	0.50
Chachoengsao	0.43	0.63	0.71	0.79	0.91	0.94	0.94	0.97	0.94	0.80	0.53	0.47
Narathiwat	0.87	0.79	0.72	0.75	0.88	0.89	0.91	0.88	0.87	0.91	0.91	0.93
Yala	0.84	0.78	0.75	0.81	0.87	0.84	0.88	0.83	0.91	0.91	0.90	0.92
Mae Hong Son	0.51	0.25	0.33	0.61	0.87	0.96	0.97	0.94	0.91	0.77	0.53	0.41
Chiang Rai	0.34	0.26	0.27	0.42	0.78	0.96	0.96	0.93	0.79	0.64	0.42	0.40
Nan	0.22	0.23	0.34	0.48	0.86	0.92	0.95	0.94	0.90	0.65	0.43	0.36
Lamphun	0.29	0.21	0.23	0.38	0.79	0.97	0.98	0.98	0.90	0.71	0.47	0.38
Phrae	0.24	0.30	0.34	0.45	0.76	0.86	0.93	0.92	0.79	0.54	0.28	0.26
Phayao	0.37	0.28	0.27	0.53	0.76	0.95	0.96	0.94	0.84	0.67	0.44	0.42
Sa Kaeo	0.50	0.49	0.67	0.80	0.94	0.97	0.97	0.96	0.92	0.71	0.56	0.58
Loei	0.31	0.33	0.49	0.68	0.88	0.97	0.97	0.98	0.92	0.73	0.50	0.42
Tak	0.35	0.38	0.44	0.67	0.91	0.96	0.96	0.97	0.93	0.75	0.52	0.43
Prachin Buri	0.36	0.50	0.62	0.75	0.92	0.96	0.97	0.97	0.94	0.78	0.62	0.49
Kanchanaburi	0.40	0.35	0.46	0.64	0.89	0.96	0.98	0.99	0.96	0.87	0.70	0.53
Satun	0.72	0.66	0.77	0.85	0.90	0.85	0.89	0.84	0.94	0.94	0.91	0.87
Nong Khai	0.29	0.37	0.48	0.66	0.90	0.95	0.96	0.95	0.87	0.69	0.46	0.36
Nakhon Pathom	0.38	0.35	0.48	0.62	0.85	0.91	0.94	0.95	0.91	0.80	0.63	0.53
Ubon Ratchathani	0.38	0.44	0.65	0.83	0.95	0.98	0.96	0.96	0.87	0.72	0.62	0.46
Samut Songkhram	0.23	0.22	0.36	0.42	0.73	0.81	0.83	0.86	0.84	0.67	0.44	0.37
Suphan buri	0.40	0.51	0.62	0.73	0.89	0.90	0.92	0.95	0.95	0.82	0.56	0.48
Phitsanulok	0.36	0.35	0.42	0.63	0.90	0.99	0.99	0.99	0.95	0.82	0.60	0.50
Trat	0.59	0.78	0.83	0.87	0.92	0.94	0.95	0.97	0.96	0.86	0.66	0.55
Nakhon Phanom	0.31	0.43	0.56	0.74	0.88	0.94	0.91	0.93	0.84	0.64	0.48	0.34
Sakon Nakhon	0.32	0.42	0.56	0.70	0.86	0.91	0.93	0.94	0.83	0.65	0.51	0.38
Udon Thani	0.35	0.39	0.47	0.68	0.92	0.98	0.98	0.98	0.92	0.72	0.50	0.39
Uttaradit	0.33	0.30	0.37	0.59	0.89	0.98	0.97	0.98	0.93	0.66	0.46	0.39
Trang	0.62	0.61	0.70	0.85	0.94	0.89	0.91	0.89	0.93	0.94	0.91	0.82
Kampangphet	0.36	0.31	0.39	0.61	0.87	0.93	0.95	0.96	0.91	0.73	0.48	0.43
Nakhon Nayok	0.40	0.51	0.65	0.79	0.92	0.98	0.97	0.96	0.94	0.76	0.60	0.47
Pichit	0.37	0.40	0.45	0.68	0.91	0.98	0.98	0.98	0.89	0.66	0.66	0.46
Phetchaboon	0.35	0.30	0.47	0.64	0.85	0.95	0.95	0.97	0.91	0.71	0.54	0.43

Stations	Jan	Feb	Mar	Apr	May	Jun	Jul	Aug	Sep	Oct	Nov	Dec
Lopburi	0.38	0.54	0.60	0.76	0.92	0.97	0.98	0.99	0.95	0.78	0.55	0.46
Singburi	0.36	0.44	0.54	0.68	0.89	0.96	0.99	0.99	0.96	0.73	0.58	0.51
Sukhothai	0.36	0.32	0.35	0.51	0.82	0.96	0.95	0.95	0.90	0.67	0.48	0.46
Angthong	0.44	0.48	0.63	0.80	0.94	0.97	0.99	1.00	0.97	0.85	0.63	0.54
Uthaitani	0.24	0.26	0.37	0.53	0.83	0.94	0.95	0.98	0.91	0.71	0.59	0.47
Kalasin	0.54	0.39	0.50	0.67	0.93	0.98	0.98	0.97	0.88	0.65	0.49	0.38
Chaiyaphom	0.35	0.43	0.53	0.66	0.91	0.97	0.98	0.99	0.91	0.67	0.55	0.44
Buriram	0.38	0.50	0.63	0.84	0.95	0.98	0.97	0.95	0.90	0.75	0.61	0.51
Mahasarakham	0.31	0.45	0.62	0.81	0.98	0.99	0.98	0.96	0.88	0.64	0.53	0.42
Mukdahan	0.35	0.41	0.59	0.73	0.89	0.94	0.92	0.92	0.85	0.68	0.58	0.46
Yasothon	0.36	0.46	0.56	0.74	0.95	0.98	0.98	0.97	0.91	0.67	0.52	0.41
Roeit	0.32	0.39	0.58	0.81	0.95	0.98	0.99	0.96	0.87	0.65	0.54	0.46
Srisaket	0.39	0.45	0.62	0.82	0.95	0.98	0.97	0.96	0.88	0.72	0.65	0.48
Surin	0.59	0.46	0.60	0.85	0.94	0.96	0.97	0.97	0.94	0.71	0.62	0.50
Nangbualamphum	0.32	0.40	0.49	0.66	0.91	0.97	0.96	0.98	0.93	0.73	0.52	0.45
Amnatcharoun	0.36	0.44	0.60	0.79	0.95	0.97	0.98	0.97	0.87	0.67	0.58	0.44
Bungkan	0.29	0.36	0.45	0.60	0.85	0.93	0.92	0.90	0.78	0.55	0.33	0.28
Chanthaburi	0.52	0.65	0.74	0.83	0.92	0.93	0.93	0.96	0.95	0.81	0.61	0.50
PhatBuri	0.30	0.23	0.37	0.40	0.71	0.80	0.84	0.86	0.81	0.70	0.52	0.39
Prachuabkirikhan	0.36	0.36	0.44	0.47	0.76	0.82	0.82	0.84	0.83	0.69	0.53	0.45
Krabi	0.56	0.53	0.60	0.73	0.81	0.77	0.82	0.78	0.84	0.85	0.82	0.77
Nakhon Srithammarat	0.77	0.73	0.76	0.84	0.93	0.93	0.95	0.90	0.96	0.96	0.89	0.86
Phatthani	0.73	0.64	0.63	0.64	0.84	0.87	0.89	0.83	0.91	0.91	0.85	0.86
Phanga	0.61	0.55	0.64	0.72	0.88	0.89	0.91	0.89	0.91	0.90	0.83	0.73
Phatthalung	0.71	0.68	0.64	0.72	0.89	0.88	0.90	0.92	0.93	0.89	0.82	0.84
Ranong	0.60	0.43	0.46	0.58	0.88	0.86	0.90	0.83	0.90	0.81	0.79	0.78
Chumphon	0.52	0.45	0.47	0.56	0.79	0.81	0.85	0.86	0.81	0.78	0.74	0.72
Chai Nat	0.33	0.31	0.42	0.65	0.89	0.95	0.95	0.97	0.95	0.76	0.52	0.51

APPENDICE Table A2 Cloud Effective Radius average monthly data on Aqua satellite.

Stations	Jan	Feb	Mar	Apr	May	Jun	Jul	Aug	Sep	Oct	Nov	Dec
Bangkok	24.18	23.33	24.52	27.17	29.44	27.64	27.83	26.50	26.65	24.95	23.65	21.86
Samut Prakan	27.81	25.70	27.14	29.83	30.34	28.39	28.65	27.84	29.11	29.49	26.68	27.79
Nonthaburi	19.19	17.53	18.88	22.39	22.41	21.60	22.37	22.00	22.12	21.39	20.97	21.36
Samut Sakhon	25.18	23.56	26.86	25.81	26.56	25.87	25.93	24.23	24.79	23.95	24.36	22.86
Pathum Thani	22.48	19.93	20.86	22.11	25.13	24.45	23.70	22.96	24.60	24.98	25.60	23.80
Phra Nakhon Si Ayutthaya	21.70	23.05	20.91	22.58	25.97	24.24	23.96	23.82	25.33	23.64	22.99	22.18
Saraburi	17.04	16.67	19.27	19.55	22.16	20.98	23.32	23.52	25.88	22.62	20.32	18.47
Ratchaburi	28.43	27.61	29.66	33.41	31.08	26.61	26.73	25.59	28.34	31.11	30.19	28.77
Rayong	27.56	26.20	29.76	33.23	32.15	29.35	29.49	26.86	29.40	29.64	28.89	30.30
Chon Buri	18.73	19.17	21.32	25.83	27.87	25.78	26.43	24.19	25.47	25.62	22.14	21.20
Chiang Mai	15.35	17.82	16.94	19.65	21.05	21.29	23.37	23.48	25.45	22.24	17.10	14.47
Lampang	15.05	16.03	18.26	19.66	22.27	21.97	24.32	24.72	25.97	23.57	18.57	15.07
Nakhon Sawan	16.67	15.14	17.99	17.90	20.57	20.53	22.38	22.17	22.28	21.59	19.17	17.89
Phuket	27.17	31.86	33.33	32.89	32.89	31.65	31.34	31.06	29.77	31.52	31.80	28.75
Surat Thani	20.22	18.19	23.97	26.80	27.81	27.77	27.29	26.40	27.34	29.16	27.60	23.25
Songkhla	21.02	20.96	21.51	25.36	27.20	28.40	28.23	26.16	27.12	27.94	28.97	24.60
Khon Kean	15.44	14.07	16.68	18.56	20.88	22.82	23.99	24.22	26.05	21.68	17.81	16.72
Nakhon Ratchasima	17.92	18.42	20.44	24.60	26.29	23.74	22.87	23.57	27.17	23.51	19.95	17.07
Chachoengsao	18.79	17.88	22.26	24.94	25.00	24.05	24.95	24.45	24.18	23.73	22.17	20.52
Narathiwat	21.72	20.08	23.05	26.99	27.64	27.90	26.65	27.24	26.56	28.61	29.74	26.15
Yala	20.39	20.16	22.24	25.35	26.94	28.26	27.40	26.31	26.01	28.77	29.07	24.63
Mae Hong Son	14.99	14.10	16.84	21.58	22.60	22.32	24.17	24.20	25.92	21.56	18.03	16.55
Chiang Rai	14.20	16.35	18.24	18.19	22.72	20.18	23.48	25.70	26.47	22.17	16.23	12.23



Stations	Jan	Feb	Mar	Apr	May	Jun	Jul	Aug	Sep	Oct	Nov	Dec
Nan	29.06	28.27	31.29	28.36	32.31	31.26	31.19	30.91	30.51	30.34	32.37	29.96
Lamphun	15.98	18.84	17.97	19.86	22.40	20.39	23.45	24.06	24.56	21.66	17.06	15.06
Phrae	19.27	17.83	22.74	24.13	24.29	24.99	26.99	25.75	30.06	26.88	20.84	17.96
Phayao	14.33	15.71	18.24	20.98	22.48	21.02	24.15	25.06	27.07	22.71	16.68	12.99
Sa Kaeo	17.15	18.72	19.08	21.69	27.52	24.56	24.02	23.74	26.46	26.18	23.65	18.73
Loei	16.60	16.77	17.56	19.58	23.07	24.19	25.47	25.58	25.69	20.43	17.12	14.87
Tak	15.37	16.22	19.10	22.34	24.19	22.99	24.33	23.83	26.56	23.62	18.16	16.84
Prochin Buri	20.00	20.14	21.55	21.73	24.75	25.47	24.18	24.73	24.97	24.02	20.56	20.55
Kanchanaburi	21.52	20.38	24.49	24.81	25.71	22.91	23.04	23.69	22.91	24.13	21.92	20.06
Satun	21.11	19.00	21.25	26.27	27.28	28.23	28.41	26.55	27.00	27.26	28.77	25.25
Nong Kai	14.89	17.28	15.41	19.28	20.12	23.74	25.47	26.36	27.60	20.42	16.99	14.08
Nakhon Pathom	27.57	23.80	27.88	31.12	28.84	27.05	26.15	24.99	25.96	26.62	25.87	25.40
Ubon Ratchathani	18.64	16.50	17.84	20.03	21.70	25.18	24.73	24.99	26.97	23.60	19.82	17.10
Samut Songkhram	30.65	30.82	29.22	33.17	31.56	26.62	27.85	26.33	27.76	28.84	30.46	28.19
Suphan buri	22.52	21.26	21.30	23.92	26.30	25.33	24.38	22.28	23.35	26.21	24.01	23.66
Phitsanulok	15.50	16.95	16.48	18.34	22.13	21.64	23.07	23.26	26.63	22.80	19.29	16.30
Trat	18.21	15.55	17.43	22.50	27.83	26.64	26.92	27.11	28.44	27.09	22.17	22.35
Nakhon Phanom	16.10	14.89	17.11	19.05	22.56	22.64	25.35	26.04	28.18	22.42	20.34	18.64
Sakon Nakhon	13.09	14.08	18.14	21.59	24.15	25.03	25.79	26.07	26.41	23.29	17.59	16.66
Udon Thani	14.84	13.50	16.45	19.12	21.57	24.88	25.08	26.26	26.45	21.53	15.86	16.72
Uttaradit	16.24	19.60	20.53	20.17	23.75	23.25	24.36	23.67	25.60	24.16	23.09	19.59
Trang	21.21	19.92	21.81	25.83	27.54	28.37	28.55	27.63	27.88	29.23	30.25	23.80
Kampangphet	20.23	19.30	18.41	22.30	24.39	23.00	23.55	23.90	24.76	22.14	21.56	18.90
Nakhon Nayok	21.36	19.32	19.76	21.14	25.55	24.54	24.67	24.11	26.16	26.44	23.88	21.37
Pichit	18.80	19.55	16.16	19.06	23.89	22.35	23.22	23.64	25.06	22.61	17.46	17.02
Phetchaboon	15.77	16.94	17.85	19.64	23.59	23.44	25.22	23.98	26.72	21.36	17.50	15.97
Lopburi	18.49	17.13	18.74	21.11	24.18	21.58	21.49	21.91	24.58	25.37	20.92	18.72
Singburi	22.99	20.28	19.96	22.93	24.07	21.47	23.14	22.63	24.45	24.36	21.70	18.75
Sukhothai	16.41	16.78	18.49	17.04	20.43	22.69	22.50	22.76	25.94	22.43	20.61	17.08
Angthong	20.69	19.85	20.69	22.21	23.87	23.26	22.60	22.91	25.47	23.92	20.98	20.22
Uthaitthani	20.66	22.22	21.78	23.09	24.79	23.72	24.25	22.91	24.13	22.62	18.87	18.63
Kalasin	15.57	14.60	19.07	19.42	20.91	23.59	24.96	24.84	25.55	21.73	17.22	15.40
Chaiyaphom	17.06	17.92	15.64	19.30	21.48	21.42	21.99	23.74	24.51	21.04	18.06	17.46
Buriram	18.20	15.76	17.76	19.91	22.00	22.80	22.76	23.35	26.93	24.64	19.69	15.57
Mahasarakham	14.06	15.61	16.07	18.21	18.64	21.56	22.87	23.43	25.49	22.53	18.68	17.60
Mukdahan	16.99	15.40	16.84	20.23	22.82	23.91	25.71	26.24	28.71	24.11	16.34	16.43
Yasothon	14.28	15.82	16.75	19.10	20.94	22.20	24.28	24.24	26.56	22.34	17.02	17.51
Roeit	16.68	13.72	16.49	18.16	20.35	21.77	23.65	24.58	25.11	22.72	18.60	18.40
Srisake	18.11	16.15	17.87	18.66	21.53	23.35	23.75	24.04	25.15	23.53	18.89	17.75
Surin	18.49	17.02	16.63	19.79	21.38	21.83	23.39	23.94	26.59	24.38	20.66	17.29
Nongbualamphum	15.61	14.75	15.36	18.27	21.50	25.76	25.32	25.73	25.95	21.38	17.24	16.52
Amnatcharoun	16.98	15.80	17.45	18.67	21.23	22.40	23.82	23.93	25.04	22.64	19.37	17.69
Bungkan	12.17	16.31	17.98	18.18	22.42	24.10	25.83	26.66	28.12	22.79	18.43	15.02
Chanthaburi	18.58	20.28	22.03	25.60	28.71	27.98	27.68	27.42	29.71	27.46	25.22	22.67
PhatBuri	30.73	27.23	31.16	32.11	31.45	27.14	28.40	25.41	28.14	29.95	29.19	29.33
Prochuabkirikhan	28.36	23.52	29.13	33.65	30.80	28.24	27.84	26.08	28.51	30.42	30.17	28.98
Krabi	24.08	27.83	28.88	34.22	32.70	32.34	31.17	32.43	31.01	31.44	33.07	28.18
Nakhon Srihammarat	20.53	20.86	23.06	26.28	28.52	28.40	27.13	26.62	26.45	29.34	29.89	24.79
Phatthani	22.04	21.33	25.06	28.12	27.83	28.04	27.95	26.15	26.97	29.68	31.28	23.98
Phanga	20.86	20.05	22.09	25.08	29.12	28.90	29.30	27.42	27.90	29.91	29.19	24.57
Phatthalung	22.88	22.77	24.75	29.87	29.74	28.94	28.26	27.15	27.35	30.66	32.78	25.93
Ranong	19.28	21.01	22.69	27.96	29.35	28.49	28.18	26.38	28.07	29.70	28.79	22.90
Chumphon	24.05	23.04	26.25	32.03	31.25	30.70	30.28	28.89	28.78	31.78	31.53	25.56
Chai Nat	20.75	19.39	21.25	21.12	24.64	23.81	23.53	22.96	23.26	23.12	22.87	19.95

APPENDICE Table A3 Cloud Optica Thickness average monthly data on Aqua satellite.

Stations	Jan	Feb	Mar	Apr	May	Jun	Jul	Aug	Sep	Oct	Nov	Dec
Bangkok	7.32	13.62	20.36	15.14	20.25	16.06	12.39	9.69	12.47	13.99	9.87	6.43
Samut Prakan	6.14	10.94	14.55	17.62	15.83	13.57	11.12	8.99	12.31	9.71	8.73	5.39
Nonthaburi	9.94	9.73	12.06	18.16	13.96	12.04	10.90	11.83	11.92	12.21	9.22	6.97
Samut Sakhon	5.24	6.50	9.15	10.44	9.70	8.10	8.01	7.89	8.95	12.21	7.30	5.71
Pathum Thani	6.46	5.19	8.53	12.01	14.99	13.73	12.55	11.79	10.58	11.47	7.04	5.87
Phra Nakhon Si Ayutthaya	6.40	4.47	8.08	9.10	13.24	12.09	11.26	10.93	11.03	11.41	8.45	6.18
Saraburi	11.67	8.59	10.76	14.80	10.36	7.81	10.00	7.21	11.64	12.91	7.70	5.09
Ratchaburi	6.00	7.81	8.21	8.83	6.02	7.28	7.30	8.20	7.08	8.49	4.86	5.55
Rayong	8.67	8.76	5.79	8.24	10.04	9.89	10.01	7.58	9.75	6.43	4.37	3.63
Chon Buri	9.25	12.55	10.91	14.91	15.44	15.47	15.37	11.90	17.48	18.30	13.70	7.36
Chiang Mai	11.79	16.18	11.71	18.49	15.00	14.17	12.26	13.28	13.44	16.25	13.87	9.50
Lampang	13.60	8.95	10.05	7.76	13.44	10.17	10.98	11.66	12.11	14.70	10.58	22.19
Nakhon Sawan	11.86	10.82	10.35	13.36	14.15	7.09	8.68	8.71	9.02	11.87	11.84	5.80
Phuket	6.65	5.81	4.58	5.44	9.83	11.20	10.03	10.17	10.71	10.70	8.48	8.40
Surat Thani	20.45	15.71	15.00	14.90	15.79	12.69	11.88	12.33	15.17	17.40	22.92	22.37
Songkhla	13.74	8.38	11.86	11.47	13.53	11.96	11.88	9.54	13.37	14.36	15.95	20.38
Khon Kean	8.93	11.89	16.59	11.82	10.87	9.18	10.75	9.01	15.38	13.44	7.06	5.86
Nakhon Ratchasima	9.12	9.26	16.20	26.77	23.55	15.14	13.13	13.18	13.09	13.86	11.88	7.95
Chachoengsao	10.36	15.12	18.00	19.91	22.35	17.93	18.96	15.75	17.81	14.41	10.53	5.86
Narathiwat	12.63	9.03	11.50	10.04	9.33	5.08	6.00	5.28	7.68	9.28	19.64	20.10
Yala	15.41	13.67	13.43	9.34	7.38	5.44	8.39	6.78	9.86	12.26	19.55	23.24
Mae Hong Son	15.45	13.08	22.52	27.59	19.74	14.04	14.75	15.48	16.74	22.59	16.37	11.58
Chiang Rai	15.01	12.84	12.78	18.04	13.52	9.69	12.48	10.86	9.61	15.46	11.74	11.74
Nan	4.74	3.27	6.24	7.83	15.92	16.42	18.25	19.01	15.87	8.19	3.93	2.73
Lamphun	14.87	7.90	12.20	11.27	13.40	9.70	10.42	10.05	13.02	14.15	15.01	9.41
Phrae	13.04	12.24	15.20	8.56	14.14	9.69	12.53	13.33	10.62	14.60	14.10	12.80
Phayao	19.20	10.55	16.72	16.09	14.11	12.86	11.74	12.85	12.45	15.25	15.00	12.22
Sa Kaeo	6.13	7.63	9.82	12.53	18.62	12.28	12.62	11.32	10.48	8.73	7.87	4.45
Loei	10.54	16.41	22.30	19.10	17.53	11.73	11.04	13.37	11.33	12.71	9.61	9.68
Tak	14.33	20.68	19.00	32.66	23.21	15.85	18.37	15.32	19.38	20.04	16.80	12.83
Prachin Buri	6.80	5.55	12.27	11.79	14.67	17.68	14.42	11.75	12.49	12.99	8.61	6.42
Kanchanaburi	6.56	5.87	9.09	8.78	9.45	8.50	9.75	10.33	9.80	15.93	14.26	8.23
Satun	10.08	9.53	11.63	13.18	9.68	8.07	11.19	9.74	13.03	14.71	16.06	12.33
Nong Khai	10.18	15.63	9.75	10.00	13.13	10.48	8.92	11.80	10.57	9.41	7.84	9.22
Nakhon Pathom	6.89	8.03	8.19	9.63	9.02	8.54	10.39	7.67	8.46	15.65	10.78	7.09
Ubon Ratchathani	7.59	7.77	10.67	14.90	15.15	11.70	10.90	10.70	11.89	15.30	9.43	6.85
Samut Songkhram	6.71	8.30	8.20	8.63	7.18	9.06	6.22	7.91	7.74	8.12	6.98	6.73
Suphan buri	8.90	8.40	9.69	14.95	14.06	8.25	10.97	8.67	9.27	12.36	9.62	4.23
Phitsanulok	13.31	7.75	14.16	7.22	10.78	8.71	10.52	10.43	12.55	19.45	16.17	12.35
Trat	12.89	14.39	15.88	17.61	17.28	17.25	21.97	21.32	21.60	22.09	14.06	9.40
Nakhon Phanom	10.33	11.85	17.59	13.21	13.24	9.13	14.85	15.37	13.86	11.84	8.54	6.58
Sakon Nakhon	12.00	17.47	19.54	19.33	20.76	12.51	15.46	13.81	15.07	11.32	10.41	7.51
Udon Thani	9.10	10.67	12.56	11.53	12.07	11.03	11.45	13.20	12.67	12.50	8.00	10.23
Uttaradit	8.24	7.82	15.77	7.93	9.85	9.39	9.11	9.54	7.03	10.23	7.11	7.13
Trang	13.30	10.63	10.25	13.56	13.12	12.05	14.49	10.69	13.25	15.72	18.15	14.63
Kampongphet	10.07	7.30	16.22	6.76	8.50	8.27	9.31	9.12	8.24	8.30	6.30	8.65
Nakhon Nayok	7.00	7.71	7.30	10.44	14.23	15.85	13.50	13.64	12.73	12.57	5.52	3.77
Pichit	13.97	7.35	14.90	11.44	10.39	7.36	8.39	8.22	7.82	9.87	9.42	6.38
Phetchaboon	13.56	12.17	16.10	15.85	13.00	8.41	10.85	10.68	15.93	18.10	13.34	11.59
Lopburi	7.85	8.68	13.41	21.18	15.25	11.70	10.88	10.82	13.11	17.79	12.65	10.31
Singburi	8.92	8.29	9.89	8.92	9.02	7.52	9.40	8.43	8.43	14.93	10.68	8.13
Sukhothai	11.69	10.42	13.22	9.98	12.40	10.21	10.53	13.81	9.89	10.09	7.81	9.94
Angthong	9.45	5.75	8.83	10.47	10.05	7.35	8.75	10.59	10.99	16.42	12.17	7.87
Uthathani	9.43	6.07	9.49	7.23	8.48	7.32	8.34	7.61	7.71	12.72	8.22	9.06

Stations	Jan	Feb	Mar	Apr	May	Jun	Jul	Aug	Sep	Oct	Nov	Dec
Kalasin	11.43	9.76	13.19	11.14	10.34	9.86	8.77	10.14	12.43	11.58	9.52	8.76
Chaiyaphom	8.92	9.06	11.13	8.13	13.39	6.73	9.89	7.93	10.28	11.14	8.91	5.27
Burirum	4.70	6.26	8.82	13.16	10.29	8.69	8.70	8.04	9.81	11.98	10.05	5.44
Mahasarakham	7.92	10.19	12.42	15.80	11.56	9.61	9.98	9.63	11.91	8.18	7.41	5.49
Mukdahan	8.41	7.87	9.96	13.99	9.79	10.35	11.91	12.73	14.91	14.53	9.45	8.66
Yasothon	8.30	8.46	9.95	12.14	10.13	10.63	9.44	9.50	11.77	8.64	8.84	6.63
Roeit	7.67	7.59	11.68	11.64	10.86	9.43	10.22	10.53	12.13	9.33	7.32	5.03
Srisaket	4.50	8.91	8.56	14.10	12.28	9.69	9.37	9.88	10.63	11.00	8.77	8.34
Surin	7.16	11.26	6.92	13.06	10.72	10.75	9.10	8.93	14.20	14.26	9.95	6.41
Nongbualamphum	9.58	11.84	13.79	12.17	10.58	9.60	10.56	13.17	11.23	11.00	11.23	8.24
Amnatcharoun	9.02	8.21	12.88	10.45	9.32	8.56	9.19	10.47	13.58	9.31	9.14	6.71
Bungkan	18.93	18.09	12.58	9.40	11.25	11.48	14.29	16.16	13.39	11.86	10.02	9.37
Chanthaburi	11.96	14.73	10.60	16.92	16.21	16.00	16.77	15.85	18.74	19.05	13.05	7.27
PhatBuri	8.95	8.51	7.75	8.90	5.93	7.58	7.76	8.11	7.03	8.75	7.85	4.42
Prochuabkirikhan	10.56	11.02	15.47	10.36	5.96	6.05	7.58	6.10	6.98	9.44	8.23	5.43
Krabi	10.64	8.68	12.96	10.52	12.49	13.66	11.84	11.77	13.55	15.84	12.72	13.79
Nakhon Srithammarat	14.50	10.86	11.13	10.83	11.46	8.76	10.82	8.70	10.84	13.81	20.75	19.78
Phatthani	11.25	8.35	10.16	5.36	9.59	7.96	7.83	6.16	8.78	10.73	18.59	20.77
Phanga	12.27	8.93	10.92	10.34	16.55	13.89	14.31	13.33	14.03	14.84	12.57	12.80
Phatthalung	14.87	5.08	8.45	5.90	11.96	12.62	10.26	9.68	9.70	13.17	17.50	19.42
Ranong	14.71	10.66	12.19	10.08	12.70	11.45	13.34	13.77	11.39	13.46	21.11	15.31
Chumphon	9.24	13.23	7.62	10.26	5.88	7.15	8.22	7.54	10.21	11.67	14.94	10.80
Chai Nat	9.28	9.92	8.60	8.70	9.72	6.32	7.89	7.18	7.73	9.47	9.37	5.92

APPENDICE Table A4 Cloud Water Path average monthly data on Aqua satellite.

Stations	Jan	Feb	Mar	Apr	May	Jun	Jul	Aug	Sep	Oct	Nov	Dec
Bangkok	84.93	163.56	305.91	223.97	327.70	265.74	210.16	159.40	204.42	206.73	132.17	68.75
Samut Prakan	66.98	138.94	217.87	288.63	247.47	216.34	184.80	143.93	208.25	152.19	123.63	56.35
Nonthaburi	92.10	85.19	148.55	266.95	203.19	182.28	151.02	162.90	168.73	161.15	108.86	73.58
Samut Sakhon	67.89	79.60	132.95	164.70	156.62	135.09	131.76	121.68	144.90	173.84	92.64	64.39
Pathum Thani	75.17	53.39	108.60	169.73	225.90	228.84	202.09	168.47	162.34	172.35	89.48	74.08
Phra Nakhon Si Ayutthaya	72.78	54.26	103.58	130.81	203.04	184.40	190.05	175.87	184.40	168.71	130.71	58.72
Saraburi	103.54	83.65	119.70	197.80	141.20	100.09	145.41	105.77	212.55	174.21	78.93	54.23
Ratchaburi	71.40	119.44	111.08	164.89	111.32	113.53	111.43	133.54	118.03	142.27	74.32	70.84
Rayong	120.45	132.22	99.69	151.33	187.23	179.85	184.21	123.63	170.28	113.16	60.31	48.55
Chon Buri	100.48	132.12	140.84	235.45	265.04	256.40	261.36	188.98	283.06	293.22	166.78	86.83
Chiang Mai	102.34	145.87	111.98	186.83	191.13	190.71	172.37	203.28	210.44	239.38	138.56	85.32
Lampang	124.83	63.65	125.17	92.01	175.31	138.34	169.09	189.70	198.57	195.33	99.52	203.65
Nakhon Sawan	99.03	92.70	98.32	154.39	191.39	87.47	119.05	125.19	131.19	172.12	136.32	55.52
Phuket	103.14	81.08	80.81	100.57	193.96	206.17	189.60	194.47	201.88	199.17	159.09	132.55
Surat Thani	268.25	193.06	227.29	256.18	266.92	222.09	205.96	200.21	253.08	293.78	385.59	320.79
Songkhla	191.41	113.31	162.94	176.76	230.13	212.68	208.55	152.68	225.93	236.39	295.55	317.08
Khon Kean	82.08	100.69	200.05	132.71	142.19	138.48	163.95	132.91	238.66	189.55	76.44	56.81
Nakhon Ratchasima	101.12	93.70	197.94	393.24	393.85	235.57	190.21	191.84	216.63	201.52	142.92	66.79
Chachoengsao	101.07	149.36	262.87	309.20	365.41	287.72	307.15	258.17	283.84	202.96	144.69	60.23
Narathiwat	177.02	120.64	182.44	169.42	153.76	83.08	102.35	87.54	124.26	161.44	361.46	344.72
Yala	203.63	190.36	197.54	147.03	123.73	87.51	141.14	109.23	164.41	209.21	355.48	367.38
Mae Hong Son	137.07	107.67	230.44	329.80	280.11	202.71	225.81	239.11	274.47	315.43	161.37	107.55
Chiang Rai	154.24	113.65	131.17	219.74	184.24	122.08	204.50	184.24	159.92	204.59	122.38	94.83
Nan	73.41	42.92	108.24	133.76	316.02	317.64	337.78	362.04	293.28	153.06	74.67	42.29
Lamphun	187.25	61.18	111.45	111.67	193.52	122.88	147.34	157.21	198.17	203.79	161.50	69.90
Phrae	131.06	106.64	145.56	120.06	221.49	145.87	206.53	205.06	194.89	236.88	175.47	111.61
Phayao	159.60	86.96	179.47	220.03	214.32	178.65	175.13	202.47	212.78	208.02	163.33	103.37
Sa Kaeo	63.78	70.42	128.09	180.52	320.01	202.07	192.25	169.26	176.06	141.87	102.60	45.19
Loei	84.28	155.43	280.78	230.57	264.76	176.11	181.73	221.65	175.58	162.18	91.19	79.04
Tak	118.40	166.96	203.33	477.82	336.64	241.81	294.96	220.39	328.62	280.32	188.28	126.67

Stations	Jan	Feb	Mar	Apr	May	Jun	Jul	Aug	Sep	Oct	Nov	Dec
Prachin Buri	76.84	60.28	156.01	178.65	236.58	282.41	243.83	191.14	210.14	207.46	98.64	62.70
Kanchanaburi	70.65	70.04	144.38	122.33	158.42	126.22	147.30	157.92	143.83	221.57	191.34	81.94
Satun	122.72	127.58	150.72	221.90	164.61	146.07	195.72	164.39	240.08	250.95	275.19	198.08
Nong Khai	92.31	170.49	86.87	119.33	170.15	166.25	155.12	200.89	187.29	127.76	76.48	74.24
Nakhon Pathom	89.41	90.32	115.32	178.95	155.75	134.94	170.99	114.39	132.99	233.73	141.58	82.17
Ubon Ratchathani	58.88	70.36	115.06	209.12	230.49	190.20	187.02	181.52	219.09	232.86	113.28	61.08
Samut Songkhram	86.99	121.38	123.29	155.17	124.22	136.49	101.54	126.75	128.86	135.17	106.85	72.87
Suphan buri	100.69	101.76	123.48	216.09	226.23	121.17	172.89	123.54	133.77	191.17	115.32	45.54
Phitsanulok	101.24	74.34	146.82	88.66	151.00	122.95	150.57	161.59	211.36	279.06	179.70	109.77
Trat	126.07	125.54	176.42	260.02	319.09	316.69	401.59	395.41	392.47	364.25	187.54	107.63
Nakhon Phanom	76.20	97.22	186.42	154.23	180.91	130.04	240.18	257.57	242.55	181.42	107.57	63.64
Sakon Nakhon	88.67	156.97	200.14	243.18	312.13	194.61	260.74	226.57	249.50	163.94	113.89	69.20
Udon Thani	84.47	90.29	115.38	126.84	174.84	172.70	186.84	223.47	215.71	166.96	77.82	96.46
Uttaradit	74.40	67.82	212.34	79.45	168.24	132.42	136.77	139.64	110.61	155.90	77.28	78.73
Trang	185.60	160.23	142.94	222.38	217.29	219.04	263.65	190.87	241.08	292.57	332.55	229.74
Kampangphet	97.17	74.38	167.80	85.53	133.08	115.19	122.97	132.47	130.55	112.85	71.01	82.64
Nakhon Nayok	75.51	96.04	84.15	145.51	215.67	250.19	218.36	228.43	218.67	212.93	72.83	43.12
Pichit	138.64	73.41	156.75	123.61	151.57	108.08	118.83	125.49	131.75	142.04	102.32	53.24
Phetchaboon	118.74	105.81	144.01	197.78	197.02	125.57	173.92	163.71	268.91	224.99	131.97	97.73
Lopburi	74.01	87.07	155.20	289.48	238.13	159.75	157.83	157.32	208.37	294.43	147.60	107.13
Singburi	89.44	95.69	108.78	124.93	128.91	101.30	146.57	120.34	129.85	221.84	131.34	70.22
Sukhothai	114.46	98.41	142.07	96.51	161.17	153.28	147.20	213.55	163.40	143.81	90.88	102.63
Angthong	91.86	64.01	113.73	153.96	141.60	109.76	132.43	165.58	190.18	235.94	148.20	70.61
Uthaitani	93.11	66.64	114.02	97.42	123.03	103.43	126.74	110.92	118.70	168.21	92.37	89.22
Kalasin	88.56	71.33	176.50	148.17	142.69	147.04	145.33	171.24	208.72	154.19	97.21	75.78
Chaiyaphom	87.99	92.71	127.04	96.78	186.73	86.75	145.96	119.99	163.84	137.99	103.68	55.33
Buriram	45.13	56.01	102.22	182.19	159.31	118.29	129.47	114.56	170.09	189.66	117.32	46.03
Maharakham	61.73	67.07	129.61	198.04	145.81	145.08	163.21	147.89	205.50	118.62	70.51	53.52
Mukdahan	71.06	58.76	104.54	189.21	132.39	156.81	190.86	213.04	256.86	218.07	94.94	82.16
Yasothon	59.62	64.90	109.04	154.44	150.83	157.70	152.42	157.88	206.51	124.71	87.92	65.25
Roeit	62.65	55.20	120.80	147.15	139.25	144.57	163.76	172.64	198.93	133.62	80.80	49.96
Srisaket	40.68	75.49	102.16	189.19	181.72	149.79	144.32	157.09	172.37	171.12	102.19	78.48
Surin	61.09	103.49	68.26	165.76	142.45	158.81	144.86	137.68	245.73	226.39	131.99	62.99
Nongbualamphum	73.30	101.06	137.29	129.11	146.01	151.92	177.74	212.02	185.47	142.97	132.85	75.31
Amnatcharoun	78.13	67.85	131.78	133.43	125.65	123.04	145.18	161.10	227.08	131.56	98.31	68.18
Bungkan	145.69	146.70	132.03	93.00	161.77	180.48	234.66	291.91	236.46	168.60	127.43	85.51
Chanthaburi	116.40	156.17	134.12	266.57	297.80	303.94	307.36	290.62	347.27	326.48	195.33	91.17
PhatBuri	122.44	121.95	126.67	172.02	105.29	118.19	128.91	124.99	114.35	152.09	127.51	59.13
Prochuabkirkhan	171.82	165.78	262.90	193.36	107.58	95.57	124.07	97.04	118.14	170.05	138.43	79.44
Krabi	147.41	131.78	214.99	193.01	228.35	251.48	223.73	217.70	252.06	291.70	253.10	224.55
Nakhon Srihammarat	180.16	140.25	176.07	175.51	201.05	155.60	197.16	148.75	178.24	238.65	372.80	317.36
Phatthani	156.16	109.14	168.74	92.89	169.93	121.63	132.80	99.98	146.68	197.69	358.71	310.03
Phanga	152.45	111.14	134.66	170.59	301.23	258.97	260.98	237.20	244.46	270.99	228.23	182.86
Phatthalung	209.67	69.50	132.28	108.76	213.81	220.55	168.31	162.79	164.73	243.15	348.59	305.60
Ranong	168.25	127.50	164.04	174.16	234.22	198.39	243.53	233.33	196.31	250.92	364.26	215.02
Chumphon	127.18	189.70	112.16	200.22	109.29	133.34	150.44	133.43	181.97	221.00	276.62	171.63
Chai Nat	94.60	73.49	98.91	114.55	147.77	87.98	117.36	102.82	122.30	132.87	107.50	60.40

APPENDICE Table A5 Cloud Top Temperature average monthly data on Aqua satellite.

Stations	Jan	Feb	Mar	Apr	May	Jun	Jul	Aug	Sep	Oct	Nov	Dec
Bangkok	-29.15	-26.42	-37.75	-45.53	-66.40	-59.24	-62.53	-60.27	-57.36	-47.02	-39.33	-42.58
Samut Prakan	-32.12	-31.02	-35.49	-45.80	-64.92	-63.10	-62.12	-61.95	-58.64	-47.60	-45.10	-48.32
Nanthaburi	-22.95	-20.14	-28.84	-39.20	-56.60	-59.15	-57.87	-61.51	-55.63	-40.86	-38.83	-38.30
Samut Sakhon	-26.57	-25.23	-38.67	-40.02	-61.35	-58.42	-59.78	-60.81	-56.11	-48.40	-46.35	-42.58
Pathum Thani	-26.58	-24.49	-32.91	-36.76	-57.47	-60.78	-60.64	-60.88	-57.42	-45.55	-47.90	-40.26
Phra Nakhon Si Ayutthaya	-25.76	-21.93	-26.00	-36.11	-55.80	-61.90	-58.47	-61.61	-55.95	-45.09	-46.35	-39.16
Saraburi	-26.42	-21.19	-23.05	-30.37	-46.45	-54.76	-57.13	-57.25	-53.95	-34.64	-32.12	-32.29

Stations	Jan	Feb	Mar	Apr	May	Jun	Jul	Aug	Sep	Oct	Nov	Dec
Ratchaburi	-45.42	-43.29	-57.88	-62.67	-70.76	-66.10	-67.38	-65.53	-60.38	-62.02	-58.80	-55.69
Rayong	-47.46	-36.23	-47.34	-53.98	-73.45	-68.55	-67.15	-66.17	-64.08	-62.75	-60.84	-60.54
Chon Buri	-28.46	-27.54	-34.37	-50.56	-69.89	-66.73	-63.75	-65.72	-62.61	-54.73	-41.00	-47.41
Chiang Mai	-22.19	-23.05	-22.30	-33.91	-38.95	-52.18	-55.68	-56.62	-52.09	-38.78	-23.34	-23.90
Lampang	-17.59	-19.31	-23.74	-24.34	-40.57	-53.29	-58.36	-56.86	-53.19	-35.25	-23.12	-20.91
Nakhon Sawan	-25.04	-16.27	-26.32	-30.85	-47.95	-50.14	-58.49	-57.87	-50.33	-34.54	-31.64	-30.99
Phuket	-55.58	-63.70	-64.01	-72.65	-72.50	-68.66	-68.54	-60.08	-68.70	-69.61	-71.48	-66.32
Surat Thani	-36.40	-32.46	-44.41	-57.07	-68.19	-67.88	-66.48	-59.06	-67.63	-66.28	-65.94	-56.26
Songkhla	-42.18	-35.92	-46.73	-53.29	-64.30	-65.37	-66.08	-55.88	-63.82	-63.50	-67.28	-57.33
Khon Kean	-22.40	-18.45	-22.44	-24.85	-43.61	-56.18	-54.70	-58.38	-60.04	-33.87	-25.26	-26.29
Nakhon Ratchasima	-31.04	-29.29	-37.68	-45.00	-55.97	-63.47	-58.99	-61.85	-57.68	-41.68	-35.89	-29.78
Chachoengsao	-32.63	-26.81	-35.99	-46.44	-64.85	-64.64	-61.84	-63.37	-58.22	-51.82	-39.40	-46.74
Narathiwat	-39.24	-36.58	-45.96	-48.17	-58.52	-56.25	-58.42	-48.81	-55.53	-59.64	-68.20	-62.61
Yala	-44.21	-39.00	-46.09	-52.23	-57.94	-63.32	-61.45	-52.36	-60.48	-59.47	-66.41	-60.72
Mae Hong Son	-24.59	-21.80	-24.95	-37.62	-43.52	-50.84	-56.73	-55.00	-51.31	-34.64	-26.62	-31.71
Chiang Rai	-19.56	-20.27	-27.72	-27.90	-40.57	-51.42	-56.94	-59.31	-52.39	-31.90	-18.99	-16.48
Nan	-48.15	-46.42	-43.85	-49.76	-71.11	-69.79	-71.84	-68.49	-65.83	-59.56	-61.85	-64.28
Lamphun	-23.26	-25.06	-24.13	-31.57	-38.53	-47.51	-55.11	-51.31	-48.86	-31.71	-21.96	-22.25
Phrae	-20.68	-17.91	-26.41	-25.78	-44.99	-54.53	-59.52	-56.73	-55.93	-36.24	-29.81	-27.95
Phayao	-19.80	-28.07	-24.10	-34.84	-40.72	-55.98	-56.87	-58.10	-53.18	-31.44	-22.72	-20.95
Sa Kaeo	-23.43	-21.66	-27.40	-35.42	-49.72	-55.49	-56.62	-55.76	-58.78	-50.06	-37.42	-39.91
Loei	-22.27	-25.58	-32.18	-34.36	-48.01	-59.61	-61.01	-63.10	-57.26	-31.40	-26.59	-18.39
Tak	-24.74	-19.24	-35.03	-44.42	-53.93	-56.48	-60.34	-58.70	-58.57	-41.50	-28.85	-28.50
Prachin Buri	-28.66	-21.31	-28.30	-32.96	-52.76	-60.56	-59.25	-61.85	-57.72	-44.41	-35.99	-36.13
Kanchanaburi	-27.18	-24.42	-29.43	-43.60	-55.78	-61.93	-59.74	-61.08	-51.97	-48.01	-40.42	-37.43
Satun	-42.05	-38.07	-46.82	-50.52	-61.08	-61.35	-65.16	-54.69	-62.25	-60.88	-63.20	-57.15
Nong Khai	-20.75	-21.85	-28.61	-27.33	-42.63	-57.73	-61.82	-62.37	-55.91	-29.02	-23.10	-19.97
Nakhon Pathom	-24.10	-19.52	-25.86	-38.07	-56.87	-57.07	-58.57	-59.91	-53.58	-47.30	-38.07	-32.37
Ubon Ratchathani	-32.27	-23.74	-25.98	-41.06	-51.05	-61.03	-58.52	-65.35	-61.41	-41.53	-31.89	-34.60
Samut Songkhram	-46.01	-49.90	-51.65	-62.36	-73.05	-67.08	-67.88	-65.16	-63.67	-60.79	-60.31	-57.85
Suphan buri	-22.12	-23.24	-25.77	-41.51	-53.37	-57.07	-58.39	-60.69	-53.24	-40.85	-41.96	-34.81
Phitsanulok	-24.50	-21.27	-29.01	-24.78	-44.93	-57.93	-56.49	-61.49	-60.99	-38.01	-26.20	-23.98
Trat	-32.29	-26.47	-34.29	-49.20	-64.25	-63.07	-63.16	-67.62	-67.96	-57.91	-45.37	-48.61
Nakhon Phanom	-26.03	-23.88	-25.28	-33.78	-50.51	-61.15	-55.29	-62.35	-59.68	-36.98	-26.56	-27.63
Sakon Nakhon	-21.72	-23.16	-26.25	-39.21	-52.92	-64.11	-62.16	-63.99	-60.72	-37.29	-28.95	-25.75
Udon Thani	-23.06	-19.22	-29.28	-25.78	-46.23	-61.61	-61.66	-64.83	-57.46	-29.68	-22.63	-23.39
Uttaradit	-16.99	-20.00	-29.81	-22.49	-38.46	-48.78	-52.73	-57.08	-50.02	-34.52	-25.92	-19.59
Trang	-40.43	-38.40	-41.50	-55.46	-69.40	-65.41	-65.06	-56.88	-64.67	-62.79	-67.52	-58.64
Kampongphet	-24.92	-24.03	-22.62	-23.66	-43.21	-47.60	-55.75	-55.58	-51.96	-31.38	-28.64	-28.25
Nakhon Nayok	-27.10	-20.98	-27.08	-34.03	-57.79	-59.80	-59.52	-61.47	-59.29	-48.50	-37.57	-38.86
Pichit	-26.28	-20.54	-24.64	-25.44	-39.68	-47.80	-55.76	-57.83	-53.66	-35.12	-25.38	-22.39
Phetchaboon	-27.95	-24.66	-30.89	-32.95	-49.04	-60.59	-61.56	-62.86	-56.35	-36.01	-30.05	-27.76
Lopburi	-28.28	-20.36	-26.37	-40.57	-57.56	-59.13	-59.05	-60.79	-57.54	-50.50	-41.37	-35.19
Singburi	-24.94	-20.86	-25.99	-36.26	-55.59	-57.08	-58.18	-60.39	-54.75	-45.95	-36.50	-26.43
Sukhothai	-20.39	-21.69	-24.99	-27.14	-39.61	-53.50	-53.54	-57.69	-50.56	-32.91	-23.53	-22.20
Angthong	-23.68	-17.16	-25.88	-37.69	-52.90	-56.98	-56.92	-60.72	-57.39	-43.49	-33.96	-32.25
Uthaihani	-27.52	-25.62	-31.01	-33.72	-46.88	-52.40	-55.95	-58.78	-51.79	-37.23	-30.36	-26.24
Kalasin	-27.48	-24.91	-26.36	-27.59	-41.64	-59.47	-56.62	-61.85	-60.10	-36.37	-26.43	-25.11
Chaiyaphom	-23.20	-25.25	-24.27	-30.68	-42.71	-56.78	-53.76	-60.21	-56.71	-39.06	-30.96	-30.20
Buriram	-27.66	-23.62	-23.27	-32.86	-46.26	-56.70	-56.19	-60.85	-57.87	-42.97	-33.83	-27.02
Maharakham	-25.99	-22.89	-21.57	-23.79	-42.44	-61.93	-56.99	-60.36	-57.40	-35.95	-30.94	-26.30
Mukdahan	-24.11	-23.70	-20.05	-24.32	-44.69	-61.04	-53.49	-60.88	-56.56	-36.93	-24.75	-27.35
Yasothorn	-21.48	-19.88	-27.60	-27.11	-43.33	-57.83	-54.20	-61.77	-60.10	-37.44	-28.90	-27.07
Roeit	-25.00	-19.07	-19.06	-24.62	-44.49	-59.21	-54.81	-62.98	-55.59	-37.07	-25.76	-28.39
Srisaket	-30.55	-23.63	-27.95	-34.85	-46.37	-60.62	-55.79	-61.29	-60.12	-42.92	-31.01	-30.54
Surin	-26.64	-25.11	-22.58	-33.71	-46.09	-58.90	-58.46	-59.49	-61.50	-39.11	-35.09	-31.49
Nongbualamphum	-23.02	-22.44	-28.54	-26.55	-40.35	-60.87	-57.75	-63.87	-57.36	-31.44	-21.81	-24.87
Amnatcharoun	-23.57	-21.66	-20.84	-27.28	-43.64	-57.42	-56.32	-61.58	-59.64	-38.50	-29.11	-30.00
Bungkan	-18.62	-25.14	-24.63	-27.02	-44.42	-62.35	-63.84	-60.48	-57.70	-33.18	-24.04	-19.01

Stations	Jan	Feb	Mar	Apr	May	Jun	Jul	Aug	Sep	Oct	Nov	Dec
Chanthaburi	-27.87	-27.78	-34.46	-51.06	-66.57	-65.34	-62.26	-65.23	-64.45	-59.98	-52.45	-50.05
PhatBuri	-52.97	-41.63	-50.02	-61.99	-75.01	-69.80	-67.45	-68.29	-67.59	-67.27	-61.25	-60.86
Prachuabkirkhan	-47.22	-38.13	-50.32	-64.48	-72.75	-69.39	-67.90	-64.89	-65.13	-63.60	-55.42	-60.23
Krabi	-44.29	-47.32	-56.85	-68.51	-74.95	-71.32	-68.64	-60.30	-67.91	-67.76	-68.04	-57.79
Nakhon Srithammarat	-34.95	-31.61	-40.50	-50.65	-65.51	-60.97	-64.22	-55.05	-61.19	-62.80	-64.39	-58.01
Phatthani	-44.36	-42.38	-48.26	-53.47	-62.42	-58.17	-62.01	-55.97	-60.70	-64.08	-66.73	-60.52
Phanga	-36.75	-36.05	-42.01	-53.01	-69.51	-68.15	-68.86	-59.72	-66.44	-65.31	-67.13	-57.39
Phatthalung	-35.55	-31.27	-40.36	-49.78	-64.92	-57.89	-62.73	-54.80	-61.91	-61.19	-66.38	-56.44
Ranong	-37.36	-38.86	-46.77	-57.77	-70.93	-65.98	-62.41	-62.45	-64.04	-67.90	-67.19	-51.94
Chumphon	-35.29	-39.07	-45.41	-62.87	-73.14	-68.58	-67.90	-60.35	-68.06	-65.71	-62.02	-52.54
Chai Nat	-27.11	-23.91	-28.24	-28.51	-46.70	-56.10	-57.31	-57.24	-53.97	-41.03	-34.97	-26.74

APPENDICE Table A6 Cloud Top Pressure average monthly data on Aqua satellite.

Stations	Jan	Feb	Mar	Apr	May	Jun	Jul	Aug	Sep	Oct	Nov	Dec
Bangkok	675.92	701.26	594.28	527.38	342.97	389.32	349.45	362.11	395.30	505.02	581.15	567.90
Samut Prakan	654.35	658.80	614.24	531.19	363.17	352.69	352.39	341.89	385.34	502.67	522.76	506.48
Nonthaburi	734.51	755.59	670.89	573.57	409.01	379.64	382.31	344.30	412.09	558.38	603.32	611.81
Samut Sakhon	711.03	723.93	590.62	580.07	390.22	396.25	378.64	358.96	409.97	491.88	516.84	568.12
Pathum Thani	705.35	721.25	636.58	601.45	412.71	375.03	361.65	358.60	393.33	526.16	513.91	592.69
Phra Nakhon Si Ayutthaya	712.87	744.11	693.78	600.74	424.66	361.26	376.32	343.32	406.17	526.02	531.39	603.06
Saraburi	695.96	729.38	710.08	649.64	498.06	418.10	385.17	378.35	424.46	612.70	648.32	661.32
Ratchaburi	511.25	546.41	395.18	375.38	301.19	314.64	291.79	300.85	355.92	358.91	398.59	434.27
Rayong	491.34	609.18	512.34	454.90	270.68	302.06	303.01	299.63	319.61	349.05	376.78	392.53
Chon Buri	685.28	691.94	623.92	478.43	306.68	316.77	334.98	318.84	345.80	427.20	562.82	524.22
Chiang Mai	729.57	711.78	686.34	581.06	542.56	423.47	374.97	364.14	426.50	546.04	705.97	729.41
Lampang	785.03	756.62	693.77	681.21	527.56	416.08	359.07	372.85	416.65	586.44	722.39	756.69
Nakhon Sawan	707.35	775.78	678.12	640.24	493.43	451.72	375.41	365.00	457.99	619.89	654.98	674.15
Phuket	424.32	358.33	364.43	290.37	283.80	299.94	294.98	373.23	287.99	294.55	286.79	325.57
Surat Thani	602.90	641.30	527.97	414.52	307.52	301.05	309.18	369.00	297.56	319.41	340.65	419.04
Songkhla	552.64	615.81	502.76	448.83	355.14	331.91	323.69	410.52	332.54	349.02	320.61	413.04
Khon Kean	745.55	755.74	708.18	689.39	517.80	411.94	412.18	383.40	379.09	628.11	709.92	710.72
Nakhon Ratchasima	652.95	646.57	555.27	510.45	406.93	337.99	365.95	338.49	383.69	546.39	611.00	683.81
Chachoengsao	629.57	687.23	596.92	508.70	341.10	324.75	336.77	320.53	376.89	443.41	569.53	517.88
Narathiwat	577.00	615.71	520.29	502.68	407.07	419.51	402.82	487.53	417.94	390.30	324.92	370.49
Yala	524.19	589.39	511.69	450.53	399.34	347.85	364.65	447.25	367.03	383.66	329.27	379.02
Mae Hong Son	685.21	699.43	638.94	515.73	464.42	409.27	359.77	372.03	407.59	560.89	643.07	616.62
Chiang Rai	770.52	739.83	643.56	637.68	517.24	427.25	370.75	354.60	423.79	606.50	750.12	801.68
Nan	502.03	526.22	542.11	488.40	286.59	280.27	255.95	278.19	304.00	378.77	365.68	367.33
Lamphun	725.34	679.68	673.61	603.42	554.29	471.76	392.43	412.10	461.83	625.12	727.07	743.95
Phrae	744.29	756.64	664.79	673.99	490.27	410.06	350.11	374.33	393.36	570.49	646.00	690.30
Phayao	760.59	650.43	680.33	572.63	521.91	387.79	364.42	360.74	408.67	609.26	705.06	745.58
Sa Kaeo	735.53	732.39	672.61	604.94	481.12	420.79	390.13	398.57	380.05	470.85	595.69	594.08
Loei	741.09	678.80	617.07	594.90	472.52	370.68	345.18	334.18	388.13	641.46	701.58	786.88
Tak	700.69	733.50	574.23	496.06	397.48	370.00	329.50	344.07	360.04	531.51	663.88	683.72
Prachin Buri	679.12	738.80	660.25	636.07	451.53	371.50	367.68	341.88	388.73	522.58	612.83	620.21
Kanchanaburi	698.61	720.35	663.12	536.98	428.90	358.45	360.47	340.53	443.21	494.26	581.75	615.65
Satun	543.81	594.49	496.49	484.08	387.10	372.71	333.12	425.36	349.11	371.79	351.17	408.03
Nong Khai	758.21	728.97	653.18	657.61	530.80	395.75	352.91	346.12	410.99	658.49	721.24	766.08
Nakhon Pathom	732.78	775.71	701.93	596.88	424.41	399.95	381.60	365.05	431.69	498.15	590.96	667.60
Ubon Ratchathani	643.45	712.21	676.93	541.18	455.08	375.38	384.32	320.16	359.96	554.41	648.96	637.84
Samut Songkhram	503.75	492.87	468.78	374.65	280.24	307.16	298.36	308.19	330.94	371.57	376.52	414.55
Suphan buri	748.70	727.99	700.31	555.97	446.10	394.95	374.54	348.57	436.43	560.53	566.98	645.31
Phitsanulok	712.27	737.37	651.97	690.32	505.17	389.54	385.68	340.18	363.86	568.19	701.84	728.04
Trat	627.67	680.61	614.98	479.29	339.57	343.81	327.00	290.42	297.16	388.00	510.87	500.84
Nakhon Phanom	704.65	705.74	677.25	600.33	450.55	367.11	407.28	349.20	380.70	584.21	688.03	701.26
Sakon Nakhon	752.00	706.98	662.09	546.01	432.59	339.59	340.36	324.58	365.83	582.84	668.10	716.18
Udon Thani	730.46	756.79	649.17	687.89	491.80	361.91	350.45	322.45	396.44	652.31	732.69	742.15

Stations	Jan	Feb	Mar	Apr	May	Jun	Jul	Aug	Sep	Oct	Nov	Dec
Uttaradit	802.69	762.14	648.32	716.52	573.07	466.13	419.46	376.12	468.47	625.76	717.41	784.68
Trang	578.03	598.94	562.33	431.78	305.10	326.03	332.20	395.93	327.49	353.82	331.63	407.23
Kampangphet	718.02	708.28	717.63	712.39	530.21	478.18	395.39	391.17	446.96	660.99	688.00	710.53
Nakhon Nayok	700.40	755.64	680.50	625.95	409.83	378.18	369.66	343.31	375.40	488.38	601.46	596.22
Pichit	700.07	740.61	693.20	686.51	557.00	481.11	394.07	369.33	426.97	612.07	719.22	757.96
Phetchaboon	677.37	696.23	630.98	611.88	465.00	356.33	340.45	325.46	395.71	595.48	653.44	697.24
Lopburi	678.02	750.78	672.16	552.75	406.85	384.25	371.79	346.68	386.35	462.76	554.93	634.38
Singburi	718.92	745.21	693.60	598.43	427.18	403.15	380.46	348.46	423.01	519.96	620.17	724.50
Sukhothai	768.70	731.92	689.33	657.79	551.07	414.84	406.47	363.90	444.68	628.30	726.01	751.91
Angthong	733.80	786.42	691.28	589.32	446.43	401.22	382.36	350.23	399.71	533.44	643.01	661.05
Uthathani	692.50	697.11	642.59	618.30	498.15	434.27	396.14	363.16	448.30	599.03	678.96	725.20
Kalasin	690.00	695.25	675.00	663.21	537.34	393.82	394.64	354.84	378.94	595.83	690.11	728.13
Chaiyaphom	739.21	698.48	695.63	639.81	527.32	411.90	420.82	363.63	407.08	580.18	660.80	682.44
Buriram	701.41	713.20	705.36	618.42	501.84	415.65	403.79	357.88	395.92	538.85	635.89	707.56
Maharakham	712.92	716.11	721.90	701.83	530.33	371.38	392.12	364.53	400.36	601.83	661.67	711.54
Mukdahan	731.72	712.19	727.78	698.12	511.48	375.20	428.31	360.02	408.14	589.63	704.80	704.83
Yasothon	748.48	747.99	657.33	671.56	521.69	402.76	421.66	357.70	377.84	589.69	669.34	701.46
Roeit	717.66	747.23	742.12	696.49	514.31	393.75	414.14	341.14	421.07	586.00	706.21	693.06
Srisaket	663.38	713.64	661.23	600.46	502.70	378.26	410.00	357.56	374.85	543.49	653.07	672.28
Surin	708.52	701.35	714.17	615.72	504.96	394.96	385.98	369.46	363.46	574.17	615.20	664.64
Nangbualamphum	734.64	724.92	652.89	674.45	545.76	372.40	381.90	333.22	394.01	645.84	742.55	731.75
Amnatcharoun	729.44	736.61	728.45	666.95	521.25	398.15	408.26	352.24	383.09	584.67	673.29	683.20
Bungkan	785.54	696.09	688.37	662.38	499.00	348.16	333.17	360.90	398.99	619.38	711.35	766.14
Chanthaburi	681.02	683.32	623.47	474.11	319.97	318.60	337.14	310.03	318.45	383.60	458.61	493.21
PhatBuri	450.78	556.21	473.99	370.53	265.22	289.17	296.24	288.91	300.72	318.95	372.72	375.69
Prachuabkirkhan	493.35	590.71	479.68	356.39	268.16	285.82	292.37	307.67	309.16	350.70	419.97	396.95
Krabi	511.41	501.41	417.73	323.55	258.81	272.44	293.10	368.23	301.27	308.71	312.54	397.47
Nakhon Srithammarat	619.89	662.24	571.15	477.93	341.41	369.05	340.89	421.99	362.95	350.83	360.67	414.84
Phatthani	528.72	571.53	502.48	462.68	368.13	400.02	364.30	424.16	362.56	348.18	335.30	391.67
Phanga	610.56	608.24	550.40	455.14	303.12	310.12	292.66	378.01	308.21	331.95	327.46	420.25
Phatthalung	609.38	667.55	572.32	496.32	352.44	395.82	353.81	419.72	354.28	373.73	341.88	424.49
Ranong	606.69	594.47	510.87	411.50	286.36	320.31	337.63	348.01	325.69	316.97	332.64	464.17
Chumphon	620.00	587.97	525.72	364.71	263.09	294.29	283.89	348.44	294.43	338.64	373.27	461.40
Chai Nat	693.72	711.77	668.62	663.82	506.53	412.56	380.98	376.51	434.07	557.33	631.12	721.41

APPENDICE B

CONFERENCE



## APPENDICE B

### Conference

Conference: Thailand Research EXPO 2023 (Oral)



Conference: The 12th Asian Aerosol Conference (AAC) 2022 (Poster)



P2-062

**Analysis of Aerosol-cloud interaction from MODIS satellite data during PM2.5 levels exceeded the standard in Bangkok.**

Oradee Pilahome<sup>1</sup>, Wichaya Ninsawan<sup>1</sup>, Yuttapichai Jankondee<sup>1</sup>, and Wilawan Kumharn<sup>1\*</sup>

<sup>1</sup> Department of Physics, Sakon Nakhon Rajabhat University, Sakon Nakhon, Thailand.

\*Corresponding author: Wilawan\_kumharn@snru.ac.th



**Analysis of Aerosol-cloud interaction from MODIS satellite data during PM2.5 levels exceeded the standard in Bangkok.**

Oradee Pilahome<sup>1</sup>, Wichaya Ninsawan<sup>1</sup>, Yuttapichai Jankondee<sup>1</sup>, and Wilawan Kumharn<sup>1\*</sup>

<sup>1</sup> Department of Physics, Sakon Nakhon Rajabhat University, Sakon Nakhon, Thailand.

\*Corresponding author: Wilawan\_kumharn@snru.ac.th

APPENDICE C

PAPER ONLINE

## APPENDICE C

### Paper Online

Paper I

Published in the Atmospheric Environment journal.

Impact 5.755



Contents lists available at ScienceDirect

Atmospheric Environment

journal homepage: [www.elsevier.com/locate/atmosenv](http://www.elsevier.com/locate/atmosenv)

## Long-term variations and comparison of aerosol optical properties based on MODIS and ground-based data in Thailand

Oradee Pilahome<sup>a</sup>, Waichaya Ninssawan<sup>a</sup>, Yuttapichai Jankondee<sup>a</sup>, Serm Janjai<sup>b</sup>,  
Wilawan Kumharn<sup>a,\*</sup>

<sup>a</sup> Department of Physics, Faculty of Science and Technology, Sakon Nakhon Rajabhat University, Sakon Nakhon, Thailand

<sup>b</sup> Department of Physics, Faculty of Science, Silpakorn University, Nakhon Pathom, Thailand

### HIGHLIGHTS

- MODIS and ground based AODs were in good agreement with  $R^2 = 0.75$ .
- Satellite and ground based AODs demonstrate increasing trends in AOD.
- Hypothesis showed 95% confidence interval of AODs retrieved from satellite data fell within the confidence range.
- Higher AOD values were observed between February to April.
- Meteorological parameters and temperature inversion more influenced AOD in February.

### ARTICLE INFO

**Keywords:**  
Aerosols  
Angstrom exponent  
MODIS  
Satellite data  
Ground-based data

### ABSTRACT

Comparison and analysis of Moderate Resolution Imaging Spectroradiometer (MODIS), Aerosol Robotic Network (AERONET), and SKYNET aerosol optical depth (AOD) products were investigated at four AERONET and two SKYNET stations in Thailand from 2006 to 2020. AERONET Level 2.0 and MODIS Deep Blue (DB) Collection 6.1 data were applied. Aqua and Terra MODIS AODs (satellite AODs) were compared to AERONET and SKYNET AODs (ground based AODs). Ground-based and satellite AODs were in good agreement, giving a high correlation ( $R^2 = 0.75$ ) in Ubon Ratchathani, associated with biomass burning. The long-term trend in AOD was analysed. Both satellite and ground based AODs demonstrate increasing trends in AOD over Thailand associated with the urbanized area and traffic congestion. Aerosol particles are categorized into dust, sea salt, and biomass burning, containing fine and coarse modes. A variation between satellite data measurements depended on surface reflectances, such as the large water body surrounding (Gongkhla) and the impact of surface albedo (Chiang Mai). Higher AOD values were observed between February to April. In addition, meteorological parameters are directly related to aerosol concentrations, while no significant connection could be developed in the observed values between Angstrom exponent (AE) and Meteorological parameters. Meteorological parameters and temperature inversion more influenced AOD concentrations in February. Nevertheless, the hypothesis showed 95% confidence interval of AODs retrieved from satellite data fell within the confidence range. Therefore, satellite aerosol products are sufficiently accurate for estimating aerosol climatology.

### 1. Introduction

Aerosol particles play a vital role in global climate change, ecosystem, and human health (Habib et al., 2019; Kumharn et al., 2012; Kuttippurath and Raj, 2021). To date, there has been increasing anxiety about the high aerosol concentration events in the atmosphere in all regions of Thailand, which cause air pollution and health problems.

Additionally, the industrial growth in Thailand leads to high levels of air pollution, which needs to improve the situation (Agsoom, 2010). Ground-based and satellite measurements of aerosol optical depth (AOD) have widely been used for aerosol studies. AOD is a parameter for indicating the extinction of a light beam as it passes through a layer of the atmosphere that contains aerosol particles. It is wavelength-dependent and typically decreases with increasing

\* Corresponding author. Department of Physics, Faculty of Science and Technology Sakon Nakhon Rajabhat University, Sakon Nakhon 47000, Thailand.  
E-mail addresses: [wilawan.kumharn@snru.ac.th](mailto:wilawan.kumharn@snru.ac.th), [wilawan.kumharn2015@gmail.com](mailto:wilawan.kumharn2015@gmail.com) (W. Kumharn).

<https://doi.org/10.1016/j.atmosenv.2022.119218>

Received 3 February 2022; Received in revised form 30 May 2022; Accepted 4 June 2022

Available online 7 June 2022

1352-2310/© 2022 Elsevier Ltd. All rights reserved.

wavelengths (Bartoszek et al., 2020; Gao et al., 2010; Schmid et al., 1997).

In Thailand, various groups have carried out several studies on satellite AODs (Jantarach et al., 2012; Kanabkaew, 2013; Nichol and Bilal, 2016; Suwanwaree et al., 2014). (Kanabkaew, 2013) examined the statistical model for predicting PM concentration in Chiang Mai using satellite AODs (Suwanwaree et al., 2014). studied the aerosol prediction index (API) for determining and mapping PM<sub>10</sub> using satellite AODs in 2009 and 2010 during burning seasons in upper northern Thailand (Jantarach et al., 2012). compared satellite AODs retrievals with ground-based measurements in the tropics (Nichol and Bilal, 2016). evaluated the new Aqua MODIS Dark Target Collection 6 AOD retrieval algorithm at 3 km resolution over Asian countries. Much of the current literature on AOD pays attention to using and comparing ground-based and satellite data. These studies indicate a relationship between long-term variations and comparison of aerosol optical properties based on satellite and ground-based data and meteorological parameters in Thailand.

Ground-based and satellite data can be used to determine AOD and AE in the atmosphere; however, various instruments could produce different AOD and AE retrievals within the exact temporal coordinates and geographic location. Recently, AOD and AE data obtained from MODIS sensors aboard two satellites (Terra and Aqua) operated by the US National Aeronautics and Space Administration (NASA) have widely been used for aerosol climatology (Mehta et al., 2016). Since many parts of Thailand lack ground-based data due to inadequate/unreliable station networks, satellite data have become essential sources for wide spatial and temporal understanding aerosols properties. However, low sensitivity of the sensor, high surface reflectivity, cloud, and low AOD could limit satellite data describing aerosol properties. Characterization of surface reflectance becomes comparatively more critical in reducing aerosol loading. Therefore, surface reflectance remains one of the essential inputs to aerosol retrieval from satellite data, especially over land surfaces. The DB algorithm utilizes blue wavelength measurements from MODIS instruments, providing helpful information about aerosol properties over bright-reflecting land surfaces. Our aerosol retrievals were obtained using the MODIS collection 6.1 DB algorithm. This study investigated AOD and AE through statistical inter-comparison analysis between satellite and ground-based products at six sites (Chiang Mai, Bangkok, Phimai, Nakhon Pathom, Ubon Ratchathani, Songkhla) in Thailand. In addition, the relationship between meteorological parameters and aerosol optical properties was examined. These results would better understand AOD climatology and its impact on tropical regions' global climate changes and human health.

## 2. Data collection

Thailand is divided into four central regions, each grouping of provinces (North, Central region, North-east, and South). Chiang Mai is the largest city in the north (Andronache, 2004), a mountainous area surrounded by high mountains and forests. Nakhon Pathom is a city in the center of a basin through which channels and rivers run. Ubon Ratchathani is a significant city in the northeast. Phimai is in Nakhon Ratchasima Province, which is about 60 km from Nakhon Ratchasima downtown, one of the four major cities in the northeast. Songkhla is in the South of the Malay Peninsula, bounded to the north by Kra Isthmus. Ground-based AOD monitoring uses Sun-photometer and Sky radiometer. The AERONET networks in Thailand are in Nakhon Pathom (13.82°N, 100.04°E), Chiang Mai (18.77°N, 98.97°E), Ubon Ratchathani (15.24°N, 104.87°E), and Songkhla (7.18°N, 100.60°E). Skynet networks are in the Bureau of Royal Rainmaking and Agricultural Aviation (BRRAA), Rang Ka Yai, Phimai, Nakhon Ratchasima (15.18°N, 102.56°E), and the meteorological department, Bangkok (13.66°N, 100.60°E) since 2005 (Fig. 1).

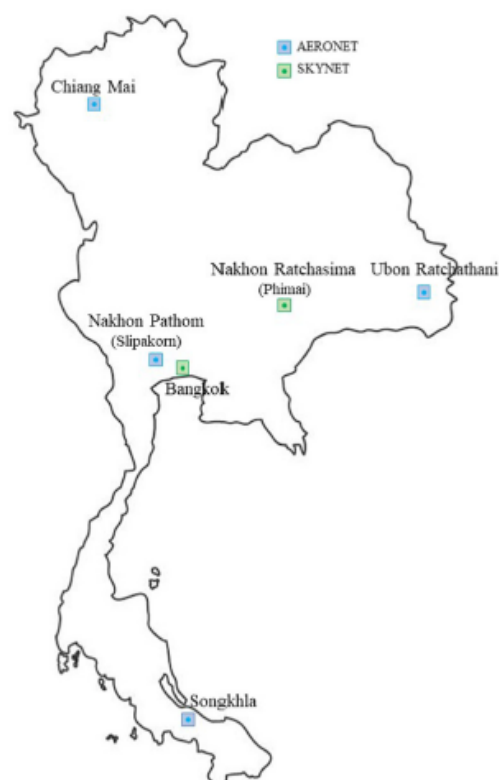


Fig. 1. Spatial distribution of synoptic stations in Thailand.

### 2.1. Ground-based and satellite data

Ground-based aerosol particles measurement using the Sun-photometer were collected from the AERONET networks at 340, 380, 440, 500, 675, 870, and 1020 nm (Giles, 2020). There are three levels in the last Version AOD data, which are Level 1.0 (unscreened), Level 1.5 (cloud-screened and quality controlled), and Level 2.0 (quality-assured) downloaded from <https://aeronet.gsfc.nasa.gov/website>. The AERONET research community adopt and validate new measurement technique and algorithms for AERONET products. Another AOD data were obtained from SKYNET networks, an observation network-related aerosol-cloud-radiation interaction under the WCRP/GAME project, focusing on East Asia. Data collections are available on <http://atmos3.cr.chiba-u.jp/skynet/website>. Satellite data retrieval was obtained from MODIS, installed on Terra and Aqua satellites, belonging to the NASA earth observing system since 1999. MODIS DB collection 6.1 Level 2 AOD products (MOD04\_L2 for Terra product and MYD04\_L2 for Aqua) has been used with the spatial resolution of a 10x10 1-km pixel array (at nadir) retrieved and downloaded from <https://ladsweb.modaps.eosdis.nasa.gov/missions-and-measurements/products> website.

Meteorological parameters (mean temperature, rainfall, RH, and wind speed) were obtained from the Thai meteorological department at local sites from 2006 to 2020.

### 3. Methodology and analysis

#### 3.1. AOD and AE calculation

AOD is the wavelength dependence that varies depending on the size, type, and chemical composition. The Angstrom equation describes the wavelength dependence (Angstrom, 1929), which is closely associated with the aerosol size distribution. Therefore, AOD can be written as follows:

$$\tau = \beta \lambda^{-\alpha} \quad (1)$$

Where  $\tau$  is the AOD;  $\beta$  is the Angstrom turbidity;  $\lambda$  is the wavelength, and  $\alpha$  is the Angstrom exponent (AE).

AE values are typically considered the independent parameter related to the size of particles (Cachorro et al., 1993, 2001; Kambezidis et al., 2001; Kumham, 2010; Shifrin, 1995; Toledano et al., 2007).

#### 3.2. Satellite AODs interpolation

Validation of satellite AODs at 550 nm is addressed by comparing the ground based AODs. Ground-based AODs 198 are retrieved at six visible channels (380, 440, 500, 675, 870, and 1020 nm) with the interpolated product at 550 199 nm. A quadratic equation is an equation having the form:

$$AOD_{550} = a_0 + a_1\lambda + a_2\lambda^2 \quad (2)$$

where  $\lambda$  represents the wavelength.  $a_0$ ,  $a_1$ , and  $a_2$  are real numbers and  $a \neq 0$ .

#### 3.3. Linear regression

Linear regression is a fundamental and commonly used predictive analysis applied for ground-based and satellite AODs as equation (3).

$$AOD_{satellite} = m \times AOD_{ground\ based} + c \quad (3)$$

where  $c$  is the intercept and  $m$  is a slope.  $AOD_{satellite}$  illustrates satellite AODs.  $R^2$  is the square of the correlation coefficient that represents the correlation between ground-based and satellite AODs. Linear trends in the time series during the study were obtained at each site.

### 4. Results and discussions

#### 4.1. Validation of ground-based and satellite data

Satellite AODs have been compared against the ground-based observations, as demonstrated in Fig. 2. Terra's orbit passes from North to South in the morning (10.30 a.m.), while Aqua passes South to North at about 1.30 p.m. Therefore, we used a pair of DB and AERONET AOD data samples considered collocated with a temporal window of  $\pm 30$  min for AERONET, and the spatial distance is within  $0.1^\circ$  (latitude/longitude). In the MODIS C6.1 validation, the validation of MODIS 10 km products against AERONET AOD data, with a  $1 \times 1$ -pixel sampling area ( $10 \times 10$  km<sup>2</sup> for the 10 km product). The correlation coefficients between satellite and ground based AODs are equal to or above 0.74 in Chiang Mai, Phimai, and Ubon Ratchathani. The highest correlation between Aqua MODIS and ground-based AODs has been found in Ubon Ratchathani with  $R^2 = 0.73$ , slope = 1.03, and Mean bias error (MBE) = 0.17, and the highest correlation between Terra MODIS and ground-based AODs has also been observed in Ubon Ratchathani with  $R^2 = 0.75$ , slope = 1.12, and MBE = 0.19. These results are likely related to the similar AOD retrieval algorithms obtained from two instruments. The lowest satellite and ground based AODs correlation coefficients are found over Nakhon Pathom. A station with a low correlation (0.5) may be due to a high level of air pollution or complex surface elements,

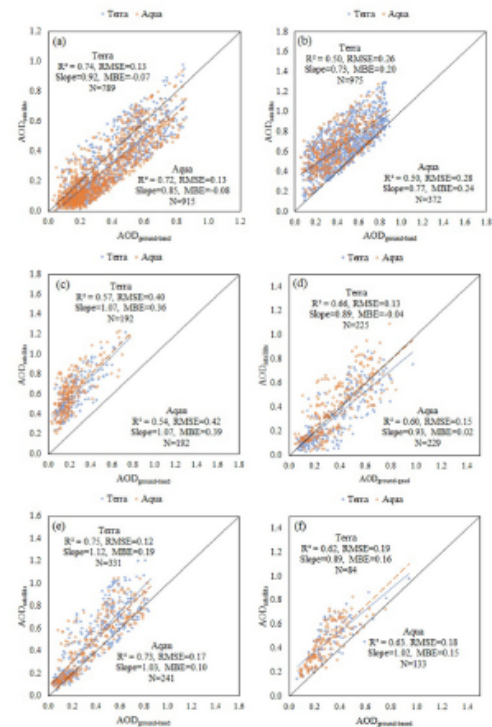


Fig. 2. Linear regression between ground based and satellite AODs in (a) Chiang Mai (b) Nakhon Pathom (c) Bangkok (d) Phimai (e) Ubon Ratchathani (f) Songkhla.

affecting lower sensitivity to aerosol properties (Cheng et al., 2006). The correlation coefficients of Terra MODIS and ground-based AODs are like those of Aqua MODIS and ground-based AODs at all sites. The satellite data underestimated AOD values that are more obvious in Chiang Mai and Phimai due to the impact of geography and surface albedo. The lowest single scattering albedo values were observed in Chiang Mai, which has the highest absorption (Janjai et al., 2012). The satellite data retrieval substantially overestimated AODs in Bangkok, Nakhon Pathom, Ubon Ratchathani, and Songkhla. This could be attributed to Songkhla's large water body, located in the South, affecting surface reflectivity. Bangkok and Nakhon Pathom, where Bangkok is the capital city of Thailand, and Nakhon Pathom is next to Bangkok, were detected with high AOD values, mainly due to human activity and transportation. Satellite AOD values are underestimated in low AOD conditions and slightly overestimated in medium or high AOD conditions (Gupta et al., 2022; Stimberg et al., 2018). In addition, areas with significant differences between spectrometers such as complex surfaces, complex aerosol types, and bright surfaces were underestimated and overestimated (Filonchik et al., 2019). As shown in Fig. 3, the satellite AEs are overestimated. This overestimation is slightly more significant in all stations except Chiang Mai. In addition, SKYNET networks (Bangkok and Phimai) have been operated for some years, and sometimes the instrument is broken, leading to missing data. Our results gave a weak correlation (0.50-0.66) at all stations. The highest correlation between Terra MODIS and ground-based AEs has been found in Chiang Mai with  $R^2=0.66$ ,

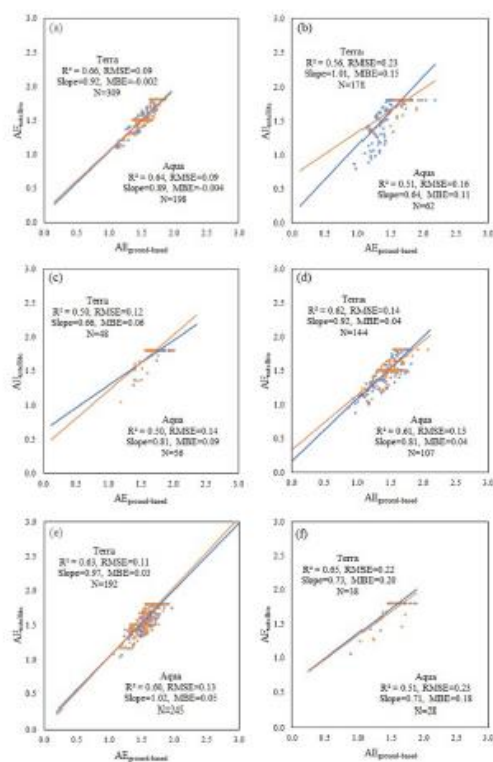


Fig. 3. Linear regression between ground based and satellite AEs in (a) Chiang Mai (b) Nakhon Pathom (c) Bangkok (d) Phimai (e) Ubon Ratchathani (f) Songkhla.

slope=0.92, and MBE=-0.002. However, many previous works also used AERONET and MODIS AE for analysis (Rupakheti et al., 2019; Sabetghadam et al., 2021; You et al., 2017).

4.2. AOD

Fig. 4 shows the monthly mean AOD obtained from satellite and ground-based data in (a) Chiang Mai, (b) Nakhon Pathom, (c) Bangkok, (d) Phimai, (e) Ubon Ratchathani, and (f) Songkhla. Seasonal variations in satellite and ground-based AODs at all stations show similar patterns, with an average of 0.41 for ground-based data and 0.53 for satellite data. Monthly ground based AOD values vary in Chiang Mai (0.12–0.72), Nakhon Pathom (0.13–0.63), Bangkok (0.43–1.29), Phimai (0.24–0.80), Ubon Ratchathani (0.15–0.67), and Songkhla (0.17–0.46). Monthly satellite AOD values vary in Chiang Mai (0.12–0.75), Nakhon Pathom (0.51–0.90), Bangkok (0.40–1.17), Phimai (0.17–0.83), Ubon Ratchathani (0.19–1.05), and Songkhla (0.38–0.98). The annual average of AOD for ground-based in Chiang Mai, Nakhon Pathom, Bangkok, Phimai, Ubon Ratchathani, and Songkhla are 0.42, 0.40, 0.60, 0.44, 0.38, and 0.24, respectively. Annual average of AOD for Terra are 0.41 (Chiang Mai), 0.70 (Nakhon Pathom), 0.70 (Bangkok), 0.40 (Phimai), 0.54 (Ubon Ratchathani), and 0.51 (Songkhla). The annual average of AODs for Aqua are 0.32 (Chiang Mai), 0.60 (Nakhon Pathom), 0.65 (Bangkok), 0.41 (Phimai), 0.50 (Ubon Ratchathani), and 0.50

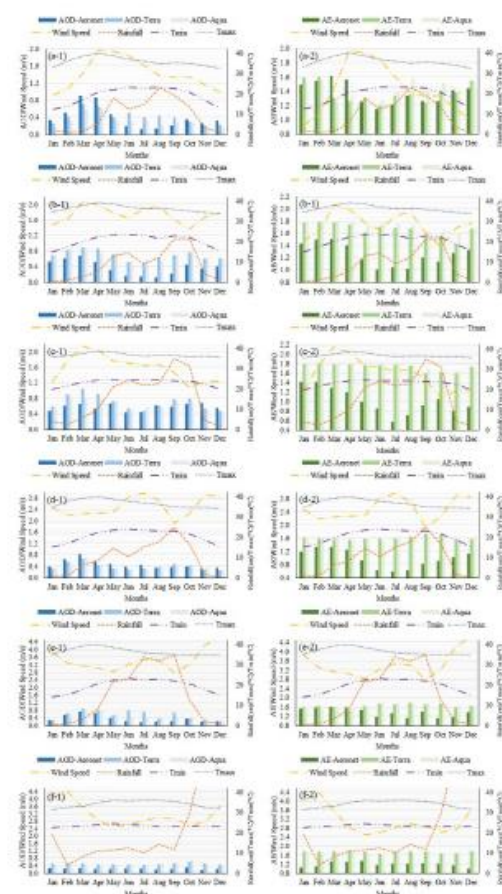


Fig. 4. Time series of monthly mean AOD and AE derived from satellite and ground based data in (a) Chiang Mai (b) Nakhon Pathom (c) Bangkok (d) Phimai (e) Ubon Ratchathani (f) Songkhla.

(Songkhla). Fig. 4 shows the monthly average of AOD for each site. Higher values of ground based and satellite AODs are observed from February to April (summer) compared with June to July (rainy season), except for Songkhla. The highest AOD value was detected at Bangkok station in April (0.91), while the lowest was observed at Phimai station (0.45). Songkhla is fewer variations of ground based AODs ranging from 0.16 to 0.36, and aerosol concentrations remain low and constant for a whole year. Low ground based and satellite AODs values were detected from June to July, which is likely due to increased rainfall and decreased atmosphere aerosol particles. Satellite and ground based AODs show high AOD values in Bangkok compared to Songkhla. Population growth, rapid urbanization, and economic development in Bangkok contribute to increased aerosol levels in the atmosphere. In contrast, a light industry with a small density of population and less human activity in Songkhla controlled aerosol particles formation, resulting in low AOD values. However, Aqua MODIS AOD annual values are slightly different from Terra MODIS AOD values because of instrument calibration or the difference in aerosol and cloud conditions. In addition, the MODIS



satellite (aboard Terra and Aqua) passes over Thailand at different times.

Illustrated in Fig. 5 is a regression analysis of satellite AODs against ground based AODs over the six sites from 2006 to 2020. Terra and Aqua MODIS, and ground based AODs have positive trends at all stations, except in Phimai (Fig. 5). In a positive direction, Aqua and Terra MODIS, and ground based AODs indicate data stability over this site. It is evident from Fig. 4 that variation in satellite AOD values is more significant. However, aerosol trends are obtained from different spectral radiometers depending on processing, calibration, and retrieval algorithms. In addition, meteorological parameters, cloud cover, anthropogenic activities, and sensors sensitivity also affect data generation.

Notably, the long-term trend indicates that the difference between satellite AODs is site-dependent which could be used for the long-term satellite performance. Both satellite and ground-based measurements indicate increasing trends in AOD over Thailand, primarily due to transportation, construction, factories, and biomass burning. The high aerosol level gradually rises toward 0.29 (an increase from 0.23 in 2006 to 0.52 in 2020) for ground-based data in Nakhon Pathom and 0.16 (from 0.66 in 2006 to 0.82 in 2020) for satellite measurements in Bangkok. As a result, satellite AOD values increased by 10.84% on average in 15 years. Similarly, there has been a gradual rise in aerosol levels for ground-based data by 6.05% in 15 years.

#### 4.3. AE

AE uses as an indicator of aerosol size distribution. Fig. 6 represents AE retrieved from ground-based and satellite data at six stations from 2006 to 2020. Analysis shows that AERONET AEs range from 0.90 to

1.66. Kumham and Hanprasert (2016) reported frequency distribution of AE values in Thailand ranging from 0.8 to 1.6, agreeing with AERONET results. Ground-based SKYNET AEs (0.62–1.14) show lower values than satellite AEs (1.00–1.66) for all stations. However, some AE values retrieved from AERONET AEs have been found high compared to satellite data in Chiang Mai. A possible explanation for this might be that Chiang Mai is the second biggest city in Thailand and is surrounded by mountains and forests, which leads to lower albedo. Low AE values (0.90–1.44) have also been found from SKYNET in Bangkok (population density of about 6,718 people per km), associated with the fine mode. It is encouraging to compare this figure with Kumham et al. (2020), who found that fine-mode aerosols showed apparent domination in the Central regions. In addition, fossil fuel consumption increased in Bangkok due to population growth and rapid urbanization, leading to many secondary anthropogenic aerosols. Aqua MODIS AEs in Chiang Mai (1.29–1.52), Nakhon Pathom (1.68–1.79), Bangkok (1.60–1.78), Phimai (1.57–1.70), Ubon Ratchathani (1.55–1.68), Songkhla (1.61–1.80) have been observed. Terra MODIS AEs in Chiang Mai, Nakhon Pathom, Bangkok, Phimai, Ubon Ratchathani, and Songkhla range from 1.38 to 1.53, 1.65–1.73, 1.59–1.77, 1.55–1.66, 1.57–1.70, and 1.64–1.80, respectively. Fig. 7 shows the frequency histogram of AE in two different frequency modes. AE frequency distribution is split into 11 groupings of 0.2 intervals. Higher AERONET AE is 56% in the range of 1.0–1.6, 30% ranges from 1.4 to 1.6, 20% is between 1.2 and 1.4, and 10% is below 1.0. MODIS AEs were observed between 1.4 and 1.8 is more than 80%. The wide range of daily frequency distribution of AE values implies the presence of different types of aerosols. High AE values indicate the dominance of fine particles. In contrast, low AE values show that aerosols consist mainly of coarse particles associated with biomass

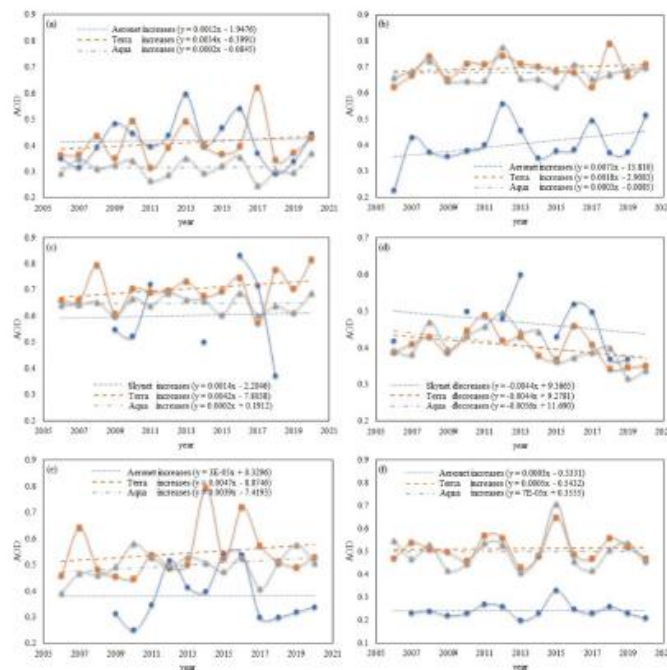


Fig. 5. Time series of year mean AOD derived from satellite and ground based data in (a) Chiang Mai (b) Nakhon Pathom (c) Bangkok (d) Phimai (e) Ubon Ratchathani (f) Songkhla.

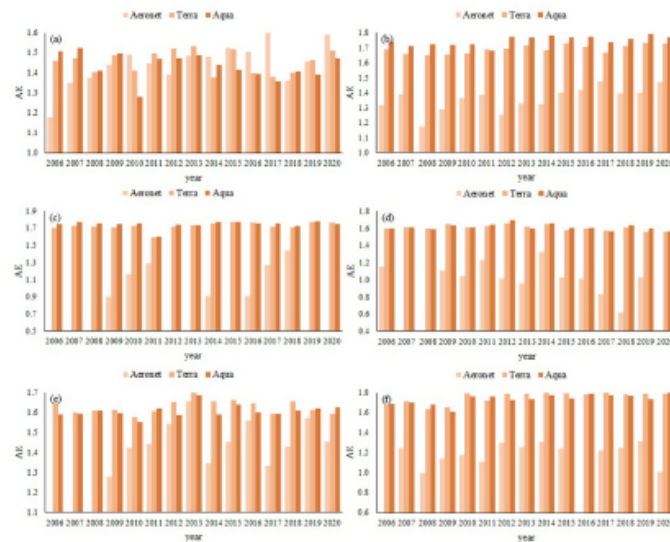


Fig. 6. AE variability in (a) Chiang Mai (b) Nakhon Pathom (c) Bangkok (d) Phimai (e) Ubon Ratchathani (f) Songkhla from satellite and ground based data for the years 2006–2020.

burning in the dry season. This finding is consistent with Kumharn et al. (2020), who found aerosol type can be categorized into anthropogenic pollution, biomass-burning smoke, and mineral dust. However, high and low AE values may come from fine mode aerosols during high-temperature periods (Lyamani et al., 2006).

#### 4.4. AOD, AE, and climate variables

In Thailand, seasons are defined as follows: winter (October–January), rainy (June–September), and summer (February–May). Mention above, higher AOD values are observed between February to April. However, the worst air pollution in Thailand is observed from December to February (winter) (Chalermpong et al., 2021; Kiangchuy et al., 2021), while the peak AOD is recorded in summer (Kumharn and Hanprasert, 2016; Kumharn et al., 2020). Air pollution in winter remains in the air for more extended periods than during the summer. However, harmful emissions from human activities in winter are low throughout the year. This result may be explained by the fact that AODs measure the extinction of solar radiation by aerosol particles in a vertical column from the Earth's surface to the top of the atmosphere. Therefore, local atmospheric and weather conditions significantly impact air pollution levels (Dejchanchaiwong et al., 2020). Our work infers that high aerosol concentrations were observed from February to April. On the question of AOD, this study found that Thailand's haze has worsened due to increase in aerosol particles caused by factors such as the transportation industry and biomass burning since 2015. Hence, this section examines AOD, AE, and climate variables during high concentrations of aerosol particles (February to April) for 2015–2020. Fig. 8 presents the results obtained from the preliminary analysis of AOD and AE from February to April at each station. As shown in Fig. 8, three months average of ground based AODs is 0.58, while Terra AOD value is 0.71 and Aqua is 0.66. High AOD from the ground is in Chiangmai at 0.90 and from Terra satellite is in Bangkok at 1.05.

The three-month average of ground-based and satellite AEs ranges from 1.07 to 1.62 and 1.29–1.80, respectively. The lower values of AE

indicate the large diameter of the aerosol particles associated with dust. In comparison, higher values of the AE show the presence of fine particles in the environment, resulting from biomass burning, sea-salt aerosols, and anthropogenic activities. High ground AEs show high values in Ubon Ratchathani and Chiangmai associated with coarse mode and low values in Bangkok, Nakhon Pathom, and Songkhla associated with fine mode, mainly due to exhaust from car engines, power plants, and agricultural waste burning from neighboring countries (Kumharn et al., 2020). Several lines of evidence suggest that the significant theories of high aerosols concentration in the winter months are the temperature inversion effect of agricultural burning, either locally or from surrounding countries (Dejchanchaiwong et al., 2020; Kayes and Kabir, 2019). Mild temperature inversions in Bangkok obtained from the Integrated Global Radiosonde Archive are observed with a high between 1,230–3,660 m, as shown in Fig. 9. Surface temperature inversions play a significant role in air quality during the winter months with a firm surface inversion. The temperature inversions trap a layer of cold air with pollution close to the ground for days or even weeks at a time (Ji et al., 2019; Khalesi and Mansouri Daneshvar, 2020). During the 2015–2020 haze period, the higher aerosol concentrations are also connected with the climate conditions that induce thermal inversions and light winds.

During high aerosol concentrations, the meteorological parameters such as high maximum temperature, low minimum temperature, light wind speed, and less or non-rainfall significantly impact aerosol concentrations in the atmosphere (He et al., 2017; Kayes and Kabir, 2019). The lower minimum temperature was recorded in February (14.06 °C) at Chiang Mai station; however, maximum and minimum temperatures changed slightly at all stations. The average wind speed is 2.40 m/s, and lower values are observed at Chiangmai station in February (1.09 m/s). Low wind speed may have resulted in aerosol particles suspended for long periods in the atmosphere, not affecting aerosol diffusion on their sedimentation. In addition, aerosol concentration increases due to the northeast monsoon that brings cooler temperatures and no/less chance of rainfall for most of Thailand. However, the average rainfall at all

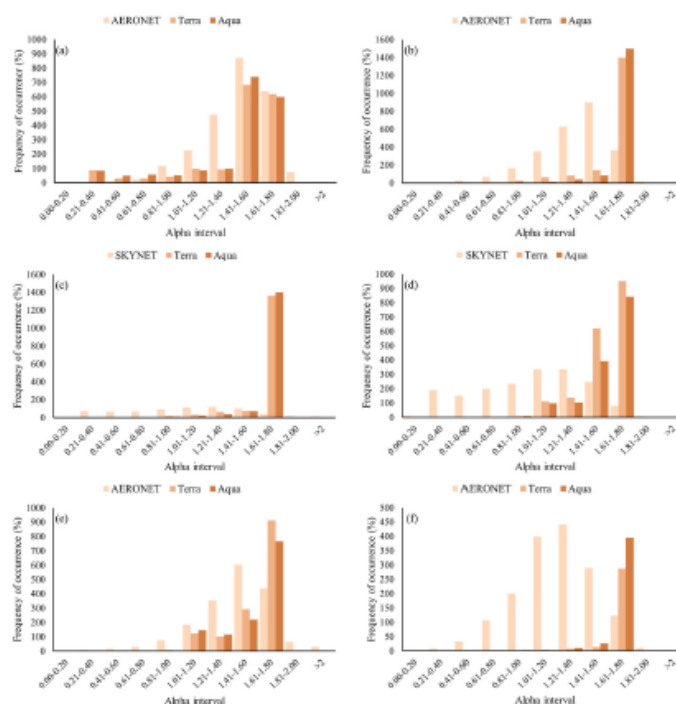


Fig. 7. The frequency histogram of AE in a) Chiang Mai (b) Nakhon Pathom (c) Bangkok (d) Phimai (e) Ubon Ratchathani (f) Songkhla from satellite and ground based data for the years 2006–2020.

stations (except in Songkhla) is detected as more petite than 10.91 nm/month in February. From the observations, it was found that climate variables (low minimum temperature ( $<14\text{ }^{\circ}\text{C}$ ), high maximum temperature ( $>36\text{ }^{\circ}\text{C}$ ), light wind speed ( $<1\text{ m/s}$ ), and less or non-rainfall ( $<10\text{ mm/month}$ ) are related to the aerosol size distribution and aerosol loading in the atmosphere. However, no significant impact of meteorological parameters on AE has been found.

## 5. Conclusions

Satellite and ground based AODs in different locations were investigated at six stations in Thailand from 2006 to 2020. The validation of the data obtained from AERONET and SKYNET ground networks was also carried out. Long-term observations have reported similar AOD trends between satellite and ground-based measurements. Satellite AODs illustrated a high correlation at most sites, indicating good agreement with ground-based observations. Satellite and ground based AODs vary depending on the season, locations, and aerosol type, with a confidence level of about 87%. Ground-based sites were used to verify sites for satellite data retrievals. Satellite data retrievals are also likely to be well-represented in Ubon Ratchathani, giving an overestimation of AOD between 1.0 and 2.0. Satellite AODs can provide a good representation of the AOD climatology almost at all sites. Generally, there is a tendency towards the gradual rise in aerosol concentration in all stations for ground-based data except in Phimai. Satellite data tend to underestimate AOD in Chiang Mai and overestimate AOD in Nakhon Pathom, Bangkok, and Songkhla. The ample water surrounding Songkhla seemed to affect the daytime satellite data, giving larger values than AERONET

measurements. Seasonal AOD variation showed a clear annual pattern with maximum summer and minimum rainy season. High AOD values contribute to the hygroscopic growth of aerosols, secondary aerosols, and pollutants. In summer, the country's whole territory is exposed to aerosol particles from North, Northeast, and neighboring countries, increasing AOD. In the rainy season, aerosol particles are scavenging because of the activity of the Southeast Monsoon, resulting in an AOD decrease. Low AOD values characterize the Phimai site, related to the station's landscape nature. Based on analyzing high AOD, it was found in Bangkok and Nakhon Pathom, which are the most polluted sites. Ground-based AEs showed lower values than satellite AEs except in Chiang Mai. Higher ground-based AEs show that aerosols consist mainly of coarse particles associated with biomass burning. The high aerosol levels covering from 2015 to 2020 were found in February with low minimum temperature ( $<14.06\text{ }^{\circ}\text{C}$ ), high maximum temperature ( $>36.26\text{ }^{\circ}\text{C}$ ), less rainfall ( $<10\text{ mm/month}$ ), and light wind speed ( $<1.09\text{ m/s}$ ), leading to high aerosol concentrations. Higher values of AE are associated with low AODs, and lower values of AE are related to high AODs. The variation in AE is primarily because of variation in AOD, which indicates that the anthropogenic aerosols contribute substantially to AOD (Deep et al., 2021). MODIS combined with AERONET and SKYNET has massive potential to ensure complex estimation of AOD, significantly reducing measurement uncertainties of AOD. To solve these issues, the expansion of monitoring networks of AERONET and SKYNET stations is essential. The results presented in this study are crucial, providing a guideline for satellite retrievals to give reliable data over a particular geographic location and AOD range over the tropic. Furthermore, in comparison to MODIS with ground-based instruments,



Fig. 8. AOD, AE, and Climate variables in a) Chiang Mai (b) Nakhon Pathom (c) Bangkok (d) Phimai (e) Ubon Ratchathani (f) Songkhla from satellite and ground based data for the years 2015–2020.

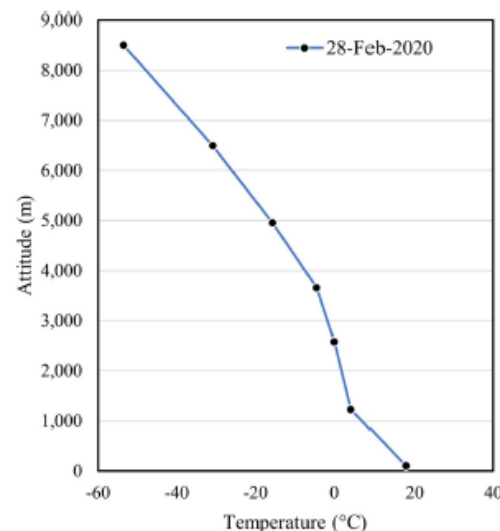


Fig. 9. Temperature inversion on February 28, 2020 in Bangkok obtained from the Integrated Global Radioonde Archive.

our knowledge of aerosols climatology over Thailand is immensely encouraging.

**CREDIT authorship contribution statement**

**Oradee Pilahome:** Methodology, Assoc. Prof. Dr, Visualization, Assoc. Prof. Dr, Software, Validation, Formal analysis, Investigation. **Walchaya Ninssawan:** Software, Investigation. **Yuttapichal Jankondee:** Investigation. **Serm Janjai:** Prof. Dr. **Wilawan Kumharn:** Conceptualization, Assoc. Prof. Dr, Methodology, Assoc. Prof. Dr, Writing – original draft, Assoc. Prof. Dr, Writing – review & editing, Assoc. Prof. Dr, Visualization, Assoc. Prof. Dr, Supervision, Assoc. Prof. Dr.

**Declaration of competing interest**

The authors declare that they have no known competing financial interests or personal relationships that could have appeared to influence the work reported in this paper.

**Acknowledgment**

This research project is supported by the National Research Council of Thailand (NRCT) (Contact No. N41A650116). In addition, we thank our colleagues from Silpakorn University for providing AERONET V-ASD data and the Center for Environmental Remote Sensing, Chiba University, for operating SKYNET V-ASD data which provided data for the research.

**References**

Agorn, S., 2010. Meteorological Observations in Thailand. Final Report of JMA/WMO Workshop on Quality Management in Surface, Climate and Upper-Air Observations in RA II (Asia), pp. 170–173. Tokyo.

Andronache, C., 2004. Precipitation removal of ultrafine aerosol particles from the atmospheric boundary layer. *J. Geophys. Res. Atmos.* 109.

Angstrom, A., 1929. On the atmospheric transmission of Sun radiation and on dust in the air. *Geogr. Ann.* 11, 156–166.

Bartoszek, K., Matuzsko, D., Soroka, J., 2020. Relationships between cloudiness, aerosol optical thickness, and sunshine duration in Poland. *Atmos. Res.* 245, 105097.

Cachorro, V.E., De Frutos, A.M., Gonzalez, M.J., 1993. Analysis of the Relationships between Junge Size Distribution and Angstrom Turbidity Parameters from Spectral Measurements of Atmospheric Aerosol Extinction, 27 A. *Atmospheric Environment - Part A General Topics*, pp. 1585–1591.

Cachorro, V.E., Viegas, P., De Frutos, A.M., 2001. A quantitative comparison of Å turbidity parameter retrieved in different spectral ranges based on spectroradiometer solar radiation measurements. *Atmos. Environ.* 35, 5117–5124.

Chalermpong, S., Thaitrakul, P., Anuchitchanchai, O., Sanghatawatana, P., 2021. Land use regression modeling for fine particulate matters in Bangkok, Thailand, using time-variant predictors: effects of seasonal factors, open biomass burning, and traffic-related factors. *Atmos. Environ.* 246, 118128.

Cheng, T., Liu, Y., Lu, D., Xu, Y., Li, H., 2006. Aerosol properties and radiative forcing in Hunshan Lake desert, northern China. *Atmos. Environ.* 40, 2169–2179.

Deep, A., et al., 2021. Aerosols optical depth and Ångström exponent over different regions in Garhwal Himalaya, India. *Environ. Monit. Assess.* 193, 324–324.

Dejchanchaiwong, R., et al., 2020. Impact of transport of fine and ultrafine particles from open biomass burning on air quality during 2019 Bangkok haze episode. *J. Environ. Sci.* 97, 149–161.

Filonchik, M., et al., 2019. Combined use of satellite and surface observations to study aerosol optical depth in different regions of China. *Sci. Rep.* 9, 6174.

Gao, W., Slusser, J., Schmoldt, D., Kerr, J., 2010. *The Brewer Spectrophotometer. UV Radiation in Global Climate Change*. Springer Berlin Heidelberg, pp. 160–191.

Giles, D.M., (2020).

Gupta, G., Venkat Ratnam, M., Madhavan, B.L., Narayanamurthy, C.S., 2022. Long-term trends in Aerosol Optical Depth across the globe obtained using multi-satellite measurements. *Atmos. Environ.*, 118953.

Habib, A., et al., 2019. Estimation and inter-comparison of dust aerosols based on MODIS, MISR and AERONET retrievals over Asian desert regions. *J. Environ. Sci.* 76, 154–166.

He, J., et al., 2017. Air pollution characteristics and their relation to meteorological conditions during 2014–2015 in major Chinese cities. *Environ. Pollut.* 223, 484–496.

Janjai, S., Nunez, M., Masiri, I., Wattan, R., Buntoung, S., Jantarach, T., Promsen, W., 2012. Aerosol optical properties at four sites in Thailand. *Atmos. Clim. Sci.* 2, 441–453.

Jantarach, T., Masiri, I., Janjai, S., 2012. Comparison of MODIS aerosol optical depth retrievals with ground-based measurements in the tropics. *Procedia Eng.* 32, 392–398.

Paper II

Published in the Advances in Space Research journal.

Impact 2.611

Available online at [www.sciencedirect.com](http://www.sciencedirect.com)

ScienceDirect

Advances in Space Research 71 (2023) 3166–3174

ADVANCES IN  
SPACE  
RESEARCH  
(a COSPAR publication)

[www.elsevier.com/locate/asr](http://www.elsevier.com/locate/asr)

## Variations in aerosols and aerosols–cloud interactions in Bangkok using MODIS satellite data during high PM<sub>2.5</sub> concentrations

Oradee Pilahome<sup>a</sup>, Waichaya Nissawan<sup>a</sup>, Yuttapichai Jankondee<sup>a</sup>, Itsara Masiri<sup>b</sup>,  
Wilawan Kumharn<sup>a,\*</sup>

<sup>a</sup> Department of Physics, Faculty of Science and Technology, Sakon Nakhon Rajabhat University, Sakon Nakhon, Thailand

<sup>b</sup> Department of Physics, Faculty of Science, Silpakorn University, Nakhon Pathom, Thailand

Received 18 August 2022; received in revised form 7 December 2022; accepted 8 December 2022

Available online 14 December 2022

### Abstract

The relationships between particulate matter with aerodynamic diameters less than 2.5  $\mu\text{m}$  (PM<sub>2.5</sub>), aerosol optical depth (AOD), and cloud parameters were investigated during high PM<sub>2.5</sub> concentrations from 1 January 2016 to 31 December 2021 in Bangkok using satellite remote sensing data from Moderate Resolution Imaging Spectroradiometer (MODIS). Cloud parameters included: Cloud effective radius (CER), Cloud fraction (CF), Cloud optical depth (COD), Cloud liquid water (CLW), Cloud top pressure (CTP), and Cloud top temperature (CTT). The analysis showed a strong negative correlation between PM<sub>2.5</sub> and CF. There was a negative correlation between CF and AOD. In addition, PM<sub>2.5</sub> showed a negative relationship with CER. In contrast, PM<sub>2.5</sub> showed a positive correlation with CTP and CTT. A negative correlation was detected between COD and PM<sub>2.5</sub>. During high PM<sub>2.5</sub> concentrations, cloud parameters are significantly influenced by PM<sub>2.5</sub> concentrations in the atmosphere. The three-month of CER, CF, CLW, COD, CTP, and CTT ranges from 16.34  $\mu\text{m}$  to 37.05  $\mu\text{m}$ , 0.22 to 0.86, 15.67  $\text{g}/\text{m}^2$  to 169.80  $\text{g}/\text{m}^2$ , 1.14 to 19.06, 261.67 hPa to 991.67 hPa, and  $-66.26\text{C}$  to  $-22.17\text{C}$ , respectively. Consequently, Altostratus clouds most appear during high PM<sub>2.5</sub> concentrations in Bangkok. The findings may help better understand Bangkok's cloud properties and atmospheric aerosols, providing more information for rainmaking during high PM<sub>2.5</sub> concentrations.

© 2022 COSPAR. Published by Elsevier B.V. All rights reserved.

**Keywords:** Aerosol; Cloud; AOD; MODIS; Angstrom exponent

### 1. Introduction

Rapid urbanization and industrialization have recently caused air pollution in Bangkok's particulate matter with aerodynamic diameters less than 2.5  $\mu\text{m}$  (PM<sub>2.5</sub>) crisis. PM<sub>2.5</sub> is a well-known parameter for polluted understanding levels of air and a substantial component of haze pollution that appears to be both increasing and decreasing

trends, depending on locations (Kumharn and Hanprasert, 2016, Kumharn et al., 2020). PM<sub>2.5</sub> are liquid/solid particles suspended in the atmosphere and play a critical role in the climate of the Earth's atmosphere. The direct effects of aerosols influence the climate directly by scattering and absorbing incoming solar radiation called aerosol–radiation interactions. The indirect effects of aerosols act as nuclei for water vapor concentrations called cloud condensation nuclei (CCN), known as aerosol–cloud interactions. Twomey [1977] first theorized such aerosol–cloud interaction, generally called the Twomey effect. This effect was found that increased anthropogenic

\* Corresponding author at: Department of Physics, Faculty of Science and Technology Sakon Nakhon Rajabhat University, Sakon Nakhon 47000, Thailand.

E-mail address: [wilawan\\_kumham@snru.ac.th](mailto:wilawan_kumham@snru.ac.th) (W. Kumham).

<https://doi.org/10.1016/j.asr.2022.12.018>

0273-1177/© 2022 COSPAR. Published by Elsevier B.V. All rights reserved.

aerosol emissions led to the radiative forcing associated with cloud albedo, which is the critical driver of effective radiative forcing due to aerosol-cloud interactions. An increase in cloud lifetime may come from CCN obtained from anthropogenic pollution, resulting increase in the amount of solar radiation reflected from clouds (Albrecht, 1989). Low clouds with small liquid water paths are observed in high accumulation mode aerosols, related to the cloud droplets having a smaller effective radius, providing the clouds with higher emissivity (Garrett and Zhao, 2006). Therefore, increased  $PM_{2.5}$  levels can enhance CCN concentrations and the density of cloud droplets. Subsequently, the droplet size declines, and the cloud albedo increases, leading to a constant liquid water content (Intergovernmental Panel on Climate Change, 2007).

Numerous studies have attempted to explain the relationship between cloud and aerosol particles (Alam et al., 2010, Brennan et al., 2005, Costantino and Bréon, 2010, Dong et al., 2019, Hasekamp et al., 2019, Myhre et al., 2007, Oreopoulos et al., 2020, Saponaro et al., 2020). Myhre Stordal (2007) showed most of the substantial rise in cloud cover with AOD using MODIS data, at least for AOD less than 0.2. Analysis of several aerosol types reveals that the cloud mask and products can be securely utilized in aerosol up to an AOD of 0.6 (Brennan, Kaufman, 2005). In addition, MODIS sees the aerosol variations of the planet's cloud regimes and rises in cloud radiative fluxes with AOD (Oreopoulos, Cho, 2020). Therefore, satellite retrievals can be provided accurate data for such as the size distribution change raises the cloud albedo so that the aerosols have a net cooling effect. Furthermore, the difference in size distribution may influence the cloud precipitation and life cycle. Unfortunately, there is little published data on aerosol-cloud interaction in Thailand. Therefore, this work aimed to explore the relationship of aerosol-cloud interaction during high  $PM_{2.5}$  concentrations in Bangkok.

## 2. Data collection

Bangkok is the capital city of Thailand with crowded and the highest pollution levels due to undergoing rapid growth in private automobile use, leading to traffic jams, and air pollution. Bangkok is in the center with 15687 km<sup>2</sup> along the Chao Phraya delta, and about Fourteen million people (22.2 %) live within the Bangkok metropolitan region. Cloud and aerosol products were collected from 1 January 2016 to 31 December 2021.

### 2.1. Cloud data

Cloud properties, including CER, CF, COD, CTP, CTT, and CLW, determine physical and radiative cloud properties and illustrate the Earth's upper-air atmosphere state. Those data were obtained from the Moderate Resolution Imaging Spectroradiometer (MODIS) with a 36-channel radiometer aboard the Terra and Aqua satellites.

This work used MODIS Cloud Product Collection 6.1 (MYD06\_L2 for Aqua), a spatial resolution of either 1 km or 5 km (at nadir), providing cloud parameters, and retrieved at wavelengths of 2.1, 1.6, and 3.7  $\mu$ m. Data were downloaded from [https://ladsweb.modaps.eosdis.nasa.gov/search/order/1/MYD06\\_L2-61](https://ladsweb.modaps.eosdis.nasa.gov/search/order/1/MYD06_L2-61).

### 2.2. AOD, AE, and $PM_{2.5}$ data

AOD and AE products (MYD04\_L2 for Aqua) were collected from MODIS Deep Blue Dark Target (DBDT) collection 6.1 Level 2 with the spatial resolution of a 10x10 1-km pixel array (at nadir) and downloaded from <https://ladsweb.modaps.eosdis.nasa.gov/missions-and-measurements/products> website. The Collection 6.1 retrieval algorithm has three channels (0.47, 0.66, and 2.12  $\mu$ m), mainly utilized for over-land aerosol retrievals. The pollution control department collected a daily average of  $PM_{2.5}$  data.  $PM_{2.5}$  data were applied.

## 3. Results and discussions

The variations in aerosol and cloud properties were examined in Bangkok from 2016 to 2021, which has faced high  $PM_{2.5}$  concentrations crisis in the last ten years. In addition, evaluating the probability of rainy clouds was observed during high  $PM_{2.5}$  concentrations for rainmaking to reduce  $PM_{2.5}$  concentrations in the atmosphere.

### 3.1. Descriptive statistics

Clouds properties (CER, CF, COD, CTP, CTT, and CLW) and aerosol properties ( $PM_{2.5}$ , AOD, AE) in Bangkok were obtained from January 2016 to December 2021 and are shown in Table 1. Average values of  $PM_{2.5}$  AOD and AE are  $22.10 \pm 9.68 \mu\text{g}/\text{m}^3$ ,  $0.66 \pm 0.15$ , and  $1.77 \pm 0.02$ , respectively. The highest annual average  $PM_{2.5}$  concentrations were found in winter ( $30.10 \mu\text{g}/\text{m}^3$ ), and the lowest annual average was observed in the rainy season ( $13.06 \mu\text{g}/\text{m}^3$ ). This result may be explained by the fact that pollution is trapped close to ground level in the winter due to low mixed boundary layer height. As a result, those pollutants remain in the air for longer than in other seasons. However, the summer months gave the highest annual average AOD (0.83) compared with the rainy season (0.58). A possible explanation for this might be that AOD is an aerosol measured in a vertical column from the Earth's surface to the top of the atmosphere, while  $PM_{2.5}$  are suspended near the ground and controlled by local weather conditions, particularly in the winter (Mhawish et al., 2020, Pilahome et al., 2022). Monthly average CER, CF, CLW, COD, CTP, and CTT are 27.16  $\mu$ m, 0.78, 102.60 g/m<sup>2</sup>, 6.38, 507.39 hPa, and -53.80C, respectively. High CER, CF, CLW, and COD were observed in the rainy season, while high CTP and CTT were detected in the summer.

Table 1  
MODIS mean and standard deviation of all parameters in Bangkok for different seasons during the period 2016 to 2021.

	Winter	Summer	Rainy	Annual
CER	27.01 ± 1.54	27.11 ± 2.06	28.05 ± 1.27	27.16 ± 1.87
CF	0.73 ± 0.05	0.68 ± 0.12	0.90 ± 0.02	0.78 ± 0.11
CLW	96.32 ± 12.83	79.84 ± 13.55	125.48 ± 9.18	102.60 ± 22.29
COD	6.65 ± 0.64	4.71 ± 0.91	7.36 ± 0.46	6.38 ± 1.25
CTP	526.02 ± 53.27	620.90 ± 119.03	400.06 ± 32.21	507.39 ± 110.07
CTT	-50.65 ± 5.98	-46.07 ± 14.79	-64.69 ± 4.58	-53.80 ± 12.44
AE	1.77 ± 0.03	1.76 ± 0.02	1.78 ± 0.02	1.77 ± 0.02
AOD	0.59 ± 0.12	0.83 ± 0.06	0.58 ± 0.10	0.66 ± 0.15
PM <sub>2.5</sub>	30.10 ± 8.92	23.35 ± 8.09	13.06 ± 1.21	22.10 ± 9.68

### 3.2. Variations in aerosols particle parameters

Seasonal variations in PM<sub>2.5</sub>, AOD, and AE were analyzed from 2016–2021. Fig. 1 presents the results from the preliminary analysis of monthly PM<sub>2.5</sub>, AOD, and AE. High PM<sub>2.5</sub> concentrations are detected from December to February, while high AOD values are observed from February to May. The weather conditions (low temperature, low relative humidity, low rainfall, and light wind) influence PM<sub>2.5</sub> concentrations measured near the ground. AEs are constant for a whole year, with an average of 1.77. PM<sub>2.5</sub> and AOD values are in the ranges of 8.45 µg/m<sup>3</sup> to 46.89 µg/m<sup>3</sup> and 0.37 to 1.05, respectively. AE values are in the range of 1.49 to 1.80; this represents the type of fine particles mainly oriented from transportation and industrial areas. Monthly PM<sub>2.5</sub> and AOD are in the same pattern except November to February due to temperature inversion which occurs about 1,230 m to 3,660 m from the ground (Pilahome, Ninssawan, 2022). The highest PM<sub>2.5</sub> and AOD are found in January (39.42 µg/m<sup>3</sup>) and February (0.88), while the lowest PM<sub>2.5</sub> and AOD are detected in June (11.81 µg/m<sup>3</sup>) and July (0.44), respectively. Wet deposition reduces aerosol concentrations in the atmosphere during the rainy season (Kumham, Janjai, 2020). As

illustrated in Fig. 2, the frequency distributions of PM<sub>2.5</sub>, AOD, and AE are much higher for the interval of 8 µg/m<sup>3</sup> to 14 µg/m<sup>3</sup> at 31 %, 0.4 to 0.6 at 42 %, and 1.7 to 1.8 at 59 %, respectively. On the question of AE, this region observed that aerosol particles show domination by fine mode, associated with human activities.

### 3.3. Variations in cloud parameters

CER, CF, COD, CLW, CTP, and CTT were analyzed for seasonal variations from 2016 to 2021 (Fig. 3). High CER, CF, CLW, and COD were observed from May to October, while high CTP and CTT were detected from February to May. Monthly CLW and COD have a similar pattern as CTP and CTT, while CF and CER have opposite ways. CER, CF, COD, CLW, CTP, and CTT values are in the range of 10.57 µm to 37.05 µm, 0.10 to 0.18, 1.14 to 19.06, 15.67 g/m<sup>2</sup> to 207.50 g/m<sup>2</sup>, 240.94 hPa to 1010.00 hPa, and -86.70 to 4.36C. It can be seen from the data in Fig. 2 that the frequency distribution of CER, CF, COD, CTP, CTT, and CLW are much higher in the range 23 µm to 29 µm (45 %), 0.8 to 1.0 (51 %), 5 to 9 (42 %), 405 hPa to 525 hPa (32 %), -60.0C to -45.1C (36 %), and 45 g/m<sup>2</sup> to 75 g/m<sup>2</sup> (22 %), respectively.

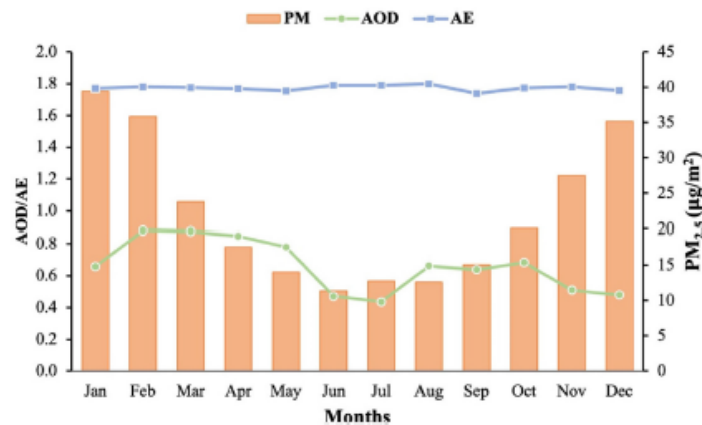


Fig. 1. Time series of monthly mean PM<sub>2.5</sub>, AOD, and AE derived from satellite in Bangkok from 2016 to 2021.

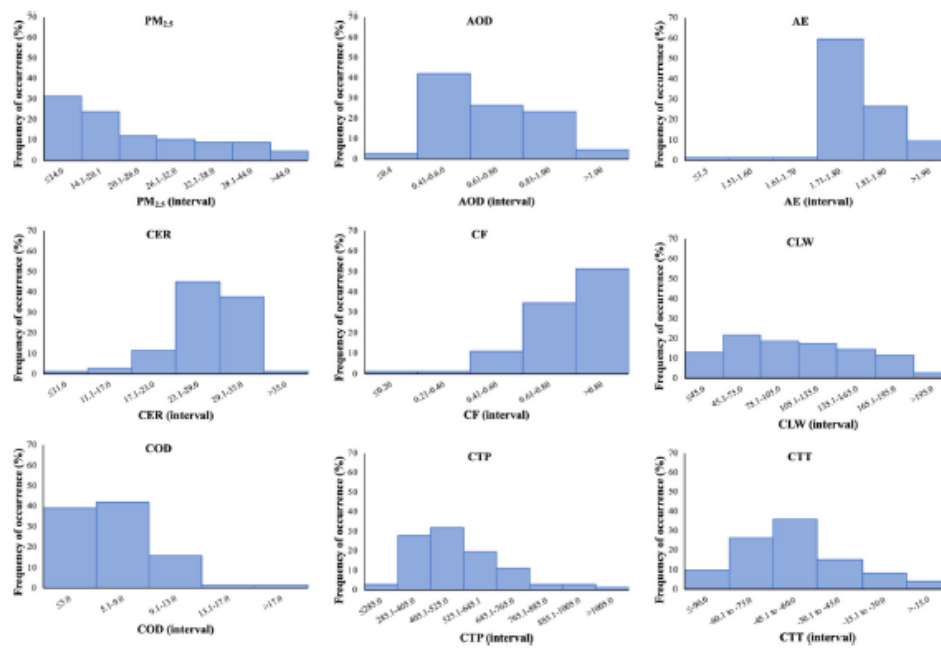


Fig. 2. Histogram of  $PM_{2.5}$ , AOD, AE, CER, CF, CLW, COD, CTP, and CTT in Bangkok from 2016 to 2021.

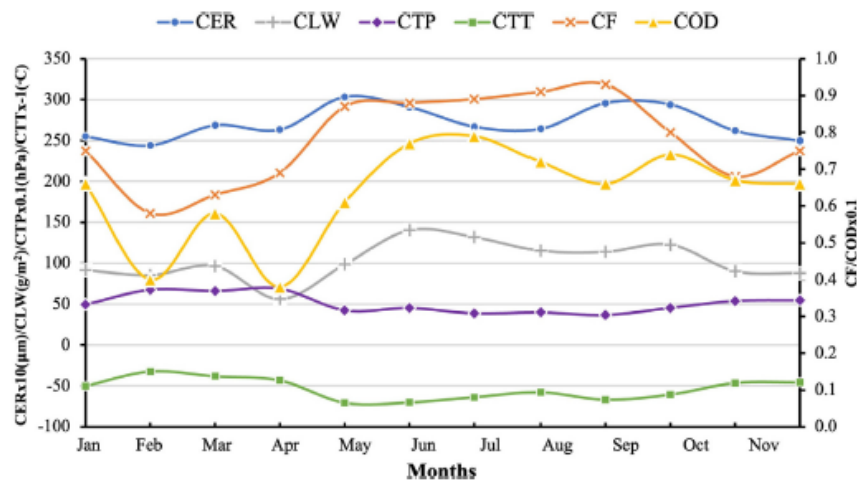


Fig. 3. Time series of monthly mean CER, CF, CLW, COD, CTP, and CTT derived from satellite in Bangkok from 2016 to 2021.

### 3.4. Relationships between $PM_{2.5}$ , AOD, and cloud parameters

$PM_{2.5}$  and AOD represent the number of aerosol particles in the atmosphere. Therefore, correlation coef-

ficients were addressed to compare the relationships between  $PM_{2.5}$ , AOD, and cloud parameters for each set of monthly parameters by using the Aqua MODIS from 2016 to 2021. AEs were not included in the analyses due to being constant for a whole year. The



relationships between aerosols properties and cloud parameters were examined.

#### 3.4.1. Relationship between $PM_{2.5}$ , AOD, and CER

The relationship between  $PM_{2.5}$  and CER has been trending weak negative.  $PM_{2.5}$  and CER values range from  $8.45 \mu\text{g}/\text{m}^3$  to  $46.89 \mu\text{g}/\text{m}^3$  and  $10.57 \mu\text{m}$  to  $37.05 \mu\text{m}$ , respectively. A weak negative correlation was also found between AOD ( $0.37 \leq \text{AOD} \leq 1.05$ ) is detected with CER ( $10.57 \mu\text{m} \leq \text{CER} \leq 37.05 \mu\text{m}$ ). As shown in Fig. 4, The findings demonstrated that the variation of CER with AOD agreed with the anti-Twomey effect due to competition for the water vapor effect in the cloud droplets, resulting in the evaporation of tiny cloud droplets. AOD is a negative correlation with CER at medium aerosol pollution ( $\text{AOD} > 0.77$ ), and CER decreased with increasing  $PM_{2.5}$  at medium to high aerosol pollution ( $PM_{2.5} > 15 \mu\text{g}/\text{m}^3$ ) (Fig. 4). The results are shown in Table 2. It is important to note that AOD and CER pass the significance test at all seasons. No Twomey effect between AOD and CER occurs in the winter ( $R^2 = 0.18$ ) and rainy seasons ( $R^2 = 0.52$ ). However, AOD and CER agreed with a slight correlation with the anti-Twomey effect in the summer seasons. There is no significant test between  $PM_{2.5}$  and CER in the winter. It reveals that  $PM_{2.5}$  and CER have a weak and negative correlation. CER values are higher during the rainy season, suggesting the possibility of aerosol hygroscopic growth. This could be due to less  $PM_{2.5}$ , causing a decrease in cloud drops and an increase in the effective cloud particle size. In addition, the enormous size of cloud droplets encourages the warm rain process (Jia et al., 2019, Zhang et al., 2020, Zhu et al., 2021). Thus, the low concentration of cloud condensation nuclei (CCN) and cloud droplets could contribute to larger CER, increasing larger droplets through the collision-coalescence process between cloud drops (Che et al., 2022, Janssen et al., 2011). On the other hand, the collision-coalescence process is controlled by a high level of aerosol concentrations, increasing the cloud droplets and leading to a decline in their effective radius. This finding is consistent with Zhu et al. (2022) and Khatri et al. (2021) result from Southeast Asia. In addition, very low aerosol concentration observed or nonexistent in the atmosphere during the rainy season, resulting in high CER.

#### 3.4.2. Relationship between $PM_{2.5}$ , AOD, and CF

CF data were obtained from MODIS using a combination of daytime for analysis. There is a decrease in CF ( $0 < \text{CF} \leq 1.0$ ) when the AOD values range from 0.1 to 1.05 (Fig. 4). The same pattern was also found with CF and  $PM_{2.5}$ . The correlations between AOD and CF in all seasons were significant (Table 2). AOD and CF give a positive correlation in the rainy ( $R^2 = 0.31$ ) and winter seasons ( $R^2 = 0.24$ ), while a negative correlation was detected in summer ( $R^2 = -0.29$ ). It is important to note that  $PM_{2.5}$  and CF pass the significance test at all seasons. Correlation coefficients for  $PM_{2.5}$  and CF are calculated with a strong

negative correlation ( $R^2 = -0.51$ ). The importance of CF was reflected, and the evident interactions between CF and aerosol properties were observed. High CF values were found in rainy, while  $PM_{2.5}$  and AOD gave low values. A study by Kaufman and Koren (2006) implied that the correlation coefficients might depend on the aerosol type. Therefore, CF may be associated with AOD level, leading to high uncertainty of AOD retrieval. In addition, the impact of CF has a significant on AOD, which CF led to ~80% missing AOD (Bi et al., 2019). Significantly, the substantial decrease in the correlation between CF and  $PM_{2.5}$  is dominated by fine mode, indicating meteorological factors influence the relationship. Clouds formed in polluted areas showed a gradual growth of cloud particles and precipitation with altitude, compared with dusty clouds. In addition, a cloud formed from desert dust by tiny droplets with effective radii only occurred when the AOD fell below 0.3 (Rosenfeld et al., 2001). From previous studies, the increasing CF value is associated with decreasing of aerosol concentrations. The change in Cloud properties is due to the changes/variations in large-scale, which may also influence  $PM_{2.5}$  concentrations (Kaufman et al., 2005).

#### 3.4.3. Relationship between $PM_{2.5}$ , AOD, and CLW

CLW is the amount of the total liquid water contained in a cloud in the atmospheric vertical column. CLW is influenced by global warming and by aerosol emission trends. There is a remarkable decrease in CLW with decreasing AOD, and CLW also decreases with decreases in  $PM_{2.5}$  (Fig. 4). The correlation between AOD and CLW and  $PM_{2.5}$  and CLW pass the significance test at all seasons. The AOD and CLW are negatively correlated with  $R^2 = -0.06$  in the summer, and  $PM_{2.5}$  and CLW are also negatively correlated with  $R^2 = -0.40$  in the summer (Table 2). A rise in the cloud droplet number concentration and a subsequent decline in CER is at an over threshold for an adequate formation of precipitation (Rosenfeld et al., 2002), enhancing CLW. Positive correlations between CER and cloud albedo are observed in the pollutant area due to the lack of drizzle size drops.

On the contrary, CER is negatively correlated with cloud albedo for clean clouds. CLW is the maximum control of liquid-cloud albedo (Gryspeerd et al., 2019). The dirty clouds have tinier cloud droplets, hence a higher cloud albedo and fewer drizzle drops (Peng et al., 2002). In addition, the cloud structure could be changed due to an increase in CLW with aerosol loading (Sporre et al., 2014). A smaller number of CCNs are likely in immaculate conditions, increasing growth quicker. Also, CLW would decrease if the clouds precipitate (Rao and Dey, 2020).

#### 3.4.4. Relationship between $PM_{2.5}$ , AOD, and COD

COD is the attenuation of solar radiation scattered and absorbed by cloud droplets in the atmosphere, which plays a vital role in Earth's radiative effect budget. As you can be seen in Fig. 4, COD is decreasing with increasing AOD. However, COD dramatically rises when  $PM_{2.5}$  values are

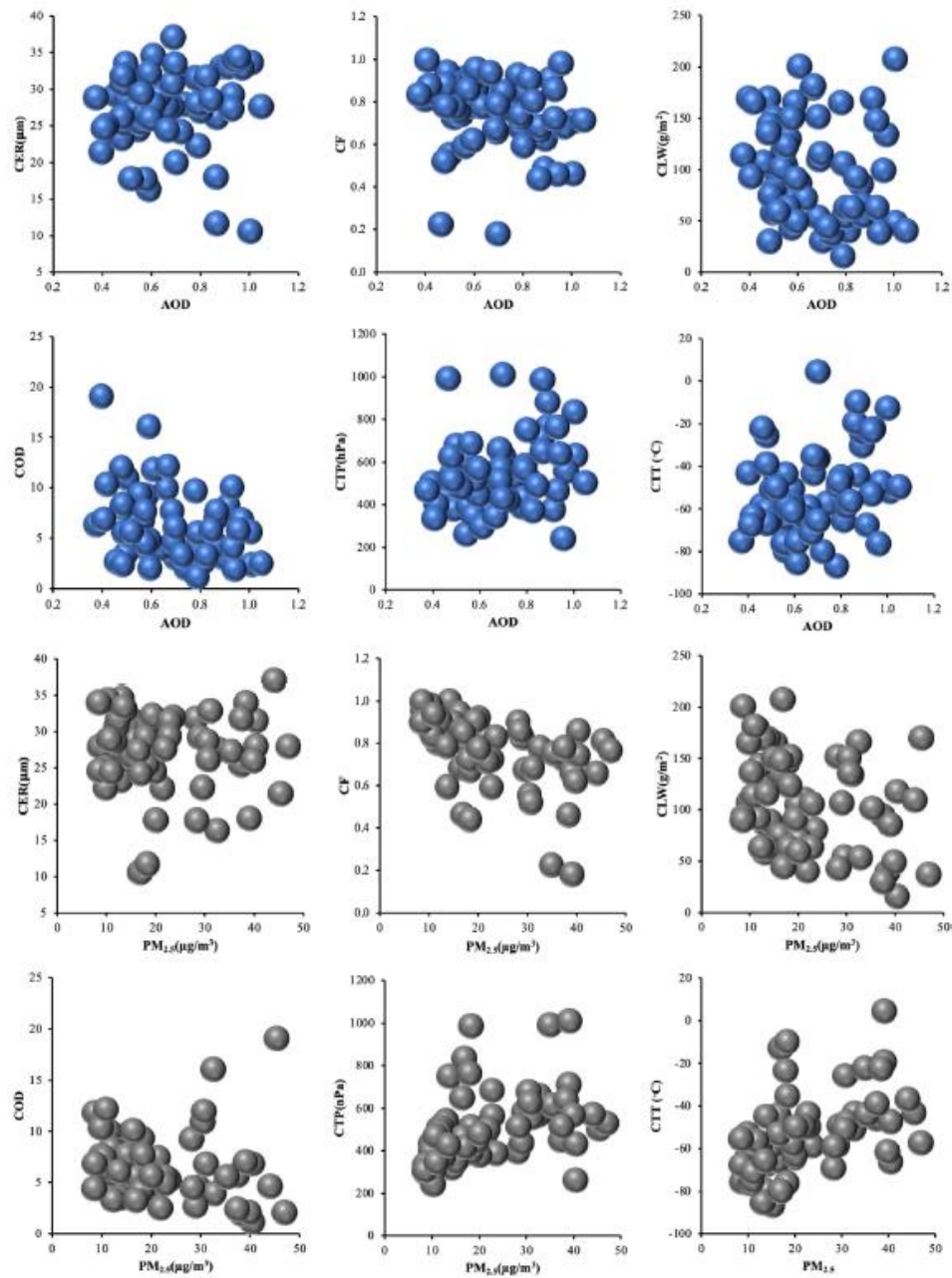


Fig. 4. The scatterplot between AOD, PM<sub>2.5</sub>, and cloud parameters in Bangkok.

Table 2  
Correlation for PM<sub>2.5</sub>, AOD, AE, CER, CF, CLW, COD, CTP, and CTT for each season.

Clouds parameters	Winter		Summer		Rainy		Annual	
	AOD	PM <sub>2.5</sub>	AOD	PM <sub>2.5</sub>	AOD	PM <sub>2.5</sub>	AOD	PM <sub>2.5</sub>
CER	0.18***	0.01	-0.11***	-0.002	0.52***	-0.11***	0.06***	-0.05***
CF	0.24***	-0.18***	-0.29*	-0.40***	0.31***	-0.29***	-0.24***	-0.51***
CLW	-0.13***	-0.03***	-0.06***	-0.31***	0.19***	-0.27***	-0.20***	-0.30***
COD	-0.24***	***	-0.31***	-0.27***	0.09***	-0.29***	-0.32***	-0.10***
CTP	-0.17***	***	0.33***	0.30***	-0.47***	0.38***	0.28***	0.39***
CTT	-0.16***	0.39***	0.39***	0.41***	0.42***	-0.21***	0.30***	0.49***

\*\*\*independent parameter is significant at the  $\alpha = 0.001$  level. \*\*independent parameter is significant at the  $\alpha = 0.01$  level.

\*Independent parameter is significant at the  $\alpha = 0.05$  level.

equal to or less than  $20 \mu\text{g}/\text{m}^3$ , and COD decreases when PM<sub>2.5</sub> values are higher than  $20 \mu\text{g}/\text{m}^3$ . Nevertheless, dust and anthropogenic aerosols within or above the clouds reduce the radiation obtained through the satellite, resulting in lower COD (Nakajima et al., 2001). This suggests that the association between AOD and COD is complex for interpretation. The finding reveals that AOD negative correlates with COD and found a high correlation in the summer ( $R^2 = -0.31$ ), and PM<sub>2.5</sub> also has a negative correlation in summer ( $R^2 = -0.27$ ) with COD (Table 2), signifying a relatively more minor influence on each other between the COD and PM<sub>2.5</sub>. Surveys such as that conducted by Chen et al. (2020) have shown that the observed effects of aerosols on warm clouds showed increasing aerosol loading caused an increase in COD. However, the apparent cloud-free atmosphere leads to a rise in the retrieved AOD, which allows the quantification of aerosol contribution at all cloud levels (Chaudhuri and Pal, 2014). The correlation between AOD and COD is positive, assuming aerosol influences COD indirectly depending on the geographical locations and climate conditions. Although the correlation between AOD and COD is negative, the correlation values are observed to be in the range of  $-0.37$  to  $0.09$ , implying a weak AOD–COD relationship. It indicates that AOD has a minor role in determining clouds' COD or radiative properties. However, the rise in aerosol concentrations may lead to numerous cloud droplets due to a reduction in droplet size at constant CLW, and consequently, growth in COD occurs. The results obtained from the preliminary analysis of COD rise due to a significant amount of CCN in the atmosphere.

#### 3.4.5. Relationship between PM<sub>2.5</sub>, AOD, and CTP

CTP is increasing with increasing AOD and PM<sub>2.5</sub>. The results are shown in Table 2. It was observed that CTP showed a positive correlation with AOD in summer ( $R^2 = 0.33$ ), while a negative correlation ( $R^2 = -0.47$ ), was observed in the rainy season (Table 2). Overall, a positive correlation was found for CTP, and AOD and PM<sub>2.5</sub>. Many historians have argued that CTP increased as AOD increased (Gopal et al., 2016, Patil et al., 2017). This may have resulted from the precipitation inhibition by expanding cloud lifetime, influencing the cloud albedo, and chang-

ing the cloud top pressure. Furthermore, decreased CTP was observed for low-AOD conditions, and increased CTP was detected for high-AOD conditions (Liu et al., 2018).

#### 3.4.6. Relationship between PM<sub>2.5</sub>, AOD and CTT

CTT plays an essential role in the net earth's radiation budget as CTT measure the atmospheric temperature at the cloud top. It was found that CTT, AOD, and PM<sub>2.5</sub> have a similar pattern to CTP. CTT increased as AOD increased (Fig. 4). The results are shown in Table 2. The correlation between AOD and CTT (Table 2) showed a positive correlation ( $R^2 = 0.30$ ), and PM<sub>2.5</sub> and CTT also gave a positive correlation ( $R^2 = 0.49$ ). A weak negative correlation between CTT and AOD ( $R^2 = -0.16$ ) was detected in the winter season, while a strong positive correlation ( $R^2 = 0.42$ ) between CTT and AOD was also seen in the rainy. The relation between CTT and PM<sub>2.5</sub> shows a similar pattern. The abovementioned observation shows that CTT could be sensitive to aerosol concentrations, mainly anthropogenic aerosols. A positive correlation is due to the AOD-CTT relationship, with climate pattern and meteorological conditions being interpreted as the contributing factors for the examined variations for further analysis. In addition, it showed a positive correlation with CTT that observed high AOD (Nyasulu et al., 2020).

#### 3.5. Cloud properties during high PM<sub>2.5</sub> concentrations

From November to January, poor air quality is observed, mainly due to less or non-rainfall substantially impacting PM<sub>2.5</sub> concentrations in the atmosphere (Pilahome, Ninssawan, 2022, Zhou et al., 2020); therefore, this work was dedicated from November to January (winter). Due to weather conditions in the winter months, pollutants are trapped in the atmosphere for longer compared to other seasons. However, human activities are minimal all over the year. Fig. 5 shows the results from the initial analysis of PM<sub>2.5</sub> and cloud parameters from November to January. As shown in Fig. 5, three-months average of PM<sub>2.5</sub> is  $33.96 \text{ g}/\text{m}^3$ , while CER, CF, CLW, COD, CTP, and CTT are  $26.15 \mu\text{m}$ ,  $0.70$ ,  $89.66 \text{ g}/\text{m}^2$ ,  $6.62$ ,  $550.39 \text{ hPa}$ , and  $-46.65\text{C}$ , respectively.

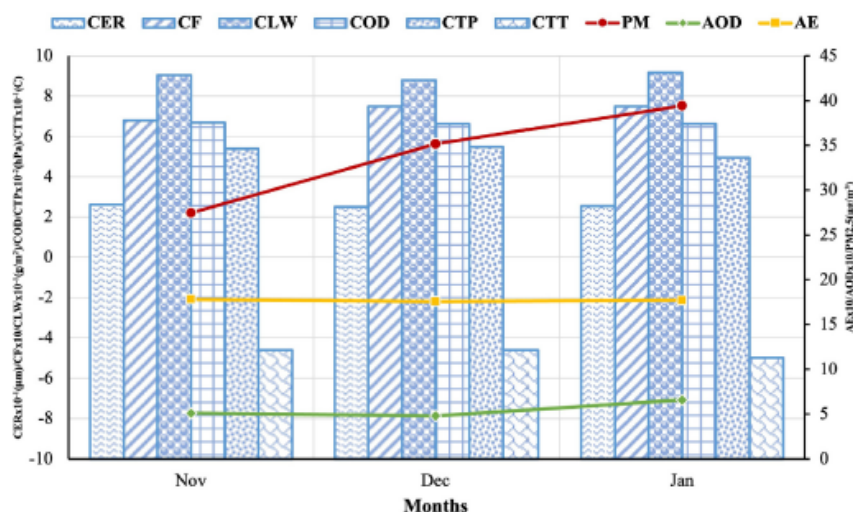


Fig. 5. PM<sub>2.5</sub>, AOD, AE, CER, CF, CLW, COD, CTP, and CTT in Bangkok for the years 2016 to 2021.

The three-month PM<sub>2.5</sub> ranges from 27.44 g/m<sup>3</sup> to 39.41 g/m<sup>3</sup>. Ground PM<sub>2.5</sub> shows high values of fine mode, primarily associated with exhaust from transportation, power plants, and biomass burning (Kumharn, Janjai, 2020). High aerosol concentrations in the winter come from agricultural waste burning locally and in surrounding provinces. Significantly, those aerosol particles are influenced by a temperature inversion (Kayee et al., 2020, Pilahome, Ninssawan, 2022)(Kayee et al., 2020; Pilahome et al., 2022). During the winter, Bangkok faces the northeast monsoon, bringing cool air and high pressure from China. This is attributed to weather conditions trapping cold air with pollutants near the Earth's surface for a few days or weeks. Therefore, high aerosol concentrations are also related to the climate conditions that cause temperature inversions during the 2016 to 2021 haze period. During high PM<sub>2.5</sub> concentrations, cloud parameters are significantly influenced by PM<sub>2.5</sub> concentrations in the atmosphere. The three-month of CER, CF, CLW, COD, CTP, and CTT ranges from 16.34 µm to 37.05 µm, 0.22 to 0.86, 15.67 g/m<sup>2</sup> to 169.80 g/m<sup>2</sup>, 1.14 to 19.06, 261.67 hPa to 991.67 hPa, and -66.26C to -22.17C, respectively. According to cloud properties, most Altostratus clouds (middle clouds) appear during high PM<sub>2.5</sub> concentrations in Bangkok (Schmunk, 2022).

#### 4. Discussion

The relationship between aerosol particles and cloud parameters was investigated during high PM<sub>2.5</sub> concentrations in Bangkok from 2016 to 2021. This study has identified the basis of the aerosol-cloud related research.

Higher AOD values were observed in the summer than in the rainy season, while high PM<sub>2.5</sub> concentrations were in the winter. CTP and CTT gave high values in summer; however, high CER, CF, CLW, and COD values were in the rainy season. Therefore, high PM<sub>2.5</sub> and cloud parameters (CTP and CTT) occurred in the same seasons. In January, the highest PM<sub>2.5</sub> levels were influenced by weather conditions (less/non-rainfall, low temperature, light wind), associated with automobile and industrial emissions combined with particles blown from the neighboring countries. Overall, the correlation analysis showed that AODs were correlated negatively with CF, CLW and COD, and positively correlated with CER, CTP, and CTT. PM<sub>2.5</sub> values indicate a negative correlation with CER, CF, CLW and COD, and have a strong negative correlation with CF. Interestingly, Altostratus clouds most appeared during high PM<sub>2.5</sub> concentrations. Our finding is helpful information for managing artificial rainmaking to reduce the polluted cities like the capital city Bangkok, Thailand.

#### Declaration of Competing Interest

The authors declare that they have no known competing financial interests or personal relationships that could have appeared to influence the work reported in this paper.

#### Acknowledgment

This research project is supported by the National Research Council of Thailand (NRCT): (Contact No. N41A650116).

## References

- Alam, K., Iqbal, M.J., Blaschke, T., Qureshi, S., Khan, G., 2010. Monitoring spatio-temporal variations in aerosols and aerosol-cloud interactions over Pakistan using MODIS data. *Adv. Space Res.* 46, 1162–1176.
- Albrecht, B.A., 1989. Aerosols, cloud microphysics, and fractional cloudiness. *Science* 245, 1227–1230.
- Bi, J., Belle, J.H., Wang, Y., Lyapustin, A.I., Wildani, A., Liu, Y., 2019. Impacts of snow and cloud covers on satellite-derived PM<sub>2.5</sub> levels. *Remote Sens. Environ.* 221, 665–674.
- Brennan, J.I., Kaufman, Y.J., Koren, I., Rong Rong, L., 2005. Aerosol-cloud interaction-misclassification of MODIS clouds in heavy aerosol. *IEEE Trans. Geosci. Remote Sens.* 43, 911.
- Chaudhuri, S., Pal, J., 2014. Cloud-aerosol coupled index in estimating the break phase of Indian summer monsoon. *Theor. Appl. Climatol.* 118, 447–464.
- Che, H., Stier, P., Watson-Parris, D., Gordon, H., Deaconu, L., 2022. Source attribution of cloud condensation nuclei and their impact on strato-cumulus clouds and radiation in the south-eastern Atlantic. *Atmos. Chem. Phys.* 22, 10789–10807.
- Chen, Y.-C., Wang, S.-H., Min, Q., et al. Aerosol impacts on warm-cloud microphysics and drizzle in a moderately polluted environment, 2020.
- Costantino, L., Bréon, F.-M., 2010. Analysis of aerosol-cloud interaction from multi-sensor satellite observations. *Geophys. Res. Lett.* 37.
- Dong, B., Wilcox, L.J., Highwood, E.J., Sutton, R.T., 2019. Impacts of recent decadal changes in Asian aerosols on the East Asian summer monsoon: roles of aerosol-radiation and aerosol-cloud interactions. *Clim. Dyn.* 53, 3235–3256.
- Garrett, T.J., Zhao, C., 2006. Increased Arctic cloud longwave emissivity associated with pollution from mid-latitudes. *Nature* 440, 787–789.
- Gopal, K.R., Obul Reddy, K.R., Balakrishnaiah, G., et al., 2016. Regional trends of aerosol optical depth and their impact on cloud properties over Southern India using MODIS data. *J. Atmos. Sol. Terr. Phys.* 146, 38–48.
- Gryspeerd, E., Goren, T., Sourdeval, O., et al., 2019. Constraining the aerosol influence on cloud liquid water path. *Atmos. Chem. Phys.* 19, 5331–5347.
- Hasekamp, O.P., Gryspeerd, E., Quaas, J., 2019. Analysis of polarimetric satellite measurements suggests stronger cooling due to aerosol-cloud interactions. *Nat. Commun.* 10, 5405.
- IPCC, 2007. *Climate Change*. Cambridge University Press.
- Janssen, R., Ganzeveld, L., Kabat, P., Kulmala, M., Nieminen, T., Roebling, R., 2011. Estimating seasonal variations in cloud droplet number concentration over the boreal forest from satellite observations. *ACPD Chem. Phys. Discuss* 11, 9999–10029.
- Jia, H., Ma, X., Quaas, J., Yin, Y., Qiu, T., 2019. Is positive correlation between cloud droplet effective radius and aerosol optical depth over land due to retrieval artifacts or real physical processes? *Atmos. Chem. Phys.* 19, 8879–8896.
- Kaufman, Y.J., Koren, I., 2006. Smoke and pollution aerosol effect on cloud cover. *Science* 313, 655–658.
- Kaufman, Y.J., Koren, I., Remer, L.A., Rosenfeld, D., Rudich, Y., 2005. The effect of smoke, dust, and pollution aerosol on shallow cloud development over the Atlantic Ocean. *Proc. Natl. Acad. Sci.* 102, 11207–11212.
- Kayee, J., Sompongchaiyakul, P., Sanwani, N., Burekul, S., Wang, X., Das, R., 2020. Metal concentrations and source apportionment of PM<sub>2.5</sub> in Chiang Rai and Bangkok, Thailand during a biomass burning season. *ACS Earth Space Chem.* 4, 1213–1226.
- Khatri, P., Hayasaka, T., Holben, B., et al. Aerosol Loading and Radiation Budget Perturbations in Densely Populated and Highly Polluted Indo-Gangetic Plain by COVID-19: Influences on Cloud Properties and Air Temperature. *Geophysical Research Letters* 48, e2021GL093796, 2021.
- Kumham, W., Hanprasert, K., 2016. Aerosol optical properties in ultraviolet ranges and respiratory diseases in Thailand. *Atmos. Environ.* 142, 221–228.
- Kumham, W., Janjai, S., Irie, H., Pilahome, O., 2020. Aerosol size distribution using Thailand ground-based instruments and climate variables. *Theor. Appl. Climatol.* 142, 599–611.
- Liu, Y., Zhang, J., Zhou, P., et al., 2018. Satellite-based estimate of the variability of warm cloud properties associated with aerosol and meteorological conditions. *Atmos. Chem. Phys.* 18, 18187–18202.
- Mhawish, A., Banerjee, T., Sorek-Hamer, M., et al., 2020. Estimation of high-resolution PM<sub>2.5</sub> over the indo-gangetic plain by fusion of satellite data, meteorology, and land use variables. *Environ. Sci. Tech.* 54, 7891–7900.
- Myhre, G., Stordal, F., Johnsrud, M., et al., 2007. Aerosol-cloud interaction inferred from MODIS satellite data and global aerosol models. *Atmos. Chem. Phys.* 7, 3081–3101.
- Nakajima, T., Higurashi, A., Kawamoto, K., Penner, J.E., 2001. A possible correlation between satellite-derived cloud and aerosol microphysical parameters. *Geophys. Res. Lett.* 28, 1171–1174.
- Nyasulu, M., Haque, M.M., Boiy, R., Kumar, K.R., Zhang, Y.-L., 2020. Seasonal climatology and relationship between AOD and cloud properties inferred from the MODIS over Malawi, Southeast Africa. *Atmos. Pollut. Res.* 11, 1933–1952.
- Oreopoulos, L., Cho, N., Lee, D. A Global Survey of Apparent Aerosol-Cloud Interaction Signals. *Journal of Geophysical Research: Atmospheres* 125, e2019JD031287, 2020.
- Patil, N., Dave, P., Venkataraman, C., 2017. Contrasting influences of aerosols on cloud properties during deficient and abundant monsoon years. *Sci. Rep.* 7, 44996.
- Peng, Y., Lohmann, U., Leaitch, R., Banić, C., Couture, M. The cloud albedo-cloud droplet effective radius relationship for clean and polluted clouds from RACE and FIRE-ACE. *Journal of Geophysical Research: Atmospheres* 107, AAC 1–AAC -6, 2002.
- Pilahome, O., Ninssawan, W., Jankondee, Y., Janjai, S., Kumham, W., 2022. Long-term variations and comparison of aerosol optical properties based on MODIS and ground-based data in Thailand. *Atmos. Environ.* 286 119218.
- Rao, S., Dey, S., 2020. Consistent signal of aerosol indirect and semi-direct effect on water clouds in the oceanic regions adjacent to the Indian subcontinent. *Atmos. Res.* 232 104677.
- Rosenfeld, D., Rudich, Y., Lahav, R., 2001. Desert dust suppressing precipitation: a possible desertification feedback loop. *PNAS* 98, 5975–5980.
- Rosenfeld, D., Lahav, R., Khain, A., Pinsky, M., 2002. The role of sea spray in cleansing air pollution over ocean via cloud processes. *Science* 297, 1667–1670.
- Saponaro, G., Sporre, M.K., Neubauer, D., et al., 2020. Evaluation of aerosol and cloud properties in three climate models using MODIS observations and its corresponding COSP simulator, as well as their application in aerosol-cloud interactions. *Atmos. Chem. Phys.* 20, 1607–1626.
- Schmunk, R. ISCCP DEFINITION OF CLOUD TYPES. 2022.
- Sporre, M.K., Swietlicki, E., Glantz, P., Kulmala, M., 2014. Aerosol indirect effects on continental low-level clouds over Sweden and Finland. *Atmos. Chem. Phys.* 14, 12167–12179.
- Zhang, Y., Zuhang, W., Zhang, L., Xie, Y., Huang, Y., Zheng, H., 2020. Study of land-sea microphysics associated with East Asian Summer Monsoon Rainband and its preliminary application to GPM DPR. *J. Atmos. Oceanic Tech.* 37.
- Zhou, Y., Yue, Y., Bai, Y., Zhang, L., 2020. Effects of Rainfall on PM<sub>2.5</sub> and PM<sub>10</sub> in the Middle Reaches of the Yangtze River. *Adv. Meteorol.*, 2398146.
- Zhu, Y., Shen, Y., Li, K., et al. Investigation of Particle Number Concentrations and New Particle Formation With Largely Reduced Air Pollutant Emissions at a Coastal Semi-Urban Site in Northern China. *Journal of Geophysical Research: Atmospheres* 126, e2021JD035419, 2021.
- Zhu, S., Xiao, Z., Che, H., Chen, Q., 2022. Impact of aerosols on warm clouds over the Sichuan Basin, China in winter based on the MERRA-2 reanalysis dataset. *Atmos. Pollut. Res.* 13 101342.

APPENDICE D  
SHORT-TERM RESEARCH

## APPENDICE D

Short-term research at The Paul Scherrer Institute, Switzerland.







APPENDICE E

A BRIEF HISTORY OF RESEARCHER

## A BRIEF HISTORY OF RESEARCHER

### PERSONAL DATA:

Name	Miss Oradee Pilahome
Academic Position	Ph.D. Student
Date of Birth	April 27, 1995
Place of Birth	Sakon Nakhon, Thailand
Nationality	Thai
Marital Status	Single
Phone	0913607130
Email	<a href="mailto:Oradee.pi60@snru.ac.th">Oradee.pi60@snru.ac.th</a>

### EDUCATION:

Bachelor's degree B.Ed.(Physics)	Sakon Nakhon Rajabhat University
Master's degree M.Sc. (Physics)	Sakon Nakhon Rajabhat University
Doctoral degree Ph.D. (Physics)	Sakon Nakhon Rajabhat University